

PART 1

ONE-DIMENSIONAL FLOWS

2

FLows ON THE LINE

2.0 Introduction

In Chapter 1, we introduced the general system

$$\begin{aligned}\dot{x}_1 &= f_1(x_1, \dots, x_n) \\ &\vdots \\ \dot{x}_n &= f_n(x_1, \dots, x_n)\end{aligned}$$

and mentioned that its solutions could be visualized as trajectories flowing through an n -dimensional phase space with coordinates (x_1, \dots, x_n) . At the moment, this idea probably strikes you as a mind-bending abstraction. So let's start slowly, beginning here on earth with the simple case $n = 1$. Then we get a single equation of the form

$$\dot{x} = f(x).$$

Here $x(t)$ is a real-valued function of time t , and $f(x)$ is a smooth real-valued function of x . We'll call such equations **one-dimensional** or **first-order systems**.

Before there's any chance of confusion, let's dispense with two fussy points of terminology:

1. The word *system* is being used here in the sense of a dynamical system, not in the classical sense of a collection of two or more equations. Thus a single equation can be a “system.”
2. We do not allow f to depend explicitly on time. Time-dependent or “nonautonomous” equations of the form $\dot{x} = f(x, t)$ are more complicated, because one needs *two* pieces of information, x and t , to predict the future state of the system. Thus $\dot{x} = f(x, t)$ should really be regarded as a *two-dimensional* or *second-order* system, and will therefore be discussed later in the book.

2.1 A Geometric Way of Thinking

Pictures are often more helpful than formulas for analyzing nonlinear systems. Here we illustrate this point by a simple example. Along the way we will introduce one of the most basic techniques of dynamics: *interpreting a differential equation as a vector field*.

Consider the following nonlinear differential equation:

$$\dot{x} = \sin x. \quad (1)$$

To emphasize our point about formulas versus pictures, we have chosen one of the few nonlinear equations that can be solved in closed form. We separate the variables and then integrate:

$$dt = \frac{dx}{\sin x},$$

which implies

$$t = \int \csc x \, dx$$

$$= -\ln|\csc x + \cot x| + C.$$

To evaluate the constant C , suppose that $x = x_0$ at $t = 0$. Then $C = \ln|\csc x_0 + \cot x_0|$.

Hence the solution is

$$t = \ln \left| \frac{\csc x_0 + \cot x_0}{\csc x + \cot x} \right|. \quad (2)$$

This result is exact, but a headache to interpret. For example, can you answer the following questions?

1. Suppose $x_0 = \pi/4$; describe the qualitative features of the solution $x(t)$ for all $t > 0$. In particular, what happens as $t \rightarrow \infty$?
2. For an arbitrary initial condition x_0 , what is the behavior of $x(t)$ as $t \rightarrow \infty$?

Think about these questions for a while, to see that formula (2) is not transparent.

In contrast, a graphical analysis of (1) is clear and simple, as shown in Figure 2.1.1. We think of t as time, x as the position of an imaginary particle moving along the real line, and \dot{x} as the velocity of that particle. Then the differential equation $\dot{x} = \sin x$ represents a **vector field** on the line: it dictates the velocity vector \dot{x} at each x . To sketch the vector field, it is convenient to plot \dot{x} versus x , and then draw arrows on the x -axis to indicate the corresponding velocity vector at each x . The arrows point to the right when $\dot{x} > 0$ and to the left when $\dot{x} < 0$.

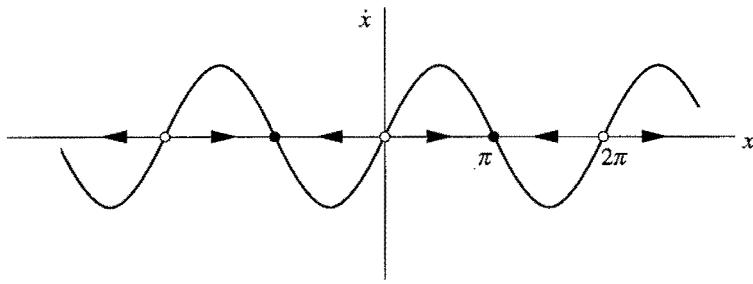


Figure 2.1.1

Here's a more physical way to think about the vector field: imagine that fluid is flowing steadily along the x -axis with a velocity that varies from place to place, according to the rule $\dot{x} = \sin x$. As shown in Figure 2.1.1, the *flow* is to the right when $\dot{x} > 0$ and to the left when $\dot{x} < 0$. At points where $\dot{x} = 0$, there is no flow; such points are therefore called *fixed points*. You can see that there are two kinds of fixed points in Figure 2.1.1: solid black dots represent *stable* fixed points (often called *attractors* or *sinks*, because the flow is toward them) and open circles represent *unstable* fixed points (also known as *repellers* or *sources*).

Armed with this picture, we can now easily understand the solutions to the differential equation $\dot{x} = \sin x$. We just start our imaginary particle at x_0 and watch how it is carried along by the flow.

This approach allows us to answer the questions above as follows:

1. Figure 2.1.1 shows that a particle starting at $x_0 = \pi/4$ moves to the right faster and faster until it crosses $x = \pi/2$ (where $\sin x$ reaches its maximum). Then the particle starts slowing down and eventually approaches the stable fixed point $x = \pi$ from the left. Thus, the qualitative form of the solution is as shown in Figure 2.1.2.

Note that the curve is concave up at first, and then concave down; this corresponds to the initial acceleration for $x < \pi/2$, followed by the deceleration toward $x = \pi$.

2. The same reasoning applies to any initial condition x_0 . Figure 2.1.1 shows that if $\dot{x} > 0$ initially, the particle heads to the right and asymptotically approaches the nearest stable fixed point. Similarly, if $\dot{x} < 0$ initially, the particle approaches the nearest stable fixed point to its left. If $\dot{x} = 0$, then x remains constant. The qualitative form of the solution for any initial condition is sketched in Figure 2.1.3.

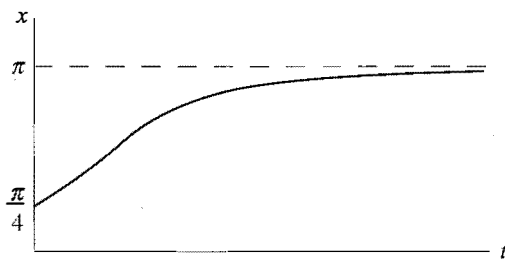


Figure 2.1.2

Qualitative form of the solution for any initial condition is sketched in Figure 2.1.3.

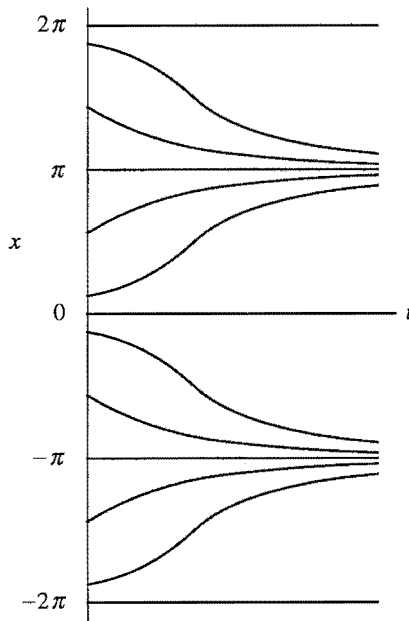


Figure 2.1.3

In all honesty, we should admit that a picture can't tell us certain *quantitative* things: for instance, we don't know the time at which the speed $|\dot{x}|$ is greatest. But in many cases *qualitative* information is what we care about, and then pictures are fine.

2.2 Fixed Points and Stability

The ideas developed in the last section can be extended to any one-dimensional system $\dot{x} = f(x)$. We just need to draw the graph of $f(x)$ and then use it to sketch the vector field on the real line (the x -axis in Figure 2.2.1).

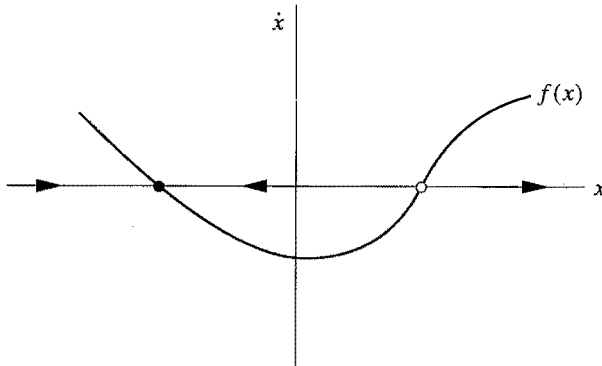


Figure 2.2.1

As before, we imagine that a fluid is flowing along the real line with a local velocity $f(x)$. This imaginary fluid is called the phase fluid, and the real line is the phase space. The flow is to the right where $f(x) > 0$ and to the left where $f(x) < 0$. To find the solution to $\dot{x} = f(x)$ starting from an arbitrary initial condition x_0 , we place an imaginary particle (known as a **phase point**) at x_0 and watch how it is carried along by the flow. As time goes on, the phase point moves along the x -axis according to some function $x(t)$. This function is called the **trajectory** based at x_0 , and it represents the solution of the differential equation starting from the initial condition x_0 . A picture like Figure 2.2.1, which shows all the qualitatively different trajectories of the system, is called a **phase portrait**.

The appearance of the phase portrait is controlled by the fixed points x^* , defined by $f(x^*) = 0$; they correspond to stagnation points of the flow. In Figure 2.2.1, the solid black dot is a stable fixed point (the local flow is toward it) and the open dot is an unstable fixed point (the flow is away from it).

In terms of the original differential equation, fixed points represent **equilibrium** solutions (sometimes called steady, constant, or rest solutions, since if $x = x^*$ initially, then $x(t) = x^*$ for all time). An equilibrium is defined to be stable if all sufficiently small disturbances away from it damp out in time. Thus stable equilibria are represented geometrically by stable fixed points. Conversely, unstable equilibria, in which disturbances grow in time, are represented by unstable fixed points.

EXAMPLE 2.2.1:

Find all fixed points for $\dot{x} = x^2 - 1$, and classify their stability.

Solution: Here $f(x) = x^2 - 1$. To find the fixed points, we set $f(x^*) = 0$ and solve for x^* . Thus $x^* = \pm 1$. To determine stability, we plot $x^2 - 1$ and then sketch the vector field (Figure 2.2.2). The flow is to the right where $x^2 - 1 > 0$ and to the left where $x^2 - 1 < 0$. Thus $x^* = -1$ is stable, and $x^* = 1$ is unstable. ■

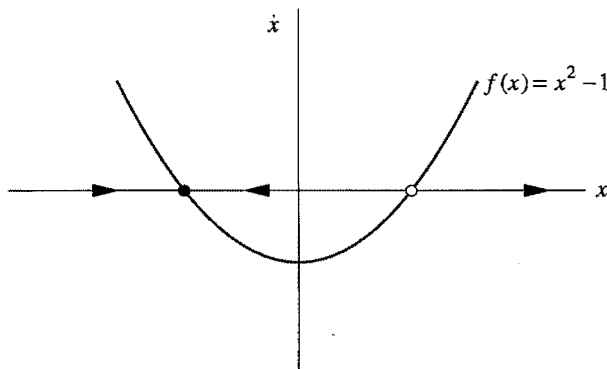


Figure 2.2.2

Note that the definition of stable equilibrium is based on *small* disturbances; certain large disturbances may fail to decay. In Example 2.2.1, all small disturbances to $x^* = -1$ will decay, but a large disturbance that sends x to the right of $x = 1$ will *not* decay—in fact, the phase point will be repelled out to $+\infty$. To emphasize this aspect of stability, we sometimes say that $x^* = -1$ is ***locally stable***, but not **globally stable**.

EXAMPLE 2.2.2:

Consider the electrical circuit shown in Figure 2.2.3. A resistor R and a capacitor C are in series with a battery of constant dc voltage V_0 . Suppose that the switch is closed at $t = 0$, and that there is no charge on the capacitor initially. Let $Q(t)$ denote the charge on the capacitor at time $t \geq 0$. Sketch the graph of $Q(t)$.

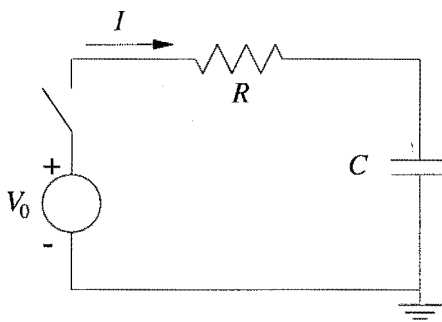


Figure 2.2.3

flowing through the resistor. This current causes charge to accumulate on the capacitor at a rate $\dot{Q} = I$. Hence

$$-V_0 + R\dot{Q} + Q/C = 0 \quad \text{or}$$

$$\dot{Q} = f(Q) = \frac{V_0}{R} - \frac{Q}{RC}.$$

The graph of $f(Q)$ is a straight line with a negative slope (Figure 2.2.4). The corresponding vector field has a fixed point where $f(Q) = 0$, which occurs at

$Q^* = CV_0$. The flow is to the right where $f(Q) > 0$ and to the left where $f(Q) < 0$. Thus the flow is always toward Q^* —it is a ***stable*** fixed point. In fact, it is ***globally stable***, in the sense that it is approached from *all* initial conditions.

To sketch $Q(t)$, we start a phase point at the origin of Figure 2.2.4 and imagine how it would move. The flow carries the phase point monotonically toward Q^* . Its speed

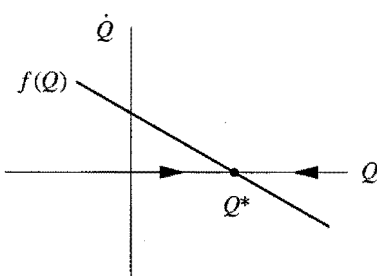


Figure 2.2.4

\dot{Q} decreases linearly as it approaches the fixed point; therefore $Q(t)$ is increasing and concave down, as shown in Figure 2.2.5. ■

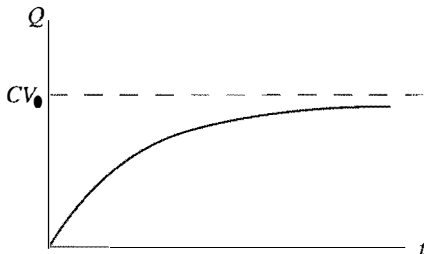


Figure 2.2.5

$x - \cos x$ looks like.

There's an easier solution, which exploits the fact that we know how to graph $y = x$ and $y = \cos x$ separately. We plot both graphs on the same axes and then observe that they intersect in exactly one point (Figure 2.2.6).

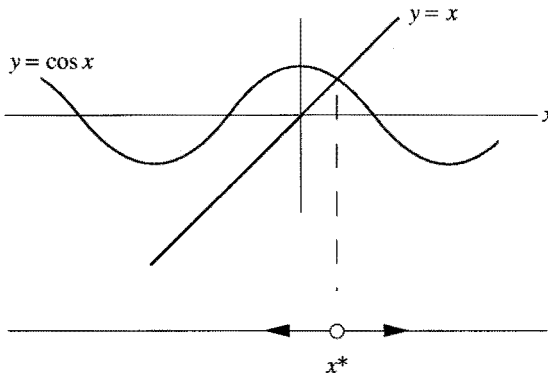


Figure 2.2.6

This intersection corresponds to a fixed point, since $x^* = \cos x^*$ and therefore $f(x^*) = 0$. Moreover, when the line lies above the cosine curve, we have $x > \cos x$ and so $\dot{x} > 0$: the flow is to the right. Similarly, the flow is to the left where the line is below the cosine curve. Hence x^* is the only fixed point, and it is unstable. Note that we can classify the stability of x^* , even though we don't have a formula for x^* itself! ■

2.3 Population Growth

The simplest model for the growth of a population of organisms is $\dot{N} = rN$, where $N(t)$ is the population at time t , and $r > 0$ is the growth rate. This model

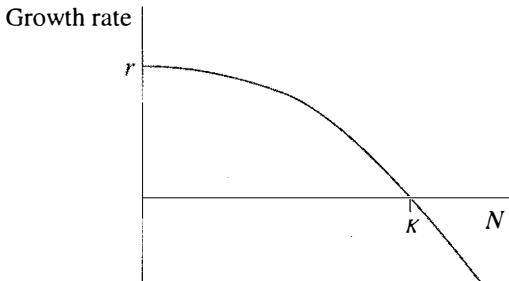


Figure 2.3.1

decreases when N becomes sufficiently large, as shown in Figure 2.3.1. For small N , the growth rate equals r , just as before. However, for populations larger than a certain **carrying capacity** K , the growth rate actually becomes negative; the death rate is higher than the birth rate.

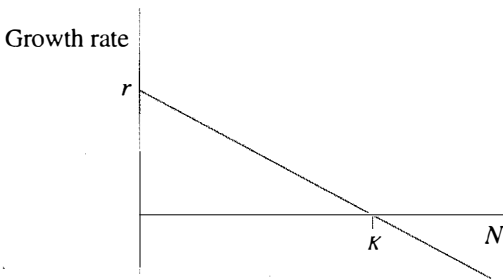


Figure 2.3.2

predicts exponential growth: $N(t) = N_0 e^{rt}$, where N_0 is the population at $t = 0$.

Of course such exponential growth cannot go on forever. To model the effects of over-crowding and limited resources, population biologists and demographers often assume that the per capita growth rate \dot{N}/N decreases linearly with N (Figure 2.3.2).

A mathematically convenient way to incorporate these ideas is to assume that the per capita growth rate \dot{N}/N decreases linearly with N (Figure 2.3.2).

This leads to the **logistic equation**

$$\dot{N} = rN \left(1 - \frac{N}{K}\right)$$

first suggested to describe the growth of human populations by Verhulst in 1838. This equation can be solved analytically (Exercise 2.3.1) but once again we prefer a graphical approach. We plot \dot{N} versus N to see what the vector field looks like. Note that we plot only $N \geq 0$, since it makes no sense to think about a negative population (Figure 2.3.3). Fixed points occur at $N^* = 0$ and $N^* = K$, as found by setting $\dot{N} = 0$ and solving for N . By looking at the flow in Figure 2.3.3, we see that $N^* = 0$ is an unstable fixed point and $N^* = K$ is a stable fixed point. In biological terms, $N = 0$ is an unstable equilibrium: a small population will grow exponentially fast and run away from $N = 0$. On the other hand, if N is disturbed slightly from K , the disturbance will decay monotonically and $N(t) \rightarrow K$ as $t \rightarrow \infty$.

In fact, Figure 2.3.3 shows that if we start a phase point at any $N_0 > 0$, it will always flow toward $N = K$. Hence *the population always approaches the carrying capacity*.

The only exception is if $N_0 = 0$; then there's nobody around to start reproducing, and so $N = 0$ for all time. (The model does not allow for spontaneous generation!)

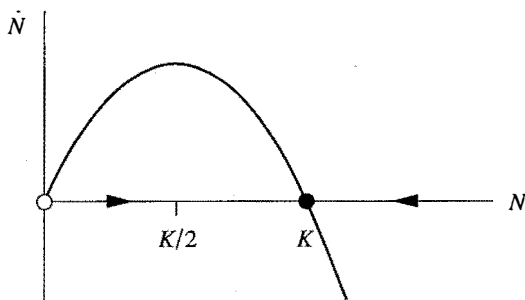


Figure 2.3.3

Figure 2.3.3 also allows us to deduce the qualitative shape of the solutions. For example, if $N_0 < K/2$, the phase point moves faster and faster until it crosses $N = K/2$, where the parabola in Figure 2.3.3 reaches its maximum. Then the phase point slows down and eventually creeps toward $N = K$. In biological terms, this means that the population initially grows in an accelerating fashion, and the graph of $N(t)$ is concave up. But after $N = K/2$, the derivative \dot{N} begins to decrease, and so $N(t)$ is concave down as it asymptotes to the horizontal line $N = K$ (Figure 2.3.4). Thus the graph of $N(t)$ is S-shaped or *sigmoid* for $N_0 < K/2$.

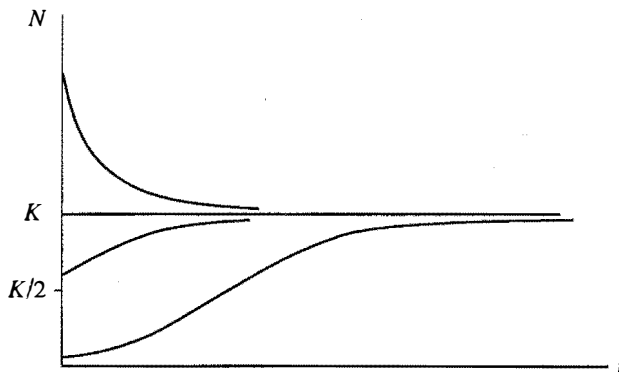


Figure 2.3.4

Something qualitatively different occurs if the initial condition N_0 lies between $K/2$ and K ; now the solutions are decelerating from the start. Hence these solutions are concave down for all t . If the population initially exceeds the carrying capacity ($N_0 > K$), then $N(t)$ decreases toward $N = K$ and is concave up. Finally, if $N_0 = 0$ or $N_0 = K$, then the population stays constant.

Critique of the Logistic Model

Before leaving this example, we should make a few comments about the biological validity of the logistic equation. The algebraic form of the model is not to be taken literally. The model should really be regarded as a metaphor for populations that have a

tendency to grow from zero population up to some carrying capacity K .

Originally a much stricter interpretation was proposed, and the model was argued to be a universal law of growth (Pearl 1927). The logistic equation was tested in laboratory experiments in which colonies of bacteria, yeast, or other simple organisms were grown in conditions of constant climate, food supply, and absence of predators. For a good review of this literature, see Krebs (1972, pp. 190–200). These experiments often yielded sigmoid growth curves, in some cases with an impressive match to the logistic predictions.

On the other hand, the agreement was much worse for fruit flies, flour beetles, and other organisms that have complex life cycles, involving eggs, larvae, pupae, and adults. In these organisms, the predicted asymptotic approach to a steady carrying capacity was never observed—instead the populations exhibited large, persistent fluctuations after an initial period of logistic growth. See Krebs (1972) for a discussion of the possible causes of these fluctuations, including age structure and time-delayed effects of overcrowding in the population.

For further reading on population biology, see Pielou (1969) or May (1981). Edelstein-Keshet (1988) and Murray (1989) are excellent textbooks on mathematical biology in general.

2.4 Linear Stability Analysis

So far we have relied on graphical methods to determine the stability of fixed points. Frequently one would like to have a more quantitative measure of stability, such as the rate of decay to a stable fixed point. This sort of information may be obtained by *linearizing* about a fixed point, as we now explain.

Let x^* be a fixed point, and let $\eta(t) = x(t) - x^*$ be a small perturbation away from x^* . To see whether the perturbation grows or decays, we derive a differential equation for η . Differentiation yields

$$\dot{\eta} = \frac{d}{dt}(x - x^*) = \dot{x},$$

since x^* is constant. Thus $\dot{\eta} = \dot{x} = f(x) = f(x^* + \eta)$. Now using Taylor's expansion we obtain

$$f(x^* + \eta) = f(x^*) + \eta f'(x^*) + O(\eta^2),$$

where $O(\eta^2)$ denotes quadratically small terms in η . Finally, note that $f(x^*) = 0$ since x^* is a fixed point. Hence

$$\dot{\eta} = \eta f'(x^*) + O(\eta^2).$$

Now if $f'(x^*) \neq 0$, the $O(\eta^2)$ terms are negligible and we may write the approximation

$$\dot{\eta} \approx \eta f'(x^*).$$

This is a linear equation in η , and is called the *linearization about x^** . It shows that *the perturbation $\eta(t)$ grows exponentially if $f'(x^*) > 0$ and decays if $f'(x^*) < 0$.* If $f'(x^*) = 0$, the $O(\eta^2)$ terms are not negligible and a nonlinear analysis is needed to determine stability, as discussed in Example 2.4.3 below.

The upshot is that the slope $f'(x^*)$ at the fixed point determines its stability. If you look back at the earlier examples, you'll see that the slope was always negative at a stable fixed point. The importance of the *sign* of $f'(x^*)$ was clear from our graphical approach; the new feature is that now we have a measure of *how stable* a fixed point is—that's determined by the *magnitude* of $f'(x^*)$. This magnitude plays the role of an exponential growth or decay rate. Its reciprocal $1/|f'(x^*)|$ is a *characteristic time scale*; it determines the time required for $x(t)$ to vary significantly in the neighborhood of x^* .

EXAMPLE 2.4.1:

Using linear stability analysis, determine the stability of the fixed points for $\dot{x} = \sin x$.

Solution: The fixed points occur where $f(x) = \sin x = 0$. Thus $x^* = k\pi$, where k is an integer. Then

$$f'(x^*) = \cos k\pi = \begin{cases} 1, & k \text{ even} \\ -1, & k \text{ odd.} \end{cases}$$

Hence x^* is unstable if k is even and stable if k is odd. This agrees with the results shown in Figure 2.1.1. ■

EXAMPLE 2.4.2:

Classify the fixed points of the logistic equation, using linear stability analysis, and find the characteristic time scale in each case.

Solution: Here $f(N) = rN(1 - \frac{N}{K})$, with fixed points $N^* = 0$ and $N^* = K$. Then $f'(N) = r - \frac{2rN}{K}$ and so $f'(0) = r$ and $f'(K) = -r$. Hence $N^* = 0$ is unstable and $N^* = K$ is stable, as found earlier by graphical arguments. In either case, the characteristic time scale is $1/|f'(N^*)| = 1/r$. ■

EXAMPLE 2.4.3:

What can be said about the stability of a fixed point when $f'(x^*) = 0$?

Solution: Nothing can be said in general. The stability is best determined on a case-by-case basis, using graphical methods. Consider the following examples:

- (a) $\dot{x} = -x^3$ (b) $\dot{x} = x^3$ (c) $\dot{x} = x^2$ (d) $\dot{x} = 0$

Each of these systems has a fixed point $x^* = 0$ with $f'(x^*) = 0$. However the stability is different in each case. Figure 2.4.1 shows that (a) is stable and (b) is unstable. Case (c) is a hybrid case we'll call *half-stable*, since the fixed point is attracting from the left and repelling from the right. We therefore indicate this type of fixed point by a half-filled circle. Case (d) is a whole line of fixed points; perturbations neither grow nor decay.

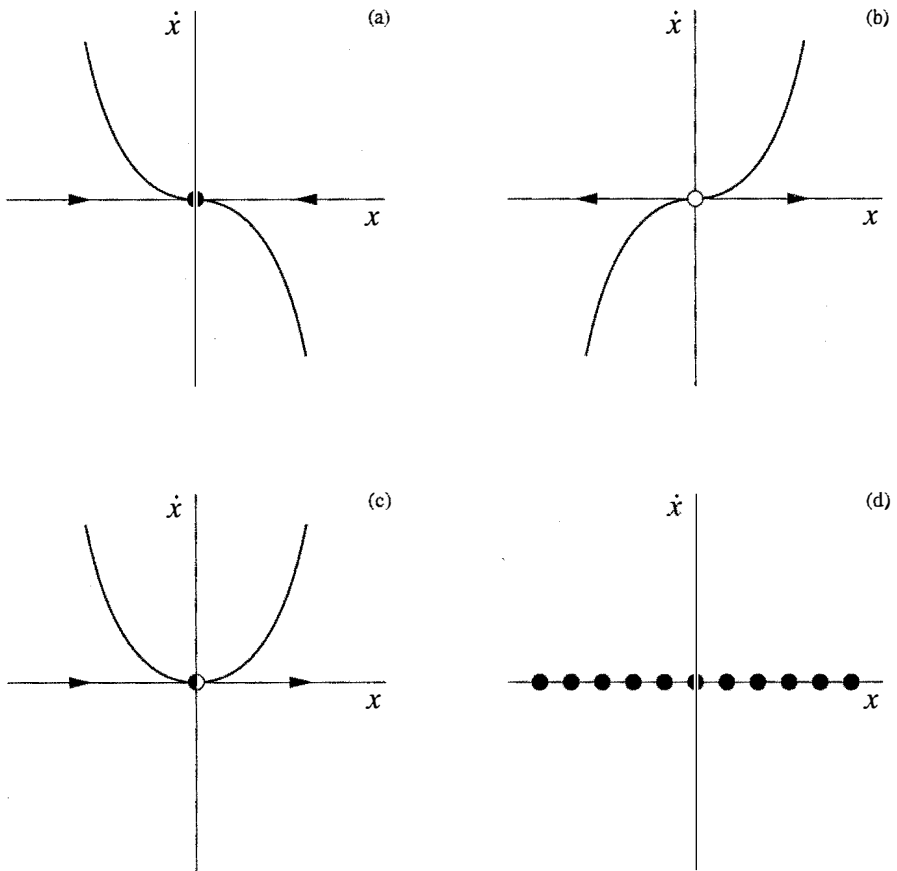


Figure 2.4.1

These examples may seem artificial, but we will see that they arise naturally in the context of *bifurcations*—more about that later. ■

2.5 Existence and Uniqueness

Our treatment of vector fields has been very informal. In particular, we have taken a cavalier attitude toward questions of existence and uniqueness of solutions to

the system $\dot{x} = f(x)$. That's in keeping with the "applied" spirit of this book. Nevertheless, we should be aware of what can go wrong in pathological cases.

EXAMPLE 2.5.1:

Show that the solution to $\dot{x} = x^{1/3}$ starting from $x_0 = 0$ is *not* unique.

Solution: The point $x = 0$ is a fixed point, so one obvious solution is $x(t) = 0$ for all t . The surprising fact is that there is *another* solution. To find it we separate variables and integrate:

$$\int x^{-1/3} dx = \int dt$$

so $\frac{3}{2} x^{2/3} = t + C$. Imposing the initial condition $x(0) = 0$ yields $C = 0$. Hence $x(t) = (\frac{2}{3}t)^{3/2}$ is also a solution! ■

When uniqueness fails, our geometric approach collapses because the phase point doesn't know how to move; if a phase point were started at the origin, would it stay there or would it move according to $x(t) = (\frac{2}{3}t)^{3/2}$? (Or as my friends in elementary school used to say when discussing the problem of the irresistible force and the immovable object, perhaps the phase point would explode!)

Actually, the situation in Example 2.5.1 is even worse than we've let on—there are *infinitely* many solutions starting from the same initial condition (Exercise 2.5.4).

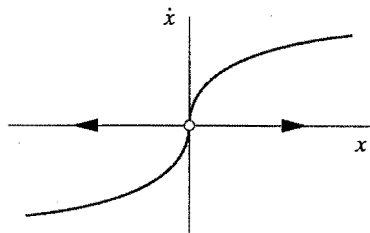


Figure 2.5.1

What's the source of the non-uniqueness? A hint comes from looking at the vector field (Figure 2.5.1). We see that the fixed point $x^* = 0$ is *very* unstable—the slope $f'(0)$ is infinite.

Chastened by this example, we state a theorem that provides sufficient conditions for existence and uniqueness of solutions to $\dot{x} = f(x)$.

Existence and Uniqueness Theorem: Consider the initial value problem

$$\dot{x} = f(x), \quad x(0) = x_0.$$

Suppose that $f(x)$ and $f'(x)$ are continuous on an open interval R of the x -axis, and suppose that x_0 is a point in R . Then the initial value problem has a solution $x(t)$ on some time interval $(-\tau, \tau)$ about $t = 0$, and the solution is unique.

For proofs of the existence and uniqueness theorem, see Borrelli and Coleman (1987), Lin and Segel (1988), or virtually any text on ordinary differential equations.

This theorem says that *if* $f(x)$ is smooth enough, then solutions exist and are unique. Even so, there's no guarantee that solutions exist forever, as shown by the

next example.

EXAMPLE 2.5.2:

Discuss the existence and uniqueness of solutions to the initial value problem $\dot{x} = 1 + x^2$, $x(0) = x_0$. Do solutions exist for all time?

Solution: Here $f(x) = 1 + x^2$. This function is continuous and has a continuous derivative for all x . Hence the theorem tells us that solutions exist and are unique for any initial condition x_0 . But *the theorem does not say that the solutions exist for all time*; they are only guaranteed to exist in a (possibly very short) time interval around $t = 0$.

For example, consider the case where $x(0) = 0$. Then the problem can be solved analytically by separation of variables:

$$\int \frac{dx}{1+x^2} = \int dt,$$

which yields

$$\tan^{-1} x = t + C$$

The initial condition $x(0) = 0$ implies $C = 0$. Hence $x(t) = \tan t$ is the solution. But notice that this solution exists only for $-\pi/2 < t < \pi/2$, because $x(t) \rightarrow \pm\infty$ as $t \rightarrow \pm\pi/2$. Outside of that time interval, there is no solution to the initial value problem for $x_0 = 0$. ■

The amazing thing about Example 2.5.2 is that the system has solutions that reach infinity *infinite time*. This phenomenon is called ***blow-up***. As the name suggests, it is of physical relevance in models of combustion and other runaway processes.

There are various ways to extend the existence and uniqueness theorem. One can allow f to depend on time t , or on several variables x_1, \dots, x_n . One of the most useful generalizations will be discussed later in Section 6.2.

From now on, we will not worry about issues of existence and uniqueness—our vector fields will typically be smooth enough to avoid trouble. If we happen to come across a more dangerous example, we'll deal with it then.

2.6 Impossibility of Oscillations

Fixed points dominate the dynamics of first-order systems. In all our examples so far, all trajectories either approached a fixed point, or diverged to $\pm\infty$. In fact, those are the *only* things that can happen for a vector field on the real line. The reason is that trajectories are forced to increase or decrease monotonically, or remain constant (Figure 2.6.1). To put it more geometrically, the phase point never reverses direction.

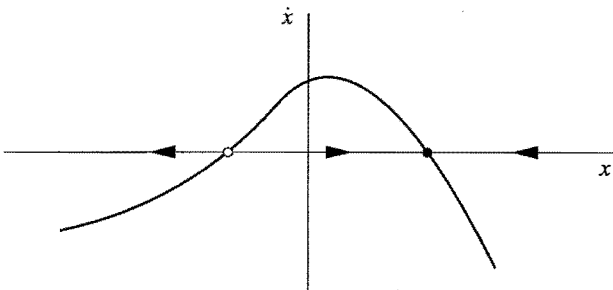


Figure 2.6.1

Thus, if a fixed point is regarded as an equilibrium solution, the approach to equilibrium is always *monotonic*—overshoot and damped oscillations can never occur in a first-order system. For the same reason, undamped oscillations are impossible. Hence *there are no periodic solutions to $\dot{x} = f(x)$* .

These general results are fundamentally topological in origin. They reflect the fact that $\dot{x} = f(x)$ corresponds to flow on a *line*. If you flow monotonically on a line, you'll never come back to your starting place—that's why periodic solutions are impossible. (Of course, if we were dealing with a *circle* rather than a line, we *could* eventually return to our starting place. Thus vector fields on the circle can exhibit periodic solutions, as we discuss in Chapter 4.)

Mechanical Analog: Overdamped Systems

It may seem surprising that solutions to $\dot{x} = f(x)$ can't oscillate. But this result becomes obvious if we think in terms of a mechanical analog. We regard $\dot{x} = f(x)$ as a limiting case of Newton's law, in the limit where the “inertia term” $m\ddot{x}$ is negligible.

For example, suppose a mass m is attached to a nonlinear spring whose restoring force is $F(x)$, where x is the displacement from the origin. Furthermore, suppose that the mass is immersed in a vat of very viscous fluid, like honey or motor oil (Figure 2.6.2), so that it is subject to a damping force $b\dot{x}$. Then Newton's law is $m\ddot{x} + b\dot{x} = F(x)$.

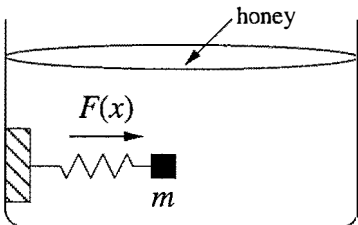


Figure 2.6.2

If the viscous damping is strong compared to the inertia term ($b\dot{x} \gg m\ddot{x}$), the system should behave like $b\dot{x} = F(x)$, or equivalently $\dot{x} = f(x)$, where $f(x) = b^{-1}F(x)$. In this **over-damped** limit, the behavior of the mechanical system is clear. The mass prefers to sit at a stable equilibrium, where $f(x) = 0$ and $f'(x) < 0$. If displaced a bit, the mass is slowly dragged back to equilibrium by the restoring force. No overshoot can occur, because the damping is enormous. And undamped oscillations are out of the question! These conclusions agree with those obtained earlier by geometric reasoning.

Actually, we should confess that this argument contains a slight swindle. The neglect of the inertia term $m\ddot{x}$ is valid, but only after a rapid initial transient during which the inertia and damping terms are of comparable size. An honest discussion of this point requires more machinery than we have available. We'll return to this matter in Section 3.5.

2.7 Potentials

There's another way to visualize the dynamics of the first-order system $\dot{x} = f(x)$, based on the physical idea of potential energy. We picture a particle sliding down the walls of a potential well, where the **potential** $V(x)$ is defined by

$$f(x) = -\frac{dV}{dx}.$$

As before, you should imagine that the particle is heavily damped—its inertia is completely negligible compared to the damping force and the force due to the potential. For example, suppose that the particle has to slog through a thick layer of goo that covers the walls of the potential (Figure 2.7.1).

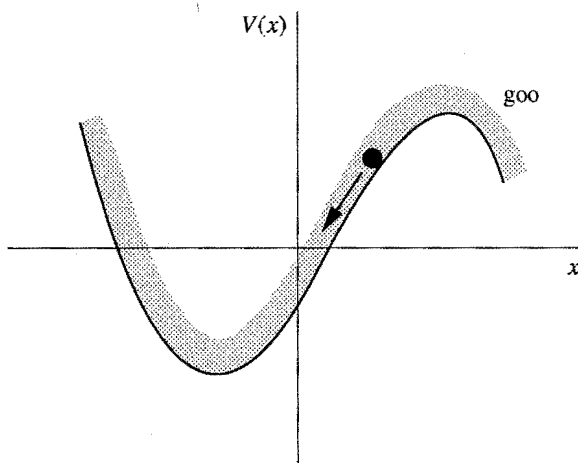


Figure 2.7.1

The negative sign in the definition of V follows the standard convention in physics; it implies that the particle always moves “downhill” as the motion proceeds. To see this, we think of x as a function of t , and then calculate the time-derivative of $V(x(t))$. Using the chain rule, we obtain

$$\frac{dV}{dt} = \frac{dV}{dx} \frac{dx}{dt}.$$

Now for a first-order system,

$$\frac{dx}{dt} = -\frac{dV}{dx},$$

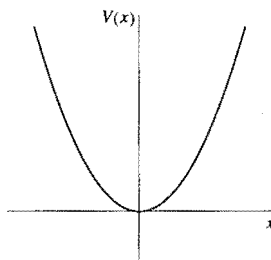
since $\dot{x} = f(x) = -dV/dx$, by the definition of the potential. Hence,

$$\frac{dV}{dt} = -\left(\frac{dV}{dx}\right)^2 \leq 0.$$

Thus $V(t)$ decreases along trajectories, and so the particle always moves toward lower potential. Of course, if the particle happens to be at an **equilibrium** point where $dV/dx = 0$, then V remains constant. This is to be expected, since $dV/dx = 0$ implies $\dot{x} = 0$; equilibria occur at the fixed points of the vector field. Note that local minima of $V(x)$ correspond to *stable* fixed points, as we'd expect intuitively, and local maxima correspond to unstable fixed points.

EXAMPLE 2.7.1:

Graph the potential for the system $\dot{x} = -x$, and identify all the equilibrium points.

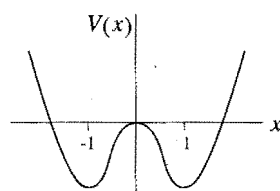


Solution: We need to find $V(x)$ such that $-dV/dx = -x$. The general solution is $V(x) = \frac{1}{2}x^2 + C$, where C is an arbitrary constant. (It always happens that the potential is only defined up to an additive constant. For convenience, we usually choose $C = 0$.) The graph of $V(x)$ is shown in Figure 2.7.2. The only equilibrium point occurs at $x = 0$, and it's stable. ■

Figure 2.7.2

EXAMPLE 2.7.2:

Graph the potential for the system $\dot{x} = x - x^3$, and identify all equilibrium points.



Solution: Solving $-dV/dx = x - x^3$ yields $V = -\frac{1}{2}x^2 + \frac{1}{4}x^4 + C$. Once again we set $C = 0$. Figure 2.7.3 shows the graph of V . The local minima at $x = \pm 1$ correspond to stable equilibria, and the local maximum at $x = 0$ corresponds to an unstable equilibrium. The potential shown in Figure 2.7.3 is often called a **double-well potential**, and the system is said to be **bistable**, since it has two stable equilibria. ■

Figure 2.7.3

2.8 Solving Equations on the Computer

Throughout this chapter we have used graphical and analytical methods to analyze first-order systems. Every budding dynamicist should master a third tool: numerical methods. In the old days, numerical methods were impractical because they required enormous amounts of tedious hand-calculation. But all that has changed, thanks to the computer. Computers enable us to approximate the solutions to analytically intractable problems, and also to visualize those solutions. In this section we take our first look at dynamics on the computer, in the context of **numerical integration** of $\dot{x} = f(x)$.

Numerical integration is a vast subject. We will barely scratch the surface. See Chapter 15 of Press et al. (1986) for an excellent treatment.

Euler's Method

The problem can be posed this way: given the differential equation $\dot{x} = f(x)$, subject to the condition $x = x_0$ at $t = t_0$, find a systematic way to approximate the solution $x(t)$.

Suppose we use the vector field interpretation of $\dot{x} = f(x)$. That is, we think of a fluid flowing steadily on the x -axis, with velocity $f(x)$ at the location x . Imagine we're riding along with a phase point being carried downstream by the fluid. Initially we're at x_0 , and the local velocity is $f(x_0)$. If we flow for a short time Δt , we'll have moved a distance $f(x_0)\Delta t$, because distance = rate \times time. Of course, that's not quite right, because our velocity was changing a little bit throughout the step. But over a sufficiently *small* step, the velocity will be nearly constant and our approximation should be reasonably good. Hence our new position $x(t_0 + \Delta t)$ is approximately $x_0 + f(x_0)\Delta t$. Let's call this approximation x_1 . Thus

$$x(t_0 + \Delta t) \approx x_1 = x_0 + f(x_0)\Delta t.$$

Now we iterate. Our approximation has taken us to a new location x_1 ; our new velocity is $f(x_1)$; we step forward to $x_2 = x_1 + f(x_1)\Delta t$; and so on. In general, the update rule is

$$x_{n+1} = x_n + f(x_n)\Delta t.$$

This is the simplest possible numerical integration scheme. It is known as **Euler's method**.

Euler's method can be visualized by plotting x versus t (Figure 2.8.1). The curve shows the exact solution $x(t)$, and the open dots show its values $x(t_n)$ at the discrete times $t_n = t_0 + n\Delta t$. The black dots show the approximate values given by the Euler method. As you can see, the approximation gets bad in a hurry unless Δt is extremely small. Hence Euler's method is not recommended in practice, but it contains the conceptual essence of the more accurate methods to be discussed next.

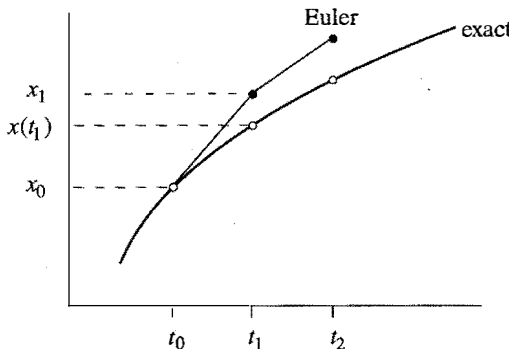


Figure 2.8.1

Refinements

One problem with the Euler method is that it estimates the derivative only at the left end of the time interval between t_n and t_{n+1} . A more sensible approach would be to use the *average* derivative across this interval. This is the idea behind the **improved Euler method**. We first take a trial step across the interval, using the Euler method. This produces a trial value $\tilde{x}_{n+1} = x_n + f(x_n)\Delta t$; the tilde above the x indicates that this is a tentative step, used only as a probe. Now that we've estimated the derivative on both ends of the interval, we average $f(x_n)$ and $f(\tilde{x}_{n+1})$, and use that to take the *real* step across the interval. Thus the improved Euler method is

$$\tilde{x}_{n+1} = x_n + f(x_n)\Delta t \quad (\text{the trial step})$$

$$x_{n+1} = x_n + \frac{1}{2}[f(x_n) + f(\tilde{x}_{n+1})]\Delta t. \quad (\text{the real step})$$

This method is more accurate than the Euler method, in the sense that it tends to make a smaller **error** $E = |x(t_n) - x_n|$ for a given **stepsize** Δt . In both cases, the error $E \rightarrow 0$ as $\Delta t \rightarrow 0$, but the error decreases *faster* for the improved Euler method. One can show that $E \propto \Delta t$ for the Euler method, but $E \propto (\Delta t)^2$ for the improved Euler method (Exercises 2.8.7 and 2.8.8). In the jargon of numerical analysis, the Euler method is first order, whereas the improved Euler method is second order.

Methods of third, fourth, and even higher orders have been concocted, but you should realize that higher order methods are not necessarily superior. Higher order methods require more calculations and function evaluations, so there's a computational cost associated with them. In practice, a good balance is achieved by the **fourth-order Runge–Kutta method**. To find x_{n+1} in terms of x_n , this method first requires us to calculate the following four numbers (cunningly chosen, as you'll see in Exercise 2.8.9):

$$\begin{aligned}k_1 &= f(x_n) \Delta t \\k_2 &= f(x_n + \frac{1}{2} k_1) \Delta t \\k_3 &= f(x_n + \frac{1}{2} k_2) \Delta t \\k_4 &= f(x_n + k_3) \Delta t.\end{aligned}$$

Then x_{n+1} is given by

$$x_{n+1} = x_n + \frac{1}{6}(k_1 + 2k_2 + 2k_3 + k_4).$$

This method generally gives accurate results without requiring an excessively small stepsize Δt . Of course, some problems are nastier, and may require small steps in certain time intervals, while permitting very large steps elsewhere. In such cases, you may want to use a Runge–Kutta routine with an automatic stepsize control; see Press et al. (1986) for details.

Now that computers are so fast, you may wonder why we don't just pick a tiny Δt once and for all. The trouble is that excessively many computations will occur, and each one carries a penalty in the form of *round-off error*. Computers don't have infinite accuracy—they don't distinguish between numbers that differ by some small amount δ . For numbers of order 1, typically $\delta \approx 10^{-7}$ for single precision and $\delta \approx 10^{-16}$ for double precision. Round-off error occurs during every calculation, and will begin to accumulate in a serious way if Δt is too small. See Hubbard and West (1991) for a good discussion.

Practical Matters

You have several options if you want to solve differential equations on the computer. If you like to do things yourself, you can write your own numerical integration routines, and plot the results using whatever graphics facilities are available. The information given above should be enough to get you started. For further guidance, consult Press et al. (1986); they provide sample routines written in Fortran, C, and Pascal.

A second option is to use existing packages for numerical methods. The software libraries by IMSL and NAG have a wide variety of state-of-the-art numerical integrators. These libraries are well documented, reliable, and flexible, and can be found at most university computing centers or networks. The packages *Matlab*, *Mathematica*, and *Maple* are more interactive and also have programs for solving ordinary differential equations.

The final option is for people who want to explore dynamics, not computing. Dynamical systems software has recently become available for personal computers. All you have to do is type in the equations and the parameters; the program solves the equations numerically and plots the results. Some recommended programs are *Phaser* (Kocak 1989) for the IBM PC or *MacMath* (Hubbard and West

1992) for the Macintosh. *MacMath* was used to generate many of the plots in this book.

These programs are easy to use, and they will help you build intuition about dynamical systems.

EXAMPLE 2.8.1:

Use *MacMath* to solve the system $\dot{x} = x(1 - x)$ numerically.

Solution: This is a logistic equation (Section 2.3) with parameters $r = 1$, $K = 1$. Previously we gave a rough sketch of the solutions, based on geometric arguments; now we can draw a more quantitative picture.

As a first step, we plot the **slope field** for the system in the (t, x) plane (Figure 2.8.2). Here the equation $\dot{x} = x(1 - x)$ is being interpreted in a new way: for each point (t, x) , the equation gives the slope dx/dt of the solution passing through that point. The slopes are indicated by little line segments in Figure 2.8.2.

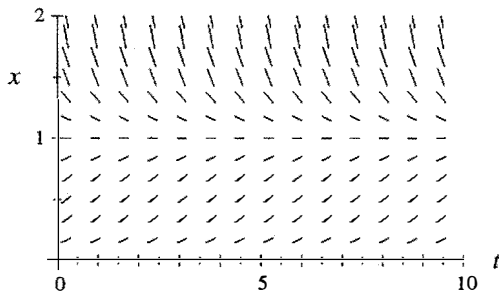


Figure 2.8.2

Finding a solution now becomes a problem of drawing a curve that is always tangent to the local slope. Figure 2.8.3 shows four solutions starting from various points in the (t, x) plane.

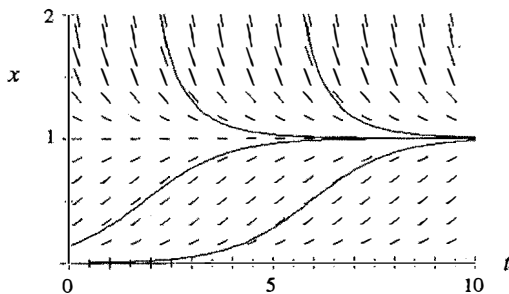


Figure 2.8.3

These numerical solutions were computed using the Runge–Kutta method with a

stepsize $\Delta t = 0.1$. The solutions have the shape expected from Section 2.3. ■

Computers are indispensable for studying dynamical systems. We will use them liberally throughout this book, and you should do likewise.

EXERCISES FOR CHAPTER 2

2.1 A Geometric Way of Thinking

In the next three exercises, interpret $\dot{x} = \sin x$ as a flow on the line.

2.1.1 Find all the fixed points of the flow.

2.1.2 At which points x does the flow have greatest velocity to the right?

2.1.3

a) Find the flow's acceleration \ddot{x} as a function of x .

b) Find the points where the flow has maximum positive acceleration.

2.1.4 (Exact solution of $\dot{x} = \sin x$) As shown in the text, $\dot{x} = \sin x$ has the solution $t = \ln|(\csc x_0 + \cot x_0)/(\csc x + \cot x)|$, where $x_0 = x(0)$ is the initial value of x .

a) Given the specific initial condition $x_0 = \pi/4$, show that the solution above can be inverted to obtain

$$x(t) = 2 \tan^{-1} \left(\frac{e^t}{1 + \sqrt{2}} \right).$$

Conclude that $x(t) \rightarrow \pi$ as $t \rightarrow \infty$, as claimed in Section 2.1. (You need to be good with trigonometric identities to solve this problem.)

b) Try to find the analytical solution for $x(t)$, given an *arbitrary* initial condition x_0 .

2.1.5 (A mechanical analog)

a) Find a mechanical system that is approximately governed by $\dot{x} = \sin x$.

b) Using your physical intuition, explain why it now becomes obvious that $x^* = 0$ is an unstable fixed point and $x^* = \pi$ is stable.

2.2 Fixed Points and Stability

Analyze the following equations graphically. In each case, sketch the vector field on the real line, find all the fixed points, classify their stability, and sketch the graph of $x(t)$ for different initial conditions. Then try for a few minutes to obtain the analytical solution for $x(t)$; if you get stuck, don't try for too long since in several cases it's impossible to solve the equation in closed form!

2.2.1 $\dot{x} = 4x^2 - 16$

2.2.3 $\dot{x} = x - x^3$

2.2.5 $\dot{x} = 1 + \frac{1}{2}\cos x$

2.2.7 $\dot{x} = e^x - \cos x$ (Hint: Sketch the graphs of e^x and $\cos x$ on the same axes, and look for intersections. You won't be able to find the fixed points explicitly, but you can still find the qualitative behavior.)

2.2.8 (Working backwards, from flows to equations) Given an equation $\dot{x} = f(x)$, we know how to sketch the corresponding flow on the real line. Here you are asked to solve the opposite problem: For the phase portrait shown in Figure 1, find an equation that is consistent with it. (There are an infinite number of correct answers—and wrong ones too.)



Figure 1

2.2.9 (Backwards again, now from solutions to equations) Find an equation $\dot{x} = f(x)$ whose solutions $x(t)$ are consistent with those shown in Figure 2.

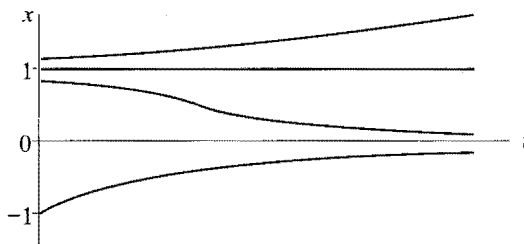


Figure 2

→ **2.2.10** (Fixed points) For each of (a)–(e), find an equation $\dot{x} = f(x)$ with the stated properties, or if there are no examples, explain why not. (In all cases, assume that $f(x)$ is a smooth function.)

- Every real number is a fixed point.
- Every integer is a fixed point, and there are no others.
- There are precisely three fixed points, and all of them are stable.
- There are no fixed points.
- There are precisely 100 fixed points.

2.2.11 (Analytical solution for charging capacitor) Obtain the analytical solution of the initial value problem $\dot{Q} = \frac{V_0}{R} - \frac{Q}{RC}$, with $Q(0) = 0$, which arose in Example 2.2.2.

2.2.12 (A nonlinear resistor) Suppose the resistor in Example 2.2.2 is replaced by a nonlinear resistor. In other words, this resistor does not have a linear

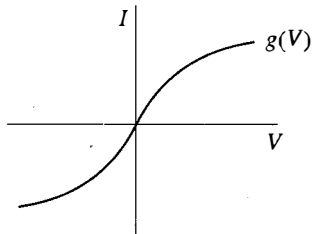


Figure 3

relation between voltage and current. Such non-linearity arises in certain solid-state devices. Instead of $I_R = V/R$, suppose we have $I_R = g(V)$, where $g(V)$ has the shape shown in Figure 3.

Redo Example 2.2.2 in this case. Derive the circuit equations, find all the fixed points, and analyze their stability. What qualitative effects does the nonlinearity introduce (if any)?

2.2.13 (Terminal velocity) The velocity $v(t)$ of a skydiver falling to the ground is governed by $m\dot{v} = mg - kv^2$, where m is the mass of the skydiver, g is the acceleration due to gravity, and $k > 0$ is a constant related to the amount of air resistance.

- Obtain the analytical solution for $v(t)$, assuming that $v(0) = 0$.
- Find the limit of $v(t)$ as $t \rightarrow \infty$. This limiting velocity is called the *terminal velocity*. (Beware of bad jokes about the word *terminal* and parachutes that fail to open.)
- Give a graphical analysis of this problem, and thereby re-derive a formula for the terminal velocity.
- An experimental study (Carlson et al. 1942) confirmed that the equation $m\dot{v} = mg - kv^2$ gives a good quantitative fit to data on human skydivers. Six men were dropped from altitudes varying from 10,600 feet to 31,400 feet to a terminal altitude of 2,100 feet, at which they opened their parachutes. The long free fall from 31,400 to 2,100 feet took 116 seconds. The average weight of the men and their equipment was 261.2 pounds. In these units, $g = 32.2 \text{ ft/sec}^2$. Compute the average velocity V_{avg} .
- Using the data given here, estimate the terminal velocity, and the value of the drag constant k . (Hints: First you need to find an exact formula for $s(t)$, the distance fallen, where $s(0) = 0$, $\dot{s} = v$, and $v(t)$ is known from part (a). You should get $s(t) = \frac{V^2}{g} \ln(\cosh \frac{gt}{V})$, where V is the terminal velocity. Then solve for V graphically or numerically, using $s = 29,300$, $t = 116$, and $g = 32.2$.)

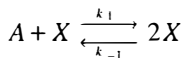
A slicker way to estimate V is to suppose $V \approx V_{\text{avg}}$, as a rough first approximation. Then show that $gt/V \approx 15$. Since $gt/V \gg 1$, we may use the approximation $\ln(\cosh x) \approx x - \ln 2$ for $x \gg 1$. Derive this approximation and then use it to obtain an analytical estimate of V . Then k follows from part (b). This analysis is from Davis (1962).

2.3 Population Growth

2.3.1 (Exact solution of logistic equation) There are two ways to solve the logistic equation $\dot{N} = rN(1 - N/K)$ analytically for an arbitrary initial condition N_0 .

- Separate variables and integrate, using partial fractions.
- Make the change of variables $x = 1/N$. Then derive and solve the resulting differential equation for x .

2.3.2 (Autocatalysis) Consider the model chemical reaction



in which one molecule of X combines with one molecule of A to form two molecules of X . This means that the chemical X stimulates its own production, a process called *autocatalysis*. This positive feedback process leads to a chain reaction, which eventually is limited by a “back reaction” in which $2X$ returns to $A + X$.

According to the *law of mass action* of chemical kinetics, the rate of an elementary reaction is proportional to the product of the concentrations of the reactants. We denote the concentrations by lowercase letters $x = [X]$ and $a = [A]$. Assume that there’s an enormous surplus of chemical A , so that its concentration a can be regarded as constant. Then the equation for the kinetics of x is

$$\dot{x} = k_1 ax - k_{-1} x^2$$

where k_1 and k_{-1} are positive parameters called *rate constants*.

- Find all the fixed points of this equation and classify their stability.
- Sketch the graph of $x(t)$ for various initial values x_0 .

2.3.3 (Tumor growth) The growth of cancerous tumors can be modeled by the Gompertz law $\dot{N} = -aN \ln(bN)$, where $N(t)$ is proportional to the number of cells in the tumor, and $a, b > 0$ are parameters.

- Interpret a and b biologically.
- Sketch the vector field and then graph $N(t)$ for various initial values.

The predictions of this simple model agree surprisingly well with data on tumor growth, as long as N is not too small; see Aroesty et al. (1973) and Newton (1980) for examples.

2.3.4 (The Allee effect) For certain species of organisms, the effective growth rate \dot{N}/N is highest at intermediate N . This is called the Allee effect (Edelstein-Keshet 1988). For example, imagine that it is too hard to find mates when N is very small, and there is too much competition for food and other resources when N is large.

- Show that $\dot{N}/N = r - a(N - b)^2$ provides an example of Allee effect, if r , a , and b satisfy certain constraints, to be determined.
- Find all the fixed points of the system and classify their stability.
- Sketch the solutions $N(t)$ for different initial conditions.
- Compare the solutions $N(t)$ to those found for the logistic equation. What are the qualitative differences, if any?

2.4 Linear Stability Analysis

Use linear stability analysis to classify the fixed points of the following systems. If linear stability analysis fails because $f'(x^*) = 0$, use a graphical argument to decide the stability.

2.4.1 $\dot{x} = x(1-x)$

2.4.2 $\dot{x} = x(1-x)(2-x)$

2.4.3 $\dot{x} = \tan x$

2.4.4 $\dot{x} = x^2(6-x)$

2.4.5 $\dot{x} = 1 - e^{-x^2}$

2.4.6 $\dot{x} = \ln x$

2.4.7 $\dot{x} = ax - x^3$, where a can be positive, negative, or zero. Discuss all three cases.

2.4.8 Using linear stability analysis, classify the fixed points of the Gompertz model of tumor growth $\dot{N} = -aN \ln(bN)$. (As in Exercise 2.3.3, $N(t)$ is proportional to the number of cells in the tumor and $a, b > 0$ are parameters.)

→ **2.4.9** (Critical slowing down) In statistical mechanics, the phenomenon of “critical slowing down” is a signature of a second-order phase transition. At the transition, the system relaxes to equilibrium much more slowly than usual. Here’s a mathematical version of the effect:

- Obtain the analytical solution to $\dot{x} = -x^3$ for an arbitrary initial condition. Show that $x(t) \rightarrow 0$ as $t \rightarrow \infty$, but that the decay is not exponential. (You should find that the decay is a much slower algebraic function of t .)
- To get some intuition about the slowness of the decay, make a numerically accurate plot of the solution for the initial condition $x_0 = 10$, for $0 \leq t \leq 10$. Then, on the same graph, plot the solution to $\dot{x} = -x$ for the same initial condition.

2.5 Existence and Uniqueness

2.5.1 (Reaching a fixed point in a finite time) A particle travels on the half-line $x \geq 0$ with a velocity given by $\dot{x} = -x^c$, where c is real and constant.

- Find all values of c such that the origin $x = 0$ is a stable fixed point.
- Now assume that c is chosen such that $x = 0$ is stable. Can the particle ever reach the origin in a *finite* time? Specifically, how long does it take for the particle to travel from $x = 1$ to $x = 0$, as a function of c ?

2.5.2 (“Blow-up”: Reaching infinity in a finite time) Show that the solution to $\dot{x} = 1 + x^{10}$ escapes to $+\infty$ in a finite time, starting from any initial condition. (Hint: Don’t try to find an exact solution; instead, compare the solutions to those of $\dot{x} = 1 + x^2$.)

2.5.3 Consider the equation $\dot{x} = rx + x^3$, where $r > 0$ is fixed. Show that $x(t) \rightarrow \pm\infty$ in finite time, starting from any initial condition $x_0 \neq 0$.

2.5.4 (Infinitely many solutions with the same initial condition) Show that the initial value problem $\dot{x} = x^{1/3}$, $x(0) = 0$, has an infinite number of solutions. (Hint:

Construct a solution that stays at $x = 0$ until some arbitrary time t_0 , after which it takes off.)

2.5.5 (A general example of non-uniqueness) Consider the initial value problem $\dot{x} = |x|^{p/q}$, $x(0) = 0$, where p and q are positive integers with no common factors.

- Show that there are an infinite number of solutions if $p < q$.
- Show that there is a unique solution if $p > q$.

2.5.6 (The leaky bucket) The following example (Hubbard and West 1991, p. 159) shows that in some physical situations, non-uniqueness is natural and obvious, not pathological.

Consider a water bucket with a hole in the bottom. If you see an empty bucket with a puddle beneath it, can you figure out when the bucket was full? No, of course not! It could have finished emptying a minute ago, ten minutes ago, or whatever. The solution to the corresponding differential equation must be non-unique when integrated backwards in time.

Here's a crude model of the situation. Let $h(t)$ = height of the water remaining in the bucket at time t ; a = area of the hole; A = cross-sectional area of the bucket (assumed constant); $v(t)$ = velocity of the water passing through the hole.

- Show that $av(t) = Ah(t)$. What physical law are you invoking?
- To derive an additional equation, use conservation of energy. First, find the change in potential energy in the system, assuming that the height of the water in the bucket decreases by an amount Δh and that the water has density ρ . Then find the kinetic energy transported out of the bucket by the escaping water. Finally, assuming all the potential energy is converted into kinetic energy, derive the equation $v^2 = 2gh$.
- Combining (b) and (c), show $\dot{h} = -C\sqrt{h}$, where $C = \sqrt{2g}(\frac{a}{A})$.
- Given $h(0) = 0$ (bucket empty at $t = 0$), show that the solution for $h(t)$ is non-unique *in backwards time*, i.e., for $t < 0$.

2.6 Impossibility of Oscillations

2.6.1 Explain this paradox: a simple harmonic oscillator $m\ddot{x} = -kx$ is a system that oscillates in one dimension (along the x -axis). But the text says one-dimensional systems can't oscillate.

→ **2.6.2** (No periodic solutions to $\dot{x} = f(x)$) Here's an analytic proof that periodic solutions are impossible for a vector field on a line. Suppose on the contrary that $x(t)$ is a nontrivial periodic solution, i.e., $x(t) = x(t + T)$ for some $T > 0$, and $x(t) \neq x(t + s)$ for all $0 < s < T$. Derive a contradiction by considering

$$\int_t^{t+T} f(x) \frac{dx}{dt} dt.$$

2.7 Potentials

For each of the following vector fields, plot the potential function $V(x)$ and identify all the equilibrium points and their stability.

2.7.1 $\dot{x} = x(1-x)$

2.7.2 $\dot{x} = 3$

2.7.3 $\dot{x} = \sin x$

2.7.4 $\dot{x} = 2 + \sin x$

2.7.5 $\dot{x} = -\sinh x$

2.7.6 $\dot{x} = r + x - x^3$, for various values of r .

2.7.7 (Another proof that solutions to $\dot{x} = f(x)$ can't oscillate) Let $\dot{x} = f(x)$ be a vector field on the line. Use the existence of a potential function $V(x)$ to show that solutions $x(t)$ cannot oscillate.

2.8 Solving Equations on the Computer

2.8.1 (Slope field) The slope is constant along horizontal lines in Figure 2.8.2. Why should we have expected this?

2.8.2 Sketch the slope field for the following differential equations. Then “integrate” the equation manually by drawing trajectories that are everywhere parallel to the local slope.

a) $\dot{x} = x$ b) $\dot{x} = 1 - x^2$ c) $\dot{x} = 1 - 4x(1-x)$ d) $\dot{x} = \sin x$

→ **2.8.3** (Calibrating the Euler method) The goal of this problem is to test the Euler method on the initial value problem $\dot{x} = -x$, $x(0) = 1$.

- Solve the problem analytically. What is the exact value of $x(1)$?
- Using the Euler method with step size $\Delta t = 1$, estimate $x(1)$ numerically—call the result $\hat{x}(1)$. Then repeat, using $\Delta t = 10^{-n}$, for $n = 1, 2, 3, 4$.
- Plot the error $E = |\hat{x}(1) - x(1)|$ as a function of Δt . Then plot $\ln E$ vs. $\ln t$. Explain the results.

→ **2.8.4** Redo Exercise 2.8.3, using the improved Euler method.

→ **2.8.5** Redo Exercise 2.8.3, using the Runge–Kutta method.

2.8.6 (Analytically intractable problem) Consider the initial value problem $\dot{x} = x + e^{-x}$, $x(0) = 0$. In contrast to Exercise 2.8.3, this problem can't be solved analytically.

- Sketch the solution $x(t)$ for $t \geq 0$.
- Using some analytical arguments, obtain rigorous bounds on the value of x at $t = 1$. In other words, prove that $a < x(1) < b$, for a, b to be determined. By being clever, try to make a and b as close together as possible. (Hint: Bound the given vector field by approximate vector fields that can be integrated analytically.)
- Now for the numerical part: Using the Euler method, compute x at $t = 1$, correct to three decimal places. How small does the stepsize need to be to obtain the desired accuracy? (Give the order of magnitude, not the exact number.)

- d) Repeat part (b), now using the Runge–Kutta method. Compare the results for stepsizes $\Delta t = 1$, $\Delta t = 0.1$, and $\Delta t = 0.01$.

2.8.7 (Error estimate for Euler method) In this question you'll use Taylor series expansions to estimate the error in taking one step by the Euler method. The exact solution and the Euler approximation both start at $x = x_0$ when $t = t_0$. We want to compare the exact value $x(t_1) \equiv x(t_0 + \Delta t)$ with the Euler approximation $x_1 = x_0 + f(x_0)\Delta t$.

- a) Expand $x(t_1) \equiv x(t_0 + \Delta t)$ as a Taylor series in Δt , through terms of $O(\Delta t^2)$. Express your answer solely in terms of x_0 , Δt , and f and its derivatives at x_0 .
b) Show that the local error $|x(t_1) - x_1| \sim C(\Delta t)^2$ and give an explicit expression for the constant C . (Generally one is more interested in the global error incurred after integrating over a time interval of fixed length $T = n\Delta t$. Since each step produces an $O(\Delta t)^2$ error, and we take $n = T/\Delta t = O(\Delta t^{-1})$ steps, the global error $|x(t_n) - x_n|$ is $O(\Delta t)$, as claimed in the text.)

2.8.8 (Error estimate for the improved Euler method) Use the Taylor series arguments of Exercise 2.8.7 to show that the local error for the improved Euler method is $O(\Delta t^3)$.

2.8.9 (Error estimate for Runge–Kutta) Show that the Runge–Kutta method produces a local error of size $O(\Delta t^5)$.

(Warning: This calculation involves massive amounts of algebra, but if you do it correctly, you'll be rewarded by seeing many wonderful cancellations. Teach yourself *Mathematica*, *Maple*, or some other symbolic manipulation language, and do the problem on the computer.)

3

BIFURCATIONS

3.0 Introduction

As we've seen in Chapter 2, the dynamics of vector fields on the line is very limited: all solutions either settle down to equilibrium or head out to $\pm\infty$. Given the triviality of the dynamics, what's interesting about one-dimensional systems? Answer: *Dependence on parameters*. The qualitative structure of the flow can change as parameters are varied. In particular, fixed points can be created or destroyed, or their stability can change. These qualitative changes in the dynamics are called **bifurcations**, and the parameter values at which they occur are called **bifurcation points**.

Bifurcations are important scientifically—they provide models of transitions and instabilities as some *control parameter* is varied. For example, consider the buckling of a beam. If a small weight is placed on top of the beam in Figure 3.0.1, the beam can support the load and remain vertical. But if the load is too heavy, the vertical position becomes unstable, and the beam may buckle.

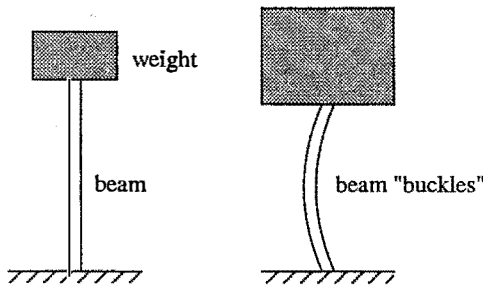


Figure 3.0.1

Here the weight plays the role of the control parameter, and the deflection of the beam from vertical plays the role of the dynamical variable x .

One of the main goals of this book is to help you develop a solid and practical understanding of bifurcations. This chapter introduces the simplest examples: bifurcations of fixed points for flows on the line. We'll use these bifurcations to model such dramatic phenomena as the onset of coherent radiation in a laser and the outbreak of an insect population. (In later chapters, when we step up to two- and three-dimensional phase spaces, we'll explore additional types of bifurcations and their scientific applications.)

We begin with the most fundamental bifurcation of all.

3.1 Saddle-Node Bifurcation

The saddle-node bifurcation is the basic mechanism by which fixed points are *created and destroyed*. As a parameter is varied, two fixed points move toward each other, collide, and mutually annihilate.

The prototypical example of a saddle-node bifurcation is given by the first-order system

$$\dot{x} = r + x^2 \quad (1)$$

where r is a parameter, which may be positive, negative, or zero. When r is negative, there are two fixed points, one stable and one unstable (Figure 3.1.1a).

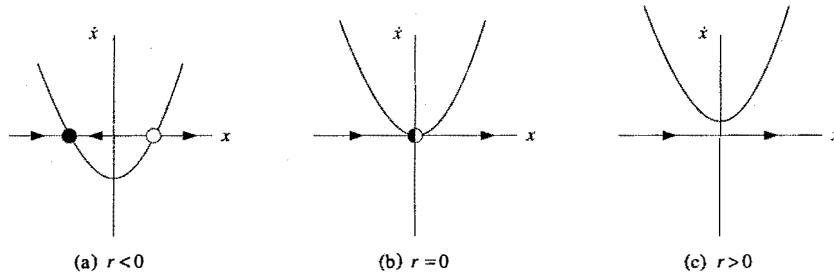


Figure 3.1.1

As r approaches 0 from below, the parabola moves up and the two fixed points move toward each other. When $r = 0$, the fixed points coalesce into a half-stable fixed point at $x^* = 0$ (Figure 3.1.1b). This type of fixed point is extremely delicate—it vanishes as soon as $r > 0$, and now there are no fixed points at all (Figure 3.1.1c).

In this example, we say that a *bifurcation* occurred at $r = 0$, since the vector fields for $r < 0$ and $r > 0$ are qualitatively different.

Graphical Conventions

There are several other ways to depict a saddle-node bifurcation. We can show a stack of vector fields for discrete values of r (Figure 3.1.2).

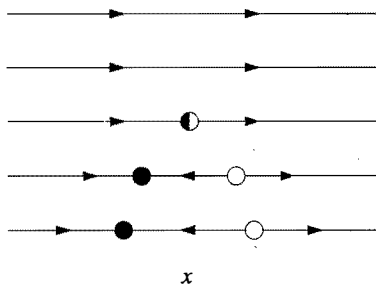


Figure 3.1.2

This representation emphasizes the dependence of the fixed points on r . In the limit of a *continuous* stack of vector fields, we have a picture like Figure 3.1.3. The curve shown is $r = -x^2$, i.e., $\dot{x} = 0$, which gives the fixed points for different r . To distinguish between stable and unstable fixed points, we use a solid line for stable points and a broken line for unstable ones.

However, the most common way to depict the bifurcation is to invert the axes of Figure 3.1.3. The rationale is that r plays the role of an independent variable, and so should be plotted horizontally

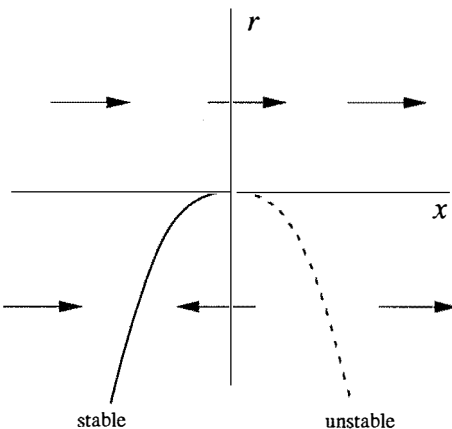


Figure 3.1.3

(Figure 3.1.4). The drawback is that now the x -axis has to be plotted vertically, which looks strange at first. Arrows are sometimes included in the picture, but not

always. This picture is called the **bifurcation diagram** for the saddle-node bifurcation.

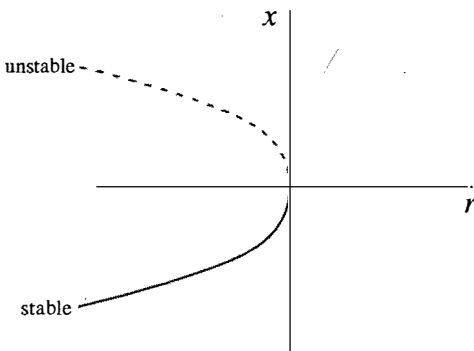


Figure 3.1.4

Terminology

Bifurcation theory is rife with conflicting terminology. The subject really hasn't settled down yet, and different people use different words for the same thing. For example, the saddle-node bifurcation

is sometimes called a *fold bifurcation* (because the curve in Figure 3.1.4 has a fold in it) or a *turning-point bifurcation* (because the point $(x, r) = (0, 0)$ is a “turning point.”) Admittedly, the term *saddle-node* doesn’t make much sense for vector fields on the line. The name derives from a completely analogous bifurcation seen in a higher-dimensional context, such as vector fields on the plane, where fixed points known as saddles and nodes can collide and annihilate (see Section 8.1).

The prize for most inventive terminology must go to Abraham and Shaw (1988), who write of a *blue sky bifurcation*. This term comes from viewing a saddle-node bifurcation in the other direction: a pair of fixed points appears “out of the clear blue sky” as a parameter is varied. For example, the vector field

$$\dot{x} = r - x^2 \quad (2)$$

has no fixed points for $r < 0$, but then one materializes when $r = 0$ and splits into two when $r > 0$ (Figure 3.1.5). Incidentally, this example also explains why we use the word “bifurcation”: it means “splitting into two branches.”

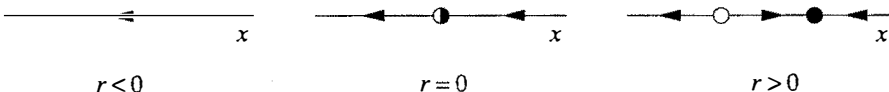


Figure 3.1.5

EXAMPLE 3.1.1:

Give a linear stability analysis of the fixed points in Figure 3.1.5.

Solution: The fixed points for $\dot{x} = f(x) = r - x^2$ are given by $x^* = \pm\sqrt{r}$. There are two fixed points for $r \geq 0$, and none for $r < 0$. To determine linear stability, we compute $f'(x^*) = -2x^*$. Thus $x^* = +\sqrt{r}$ is stable, since $f'(x^*) < 0$. Similarly $x^* = -\sqrt{r}$ is unstable. At the bifurcation point $r = 0$, we find $f'(x^*) = 0$; the linearization vanishes when the fixed points coalesce. ■

EXAMPLE 3.1.2:

Show that the first-order system $\dot{x} = r - x - e^{-x}$ undergoes a saddle-node bifurcation as r is varied, and find the value of r at the bifurcation point.

Solution: The fixed points satisfy $f(x) = r - x - e^{-x} = 0$. But now we run into a difficulty—in contrast to Example 3.1.1, we can’t find the fixed points explicitly as a function of r . Instead we adopt a geometric approach. One method would be to graph the function $f(x) = r - x - e^{-x}$ for different values of r , look for its roots x^* , and then sketch the vector field on the x -axis. This method is

fine, but there's an easier way. The point is that the two functions $r - x$ and e^{-x} have much more familiar graphs than their difference $r - x - e^{-x}$. So we plot $r - x$ and e^{-x} on the same picture (Figure 3.1.6a). Where the line $r - x$ intersects the curve e^{-x} , we have $r - x = e^{-x}$ and so $f(x) = 0$. Thus, *intersections of the line and the curve correspond to fixed points for the system*. This picture also allows us to read off the direction of flow on the x -axis: the flow is to the right where the line lies above the curve, since $r - x > e^{-x}$ and therefore $\dot{x} > 0$. Hence, the fixed point on the right is stable, and the one on the left is unstable.

Now imagine we start decreasing the parameter r . The line $r - x$ slides down and the fixed points approach each other. At some critical value $r = r_c$, the line becomes *tangent* to the curve and the fixed points coalesce in a saddle-node bifurcation (Figure 3.1.6b). For r below this critical value, the line lies below the curve and there are no fixed points (Figure 3.1.6c).

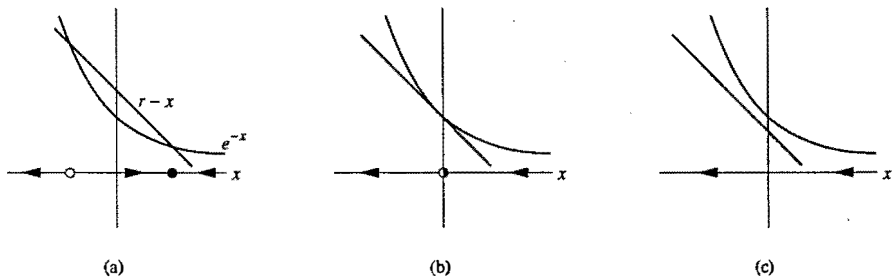


Figure 3.1.6

To find the bifurcation point r_c , we impose the condition that the graphs of $r - x$ and e^{-x} intersect *tangentially*. Thus we demand equality of the functions *and* their derivatives:

$$e^{-x} = r - x$$

and

$$\frac{d}{dx} e^{-x} = \frac{d}{dx}(r - x).$$

The second equation implies $-e^{-x} = -1$, so $x = 0$. Then the first equation yields $r = 1$. Hence the bifurcation point is $r_c = 1$, and the bifurcation occurs at $x = 0$. ■

Normal Forms

In a certain sense, the examples $\dot{x} = r - x^2$ or $\dot{x} = r + x^2$ are representative of *all* saddle-node bifurcations; that's why we called them "prototypical." The idea is that, close to a saddle-node bifurcation, the dynamics typically look like $\dot{x} = r - x^2$ or $\dot{x} = r + x^2$.

For instance, consider Example 3.1.2 near the bifurcation at $x=0$ and $r=1$. Using the Taylor expansion for e^{-x} about $x=0$, we find

$$\begin{aligned}\dot{x} &= r - x - e^{-x} \\ &= r - x - \left[1 - x + \frac{x^2}{2!} + \dots \right] \\ &= (r-1) - \frac{x^2}{2} + \dots\end{aligned}$$

to leading order in x . This has the same algebraic form as $\dot{x} = r - x^2$, and can be made to agree exactly by appropriate rescalings of x and r .

It's easy to understand why saddle-node bifurcations typically have this algebraic form. We just ask ourselves: how can two fixed points of $\dot{x} = f(x)$ collide and disappear as a parameter r is varied? Graphically, fixed points occur where the graph of $f(x)$ intersects the x -axis. For a saddle-node bifurcation to be possible, we need two nearby roots of $f(x)$; this means $f(x)$ must look locally "bowl-shaped" or parabolic (Figure 3.1.7).

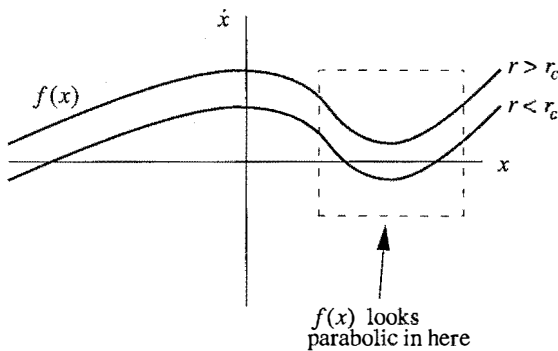


Figure 3.1.7

Now we use a microscope to zoom in on the behavior near the bifurcation. As r varies, we see a parabola intersecting the x -axis, then becoming tangent to it, and then failing to intersect. This is exactly the scenario in the prototypical Figure 3.1.1.

Here's a more algebraic version of the same argument. We regard f as a function of both x and r , and examine the behavior of $\dot{x} = f(x, r)$ near the bifurcation at $x = x^*$ and $r = r_c$. Taylor's expansion yields

$$\begin{aligned}\dot{x} &= f(x, r) \\ &= f(x^*, r_c) + (x - x^*) \frac{\partial f}{\partial x} \Big|_{(x^*, r_c)} + (r - r_c) \frac{\partial f}{\partial r} \Big|_{(x^*, r_c)} + \frac{1}{2} (x - x^*)^2 \frac{\partial^2 f}{\partial x^2} \Big|_{(x^*, r_c)} + \dots\end{aligned}$$

where we have neglected quadratic terms in $(r - r_c)$ and cubic terms in $(x - x^*)$. Two of the terms in this equation vanish: $f(x^*, r_c) = 0$ since x^* is a fixed point, and $\partial f / \partial x|_{(x^*, r_c)} = 0$ by the tangency condition of a saddle-node bifurcation. Thus

$$\dot{x} = a(r - r_c) + b(x - x^*)^2 + \dots \quad (3)$$

where $a = \partial f / \partial r|_{(x^*, r_c)}$ and $b = \frac{1}{2} \partial^2 f / \partial x^2|_{(x^*, r_c)}$. Equation (3) agrees with the form of our prototypical examples. (We are assuming that $a, b \neq 0$, which is the typical case; for instance, it would be a very special situation if the second derivative $\partial^2 f / \partial x^2$ also happened to vanish at the fixed point.)

What we have been calling prototypical examples are more conventionally known as ***normal forms*** for the saddle-node bifurcation. There is much, much more to normal forms than we have indicated here. We will be seeing their importance throughout this book. For a more detailed and precise discussion, see Guckenheimer and Holmes (1983) or Wiggins (1990).

3.2 Transcritical Bifurcation

There are certain scientific situations where a fixed point must exist for all values of a parameter and can never be destroyed. For example, in the logistic equation and other simple models for the growth of a single species, there is a fixed point at zero population, regardless of the value of the growth rate. However, such a fixed point may *change its stability* as the parameter is varied. The transcritical bifurcation is the standard mechanism for such changes in stability.

The normal form for a transcritical bifurcation is

$$\dot{x} = rx - x^2. \quad (1)$$

This looks like the logistic equation of Section 2.3, but now we allow x and r to be either positive or negative.

Figure 3.2.1 shows the vector field as r varies. Note that there is a fixed point at $x^* = 0$ for *all* values of r .

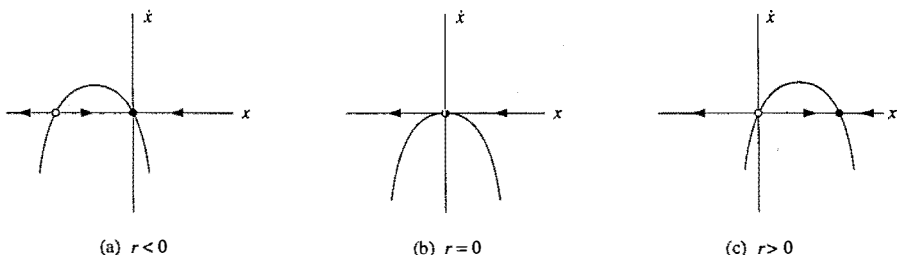


Figure 3.2.1

For $r < 0$, there is an unstable fixed point at $x^* = r$ and a stable fixed point at $x^* = 0$. As r increases, the unstable fixed point approaches the origin, and coalesces with it when $r = 0$. Finally, when $r > 0$, the origin has become unstable, and $x^* = r$ is now stable. Some people say that an *exchange of stabilities* has taken place between the two fixed points.

Please note the important difference between the saddle-node and transcritical bifurcations: in the transcritical case, the two fixed points don't disappear after the bifurcation—instead they just switch their stability.

Figure 3.2.2 shows the bifurcation diagram for the transcritical bifurcation. As in Figure 3.1.4, the parameter r is regarded as the independent variable, and the fixed points $x^* = 0$ and $x^* = r$ are shown as dependent variables.

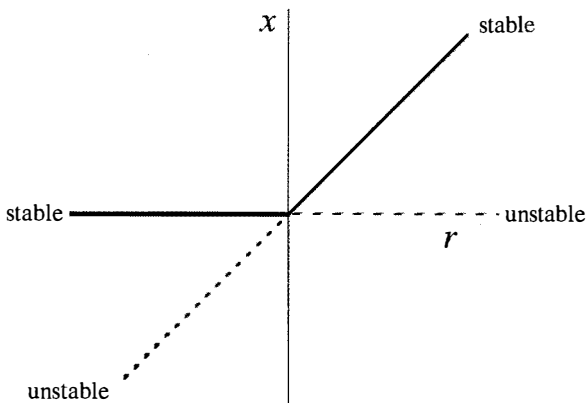


Figure 3.2.2

EXAMPLE 3.2.1:

Show that the first-order system $\dot{x} = x(1 - x^2) - a(1 - e^{-bx})$ undergoes a transcritical bifurcation at $x = 0$ when the parameters a, b satisfy a certain equation, to be determined. (This equation defines a *bifurcation curve* in the (a, b) parameter space.) Then find an approximate formula for the fixed point that bifurcates from $x = 0$, assuming that the parameters are close to the bifurcation curve.

Solution: Note that $x = 0$ is a fixed point for all (a, b) . This makes it plausible that the fixed point will bifurcate transcritically, if it bifurcates at all. For small x , we find

$$\begin{aligned} 1 - e^{-bx} &= 1 - [1 - bx + \frac{1}{2}b^2x^2 + O(x^3)] \\ &= bx - \frac{1}{2}b^2x^2 + O(x^3) \end{aligned}$$

and so

$$\begin{aligned} \dot{x} &= x - a(bx - \frac{1}{2}b^2x^2) + O(x^3) \\ &= (1 - ab)x + (\frac{1}{2}ab^2)x^2 + O(x^3). \end{aligned}$$

Hence a transcritical bifurcation occurs when $ab = 1$; this is the equation for the bifurcation curve. The nonzero fixed point is given by the solution of $1 - ab + (\frac{1}{2}ab^2)x \approx 0$, i.e.,

$$x^* \approx \frac{2(ab-1)}{ab^2}.$$

This formula is approximately correct only if x^* is small, since our series expansions are based on the assumption of small x . Thus the formula holds only when ab is close to 1, which means that the parameters must be close to the bifurcation curve. ■

EXAMPLE 3.2.2:

Analyze the dynamics of $\dot{x} = r \ln x + x - 1$ near $x = 1$, and show that the system undergoes a transcritical bifurcation at a certain value of r . Then find new variables X and R such that the system reduces to the approximate normal form $\dot{X} \approx RX - X^2$ near the bifurcation.

Solution: First note that $x = 1$ is a fixed point for all values of r . Since we are interested in the dynamics near this fixed point, we introduce a new variable $u = x - 1$, where u is small. Then

$$\begin{aligned}\dot{u} &= \dot{x} \\ &= r \ln(1+u) + u \\ &= r \left[u - \frac{1}{2}u^2 + O(u^3) \right] + u \\ &\approx (r+1)u - \frac{1}{2}ru^2 + O(u^3).\end{aligned}$$

Hence a transcritical bifurcation occurs at $r_c = -1$.

To put this equation into normal form, we first need to get rid of the coefficient of u^2 . Let $u = av$, where a will be chosen later. Then the equation for v is

$$\dot{v} = (r+1)v - (\frac{1}{2}ra)v^2 + O(v^3).$$

So if we choose $a = 2/r$, the equation becomes

$$\dot{v} = (r+1)v - v^2 + O(v^3).$$

Now if we let $R = r+1$ and $X = v$, we have achieved the approximate normal form $\dot{X} \approx RX - X^2$, where cubic terms of order $O(X^3)$ have been neglected. In terms of the original variables, $X = v = u/a = \frac{1}{2}r(x-1)$. ■

To be a bit more accurate, the theory of normal forms assures us that we can find a change of variables such that the system becomes $\dot{X} = RX - X^2$, with *strict*, rather than approximate, equality. Our solution above gives an approximation to the necessary change of variables. If we wanted a better approximation, we would

retain the cubic terms in the series expansions (and perhaps even higher-order terms if we're really feeling heroic) and we would have to do a more elaborate calculation to eliminate these higher-order terms. See Exercises 3.2.6 and 3.2.7 for a taste of such calculations, or see the books of Guckenheimer and Holmes (1983), Wiggins (1990), or Manneville (1990).

3.3 Laser Threshold

Now it's time to apply our mathematics to a scientific example. We analyze an extremely simplified model for a laser, following the treatment given by Haken (1983).

Physical Background

We are going to consider a particular type of laser known as a solid-state laser, which consists of a collection of special "laser-active" atoms embedded in a solid-state matrix, bounded by partially reflecting mirrors at either end. An external energy source is used to excite or "pump" the atoms out of their ground states (Figure 3.3.1).

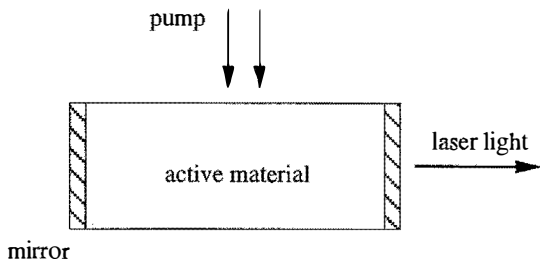


Figure 3.3.1

Each atom can be thought of as a little antenna radiating energy. When the pumping is relatively weak, the laser acts just like an ordinary *lamp*: the excited atoms oscillate independently of one another and emit randomly phased light waves.

Now suppose we increase the strength of the pumping. At first nothing different happens, but then suddenly, when the pump strength exceeds a certain threshold, the atoms begin to oscillate in phase—the lamp has turned into a *laser*. Now the trillions of little antennas act like one giant antenna and produce a beam of radiation that is much more coherent and intense than that produced below the laser threshold.

This sudden onset of coherence is amazing, considering that the atoms are being excited completely at random by the pump! Hence the process is *self-organizing*: the coherence develops because of a cooperative interaction among the atoms themselves.

Model

A proper explanation of the laser phenomenon would require us to delve into quantum mechanics. See Milonni and Eberly (1988) for an intuitive discussion.

Instead we consider a simplified model of the essential physics (Haken 1983, p. 127). The dynamical variable is the number of photons $n(t)$ in the laser field. Its rate of change is given by

$$\begin{aligned}\dot{n} &= \text{gain} - \text{loss} \\ &= Gn - kn.\end{aligned}$$

The gain term comes from the process of *stimulated emission*, in which photons stimulate excited atoms to emit additional photons. Because this process occurs via random encounters between photons and excited atoms, it occurs at a rate proportional to n and to the number of excited atoms, denoted by $N(t)$. The parameter $G > 0$ is known as the gain coefficient. The loss term models the escape of photons through the endfaces of the laser. The parameter $k > 0$ is a rate constant; its reciprocal $\tau = 1/k$ represents the typical lifetime of a photon in the laser.

Now comes the key physical idea: after an excited atom emits a photon, it drops down to a lower energy level and is no longer excited. Thus N decreases by the emission of photons. To capture this effect, we need to write an equation relating N to n . Suppose that in the absence of laser action, the pump keeps the number of excited atoms fixed at N_0 . Then the *actual* number of excited atoms will be reduced by the laser process. Specifically, we assume

$$N(t) = N_0 - \alpha n,$$

where $\alpha > 0$ is the rate at which atoms drop back to their ground states. Then

$$\begin{aligned}\dot{n} &= Gn(N_0 - \alpha n) - kn \\ &= (GN_0 - k)n - (\alpha G)n^2.\end{aligned}$$

We're finally on familiar ground—this is a first-order system for $n(t)$. Figure 3.3.2 shows the corresponding vector field for different values of the pump strength N_0 . Note that only positive values of n are physically meaningful.

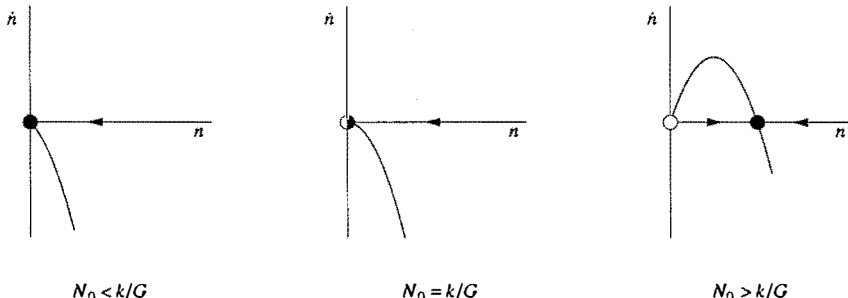


Figure 3.3.2

When $N_0 < k/G$, the fixed point at $n^* = 0$ is stable. This means that there is no stimulated emission and the laser acts like a lamp. As the pump strength N_0 is increased, the system undergoes a transcritical bifurcation when $N_0 = k/G$. For $N_0 > k/G$, the origin loses stability and a stable fixed point appears at $n^* = (GN_0 - k)/\alpha G > 0$, corresponding to spontaneous laser action. Thus $N_0 = k/G$ can be interpreted as the ***laser threshold*** in this model. Figure 3.3.3 summarizes our results.

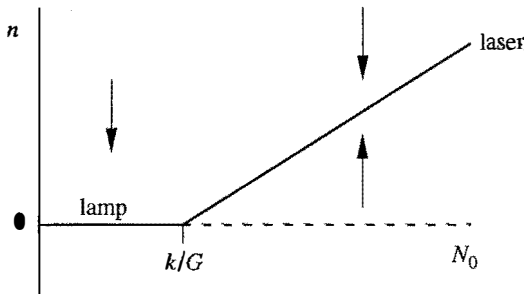


Figure 3.3.3

Although this model correctly predicts the existence of a threshold, it ignores the dynamics of the excited atoms, the existence of spontaneous emission, and several other complications. See Exercises 3.3.1 and 3.3.2 for improved models.

3.4 Pitchfork Bifurcation

We turn now to a third kind of bifurcation, the so-called pitchfork bifurcation. This bifurcation is common in physical problems that have a ***symmetry***. For example, many problems have a spatial symmetry between left and right. In such cases, fixed points tend to appear and disappear in symmetrical pairs. In the buckling example of Figure 3.0.1, the beam is stable in the vertical position if the load is small. In this case there is a stable fixed point corresponding to zero deflection. But if the load exceeds the buckling threshold, the beam may buckle to either the left or the right. The vertical position has gone unstable, and two new symmetrical fixed points, corresponding to left- and right-buckled configurations, have been born.

There are two very different types of pitchfork bifurcation. The simpler type is called ***supercritical***, and will be discussed first.

Supercritical Pitchfork Bifurcation

The normal form of the supercritical pitchfork bifurcation is

$$\dot{x} = rx - x^3. \quad (I)$$

Note that this equation is *invariant* under the change of variables $x \rightarrow -x$. That is, if we replace x by $-x$ and then cancel the resulting minus signs on both sides of the equation, we get (1) back again. This invariance is the mathematical expression of the left-right symmetry mentioned earlier. (More technically, one says that the vector field is *equivariant*, but we'll use the more familiar language.)

Figure 3.4.1 shows the vector field for different values of r .

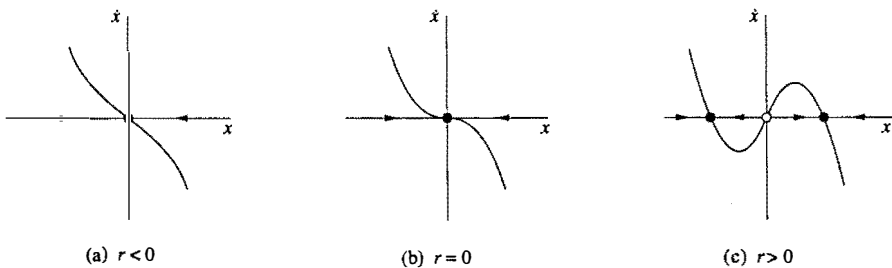


Figure 3.4.1

When $r < 0$, the origin is the only fixed point, and it is stable. When $r = 0$, the origin is still stable, but much more weakly so, since the linearization vanishes. Now solutions no longer decay exponentially fast—instead the decay is a much slower algebraic function of time (recall Exercise 2.4.9). This lethargic decay is called *critical slowing down* in the physics literature. Finally, when $r > 0$, the origin has become unstable. Two new stable fixed points appear on either side of the origin, symmetrically located at $x^* = \pm\sqrt{r}$.

The reason for the term “pitchfork” becomes clear when we plot the bifurcation diagram (Figure 3.4.2). Actually, pitchfork trifurcation might be a better word!

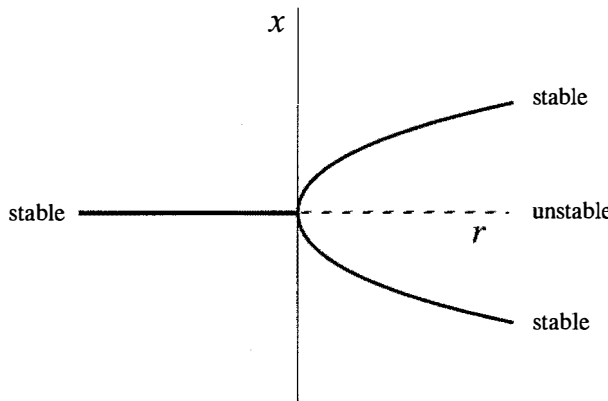


Figure 3.4.2

EXAMPLE 3.4.1:

Equations similar to $\dot{x} = -x + \beta \tanh x$ arise in statistical mechanical models of magnets and neural networks (see Exercise 3.6.7 and Palmer 1989). Show that this equation undergoes a supercritical pitchfork bifurcation as β is varied. Then give a *numerically accurate* plot of the fixed points for each β .

Solution: We use the strategy of Example 3.1.2 to find the fixed points. The graphs of $y = x$ and $y = \beta \tanh x$ are shown in Figure 3.4.3; their intersections correspond to fixed points. The key thing to realize is that as β increases, the tanh curve becomes steeper at the origin (its slope there is β). Hence for $\beta < 1$ the origin is the only fixed point. A pitchfork bifurcation occurs at $\beta = 1$, $x^* = 0$, when the tanh curve develops a slope of 1 at the origin. Finally, when $\beta > 1$, two new stable fixed points appear, and the origin becomes unstable.

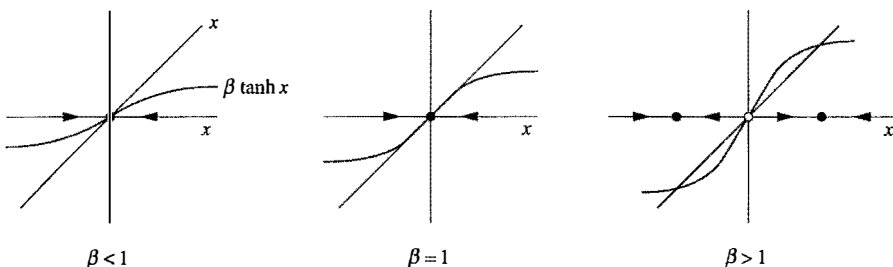


Figure 3.4.3

Now we want to compute the fixed points x^* for each β . Of course, one fixed point always occurs at $x^* = 0$; we are looking for the other, nontrivial fixed points.

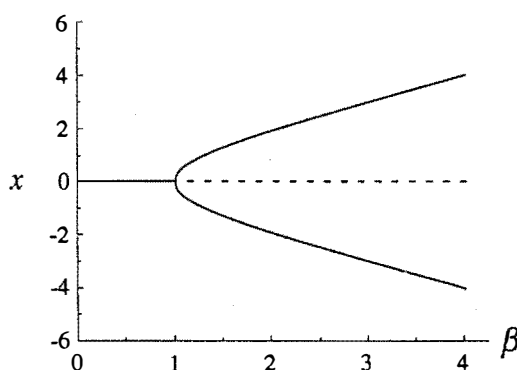


Figure 3.4.4

then compute $\beta = x^*/\tanh x^*$. This gives us a table of pairs (x^*, β) . For each pair, we plot β horizontally and x^* vertically. This yields the bifurcation diagram (Figure 3.4.4).

One approach is to solve the equation $x^* = \beta \tanh x^*$ numerically, using the Newton-Raphson method or some other root-finding scheme. (See Press et al. (1986) for a friendly and informative discussion of numerical methods.)

But there's an easier way, which comes from changing our point of view. Instead of studying the dependence of x^* on β , we think of x^* as the *independent* variable, and

The shortcut used here exploits the fact that $f(x, \beta) = -x + \beta \tanh x$ depends more simply on β than on x . This is frequently the case in bifurcation problems—the dependence on the control parameter is usually simpler than the dependence on x . ■

EXAMPLE 3.4.2:

Plot the potential $V(x)$ for the system $\dot{x} = rx - x^3$, for the cases $r < 0$, $r = 0$, and $r > 0$.

Solution: Recall from Section 2.7 that the potential for $\dot{x} = f(x)$ is defined by $f(x) = -dV/dx$. Hence we need to solve $-dV/dx = rx - x^3$. Integration yields $V(x) = -\frac{1}{2}rx^2 + \frac{1}{4}x^4$, where we neglect the arbitrary constant of integration. The corresponding graphs are shown in Figure 3.4.5.

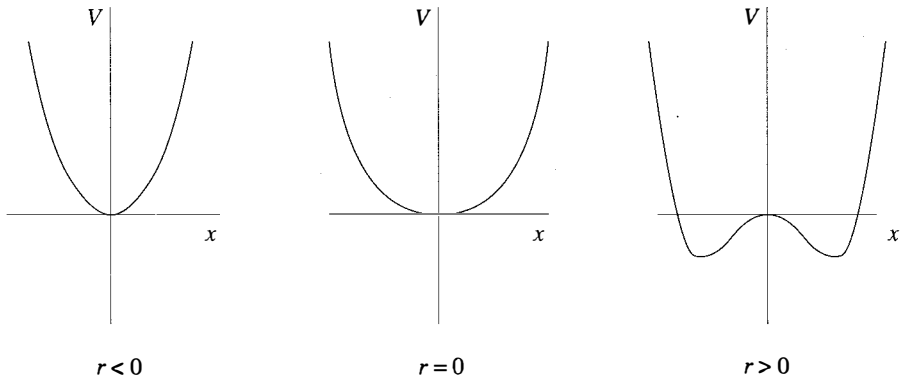


Figure 3.4.5

When $r < 0$, there is a quadratic minimum at the origin. At the bifurcation value $r = 0$, the minimum becomes a much flatter quartic. For $r > 0$, a local *maximum* appears at the origin, and a symmetric pair of minima occur to either side of it. ■

Subcritical Pitchfork Bifurcation

In the supercritical case $\dot{x} = rx - x^3$ discussed above, the cubic term is *stabilizing*: it acts as a restoring force that pulls $x(t)$ back toward $x = 0$. If instead the cubic term were *destabilizing*, as in

$$\dot{x} = rx + x^3, \quad (2)$$

then we'd have a **subcritical** pitchfork bifurcation. Figure 3.4.6 shows the bifurcation diagram.

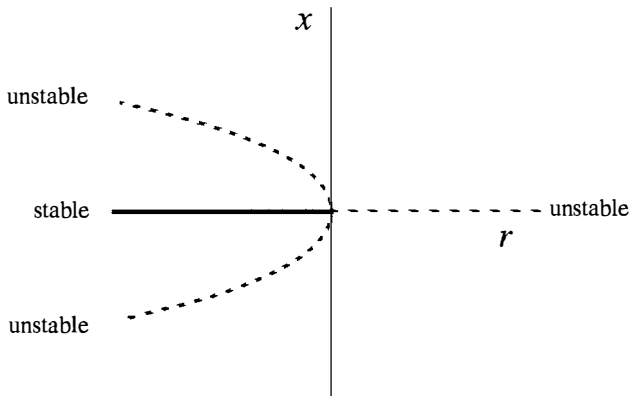


Figure 3.4.6

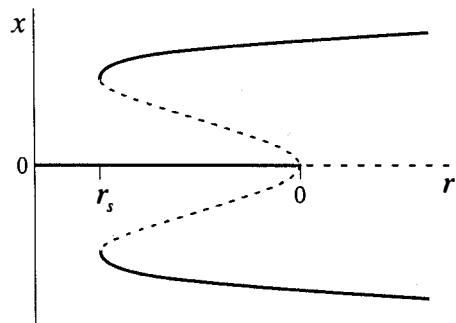
Compared to Figure 3.4.2, the pitchfork is inverted. The nonzero fixed points $x^* = \pm\sqrt{-r}$ are *unstable*, and exist only *below* the bifurcation ($r < 0$), which motivates the term “subcritical.” More importantly, the origin is stable for $r < 0$ and unstable for $r > 0$, as in the supercritical case, but now the instability for $r > 0$ is not opposed by the cubic term—in fact the cubic term lends a helping hand in driving the trajectories out to infinity! This effect leads to *blow-up*: one can show that $x(t) \rightarrow \pm\infty$ in finite time, starting from any initial condition $x_0 \neq 0$ (Exercise 2.5.3).

In real physical systems, such an explosive instability is usually opposed by the stabilizing influence of higher-order terms. Assuming that the system is still symmetric under $x \rightarrow -x$, the first stabilizing term must be x^5 . Thus the canonical example of a system with a subcritical pitchfork bifurcation is

$$\dot{x} = rx + x^3 - x^5. \quad (3)$$

There’s no loss in generality in assuming that the coefficients of x^3 and x^5 are 1 (Exercise 3.5.8).

The detailed analysis of (3) is left to you (Exercises 3.4.14 and 3.4.15). But we will summarize the main results here. Figure 3.4.7 shows the bifurcation diagram for (3).



For small x , the picture looks just like Figure 3.4.6: the origin is locally stable for $r < 0$, and two backward-bending branches of unstable fixed points bifurcate from the origin when $r = 0$. The new feature, due to the x^5 term, is that the unstable branches turn around and become stable at $r = r_s$, where $r_s < 0$. These stable **large-amplitude** branches exist for all $r > r_s$.

Figure 3.4.7

There are several things to note about Figure 3.4.7:

1. In the range $r_s < r < 0$, two qualitatively different stable states coexist, namely the origin and the large-amplitude fixed points. The initial condition x_0 determines which fixed point is approached as $t \rightarrow \infty$. One consequence is that the origin is stable to small perturbations, but not to large ones—in this sense the origin is *locally* stable, but not *globally* stable.
2. The existence of different stable states allows for the possibility of **jumps** and **hysteresis** as r is varied. Suppose we start the system in the state $x^* = 0$, and then slowly increase the parameter r (indicated by an arrow along the r -axis of Figure 3.4.8).

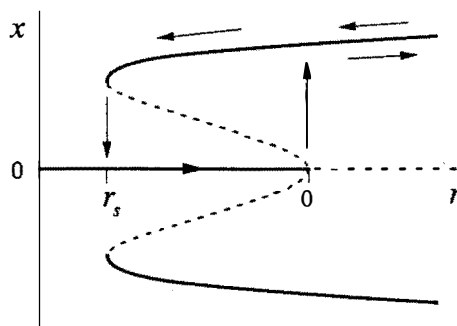


Figure 3.4.8

Then the state remains at the origin until $r = 0$, when the origin loses stability. Now the slightest nudge will cause the state to *jump* to one of the large-amplitude branches. With further increases of r , the state moves out along the large-amplitude branch. If r is now decreased, the state remains on the large-amplitude branch, even when r is decreased below 0! We have to lower r even further (down past r_s) to get the state to jump back to the origin. This lack of reversibility as a parameter is varied is called *hysteresis*.

3. The bifurcation at r_s is a saddle-node bifurcation, in which stable and unstable fixed points are born “out the clear blue sky” as r is increased (see Section 3.1).

Terminology

As usual in bifurcation theory, there are several other names for the bifurcations discussed here. The supercritical pitchfork is sometimes called a forward bifurcation, and is closely related to a continuous or second-order phase transition in sta-

tical mechanics. The subcritical bifurcation is sometimes called an inverted or backward bifurcation, and is related to discontinuous or first-order phase transitions. In the engineering literature, the supercritical bifurcation is sometimes called soft or safe, because the nonzero fixed points are born at small amplitude; in contrast, the subcritical bifurcation is hard or dangerous, because of the jump from zero to large amplitude.

3.5 Overdamped Bead on a Rotating Hoop

In this section we analyze a classic problem from first-year physics, the bead on a rotating hoop. This problem provides an example of a bifurcation in a mechanical system. It also illustrates the subtleties involved in replacing Newton's law, which is a second-order equation, by a simpler first-order equation.

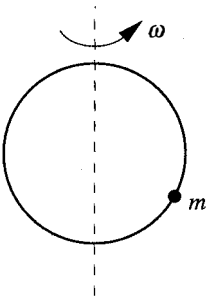


Figure 3.5.1

The mechanical system is shown in Figure 3.5.1. A bead of mass m slides along a wire hoop of radius r . The hoop is constrained to rotate at a constant angular velocity ω about its vertical axis. The problem is to analyze the motion of the bead, given that it is acted on by both gravitational and centrifugal forces. This is the usual statement of the problem, but now we want to add a new twist: suppose that there's also a frictional force on the bead that opposes its motion. To be specific, imagine that the whole system is immersed in a vat of molasses or some other very viscous fluid, and that the friction is due to viscous damping.

Let ϕ be the angle between the bead and the downward vertical direction. By convention, we restrict ϕ to the range $-\pi < \phi \leq \pi$, so there's only one angle for each point on the hoop. Also, let $\rho = r \sin \phi$ denote the distance of the bead from the vertical axis. Then the coordinates are as shown in Figure 3.5.2.

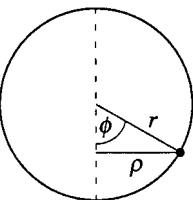


Figure 3.5.2

Now we write Newton's law for the bead. There's a downward gravitational force mg , a sideways centrifugal force $m\rho\omega^2$, and a tangential damping force $b\dot{\phi}$. (The constants g and b are taken to be positive; negative signs will be added later as needed.) The hoop is assumed to be rigid, so we only have to resolve the forces along the tangential direction, as shown in Figure 3.5.3. After substituting $\rho = r \sin \phi$ in the centrifugal term, and recalling that the tangential acceleration is $r\ddot{\phi}$, we obtain the governing equation

$$mr\ddot{\phi} = -b\dot{\phi} - mg \sin \phi + mr\omega^2 \sin \phi \cos \phi. \quad (1)$$

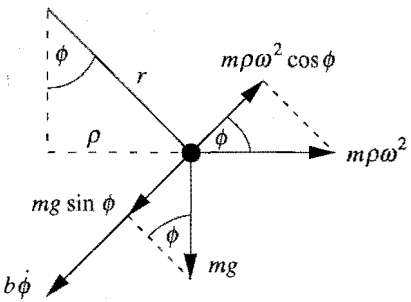


Figure 3.5.3

like it! But we will for now, and then at the end of this section we'll try to find a regime where our approximation is valid.

This is a *second-order* differential equation, since the second derivative $\ddot{\phi}$ is the highest one that appears. We are not yet equipped to analyze second-order equations, so we would like to find some conditions under which we can safely neglect the $mr\ddot{\phi}$ term. Then (1) reduces to a first-order equation, and we can apply our machinery to it.

Of course, this is a dicey business: we can't just neglect terms because we feel

Analysis of the First-Order System

Our concern now is with the first-order system

$$\begin{aligned} b\dot{\phi} &= -mg \sin \phi + mr\omega^2 \sin \phi \cos \phi \\ &= mg \sin \phi \left(\frac{r\omega^2}{g} \cos \phi - 1 \right). \end{aligned} \quad (2)$$

The fixed points of (2) correspond to equilibrium positions for the bead. What's your intuition about where such equilibria can occur? We would expect the bead to remain at rest if placed at the top or the bottom of the hoop. Can other fixed points occur? And what about stability? Is the bottom always stable?

Equation (2) shows that there are always fixed points where $\sin \phi = 0$, namely $\phi^* = 0$ (the bottom of the hoop) and $\phi^* = \pi$ (the top). The more interesting result is that there are two *additional* fixed points if

$$\frac{r\omega^2}{g} > 1,$$

that is, if the hoop is spinning fast enough. These fixed points satisfy $\phi^* = \pm \cos^{-1}(g/r\omega^2)$. To visualize them, we introduce a parameter

$$\gamma = \frac{r\omega^2}{g}$$

and solve $\cos \phi^* = 1/\gamma$ graphically. We plot $\cos \phi$ vs. ϕ , and look for intersections with the constant function $1/\gamma$, shown as a horizontal line in Figure 3.5.4. For $\gamma < 1$ there are no intersections, whereas for $\gamma > 1$ there is a symmetrical pair of in-

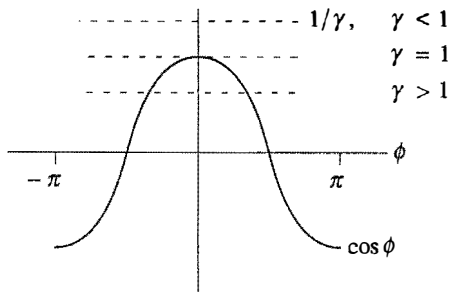


Figure 3.5.4

tersections to either side of $\phi^* = 0$. As $\gamma \rightarrow \infty$, these intersections approach $\pm\pi/2$. Figure 3.5.5 plots the fixed points on the hoop for the cases $\gamma < 1$ and $\gamma > 1$.

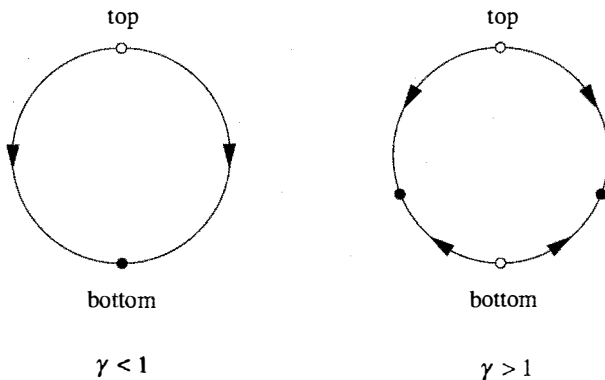


Figure 3.5.5

To summarize our results so far, let's plot *all* the fixed points as a function of the parameter γ (Figure 3.5.6). As usual, solid lines denote stable fixed points and broken lines denote unstable fixed points.

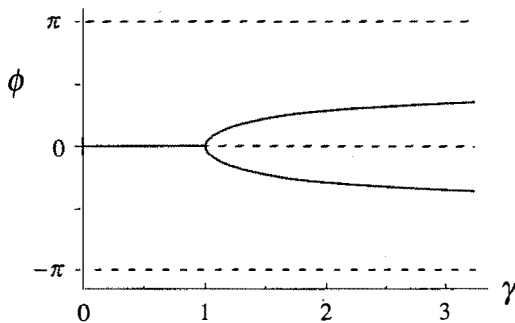


Figure 3.5.6

We now see that a ***supercritical pitchfork bifurcation*** occurs at $\gamma = 1$. It's left to you to check the stability of the fixed points, using linear stability analysis or graphical methods (Exercise 3.5.2).

Here's the physical interpretation of the results: When $\gamma < 1$, the hoop is rotating slowly and the centrifugal force is too weak to balance the force of gravity. Thus the bead slides down to the bottom and stays there. But if $\gamma > 1$, the hoop is spinning fast enough that the bottom becomes unstable. Since the centrifugal force grows as the bead moves farther from the bottom, any slight displacement of the bead will be *amplified*. The bead is therefore pushed up the hoop until gravity balances the centrifugal force; this balance occurs at $\phi^* = \pm \cos^{-1}(g/r\omega^2)$. Which of these two fixed points is actually selected depends on the initial disturbance. Even though the two fixed points are entirely symmetrical, an asymmetry in the initial conditions will lead to one of them being chosen—physicists sometimes refer to these as ***symmetry-broken*** solutions. In other words, the solution has less symmetry than the governing equation.

What *is* the symmetry of the governing equation? Clearly the left and right halves of the hoop are physically equivalent—this is reflected by the invariance of (1) and (2) under the change of variables $\phi \rightarrow -\phi$. As we mentioned in Section 3.4, pitchfork bifurcations are to be expected in situations where such a symmetry exists.

Dimensional Analysis and Scaling

Now we need to address the question: When is it valid to neglect the inertia term $mr\ddot{\phi}$ in (1)? At first sight the limit $m \rightarrow 0$ looks promising, but then we notice that we're throwing out the baby with the bathwater: the centrifugal and gravitational terms vanish in this limit too! So we have to be more careful.

In problems like this, it is helpful to express the equation in ***dimensionless*** form (at present, all the terms in (1) have the dimensions of force.) The advantage of a dimensionless formulation is that we know how to define *small*—it means “much less than 1.” Furthermore, nondimensionalizing the equation reduces the number of parameters by lumping them together into ***dimensionless groups***. This reduction always simplifies the analysis. For an excellent introduction to dimensional analysis, see Lin and Segel (1988).

There are often several ways to nondimensionalize an equation, and the best choice might not be clear at first. Therefore we proceed in a flexible fashion. We define a dimensionless time τ by

$$\tau = \frac{t}{T}$$

where T is a ***characteristic time scale*** to be chosen later. When T is chosen correctly, the new derivatives $d\phi/d\tau$ and $d^2\phi/d\tau^2$ should be $O(1)$, i.e., of order

unity. To express these new derivatives in terms of the old ones, we use the chain rule:

$$\dot{\phi} \equiv \frac{d\phi}{dt} = \frac{d\phi}{d\tau} \frac{d\tau}{dt} = \frac{1}{T} \frac{d\phi}{d\tau}$$

and similarly

$$\ddot{\phi} = \frac{1}{T^2} \frac{d^2\phi}{d\tau^2}.$$

(The easy way to remember these formulas is to formally substitute $T\tau$ for t .) Hence (1) becomes

$$\frac{mr}{T^2} \frac{d^2\phi}{d\tau^2} = -\frac{b}{T} \frac{d\phi}{d\tau} - mg \sin \phi + mr\omega^2 \sin \phi \cos \phi.$$

Now since this equation is a balance of forces, we nondimensionalize it by dividing by a force mg . This yields the dimensionless equation

$$\left(\frac{r}{gT^2} \right) \frac{d^2\phi}{d\tau^2} = -\left(\frac{b}{mgT} \right) \frac{d\phi}{d\tau} - \sin \phi + \left(\frac{r\omega^2}{g} \right) \sin \phi \cos \phi. \quad (3)$$

Each of the terms in parentheses is a dimensionless group. We recognize the group $r\omega^2/g$ in the last term—that's our old friend γ from earlier in the section.

We are interested in the regime where the left-hand side of (3) is negligible compared to all the other terms, and where all the terms on the right-hand side are of comparable size. Since the derivatives are $O(1)$ by assumption, and $\sin \phi \approx O(1)$, we see that we need

$$\frac{b}{mgT} \approx O(1), \text{ and } \frac{r}{gT^2} \ll 1.$$

The first of these requirements sets the time scale T : a natural choice is

$$T = \frac{b}{mg}.$$

Then the condition $r/gT^2 \ll 1$ becomes

$$\frac{r}{g} \left(\frac{mg}{b} \right)^2 \ll 1, \quad (4)$$

or equivalently,

$$b^2 \gg m^2 gr.$$

This can be interpreted as saying that the *damping is very strong*, or that the mass is very small, now in a precise sense.

The condition (4) motivates us to introduce a dimensionless group

$$\varepsilon = \frac{m^2 gr}{b^2} . \quad (5)$$

Then (3) becomes

$$\varepsilon \frac{d^2\phi}{d\tau^2} = -\frac{d\phi}{d\tau} - \sin \phi + \gamma \sin \phi \cos \phi . \quad (6)$$

As advertised, the dimensionless Equation (6) is simpler than (1): the five parameters m , g , r , ω , and b have been replaced by two dimensionless groups γ and ε .

In summary, our dimensional analysis suggests that in the **overdamped** limit $\varepsilon \rightarrow 0$, (6) should be well approximated by the first-order system

$$\frac{d\phi}{d\tau} = f(\phi) \quad (7)$$

where

$$\begin{aligned} f(\phi) &= -\sin \phi + \gamma \sin \phi \cos \phi \\ &= \sin \phi (\gamma \cos \phi - 1). \end{aligned}$$

A Paradox

Unfortunately, there is something fundamentally wrong with our idea of replacing a second-order equation by a first-order equation. The trouble is that a second-order equation requires *two* initial conditions, whereas a first-order equation has only *one*. In our case, the bead's motion is determined by its initial position and velocity. These two quantities can be chosen completely independent of each other. But that's not true for the first-order system: given the initial position, the initial velocity is dictated by the equation $d\phi/d\tau = f(\phi)$. Thus the solution to the first-order system will not, in general, be able to satisfy *both* initial conditions.

We seem to have run into a paradox. Is (7) valid in the overdamped limit or not? If it is valid, how can we satisfy the two arbitrary initial conditions demanded by (6)?

The resolution of the paradox requires us to analyze the second-order system (6). We haven't dealt with second-order systems before—that's the subject of Chapter 5. But read on if you're curious; some simple ideas are all we need to finish the problem.

Phase Plane Analysis

Throughout Chapters 2 and 3, we have exploited the idea that a first-order sys-

tem $\dot{x} = f(x)$ can be regarded as a vector field on a line. By analogy, the second-order system (6) can be regarded as a vector field on a *plane*, the so-called **phase plane**.

The plane is spanned by two axes, one for the angle ϕ and one for the angular velocity $d\phi/d\tau$. To simplify the notation, let

$$\Omega = \phi' \equiv d\phi/d\tau$$

where prime denotes differentiation with respect to τ . Then an initial condition for (6) corresponds to a point (ϕ_0, Ω_0) in the phase plane (Figure 3.5.7). As time evolves, the phase point $(\phi(t), \Omega(t))$ moves around in the phase plane along a **trajectory** determined by the solution to (6).

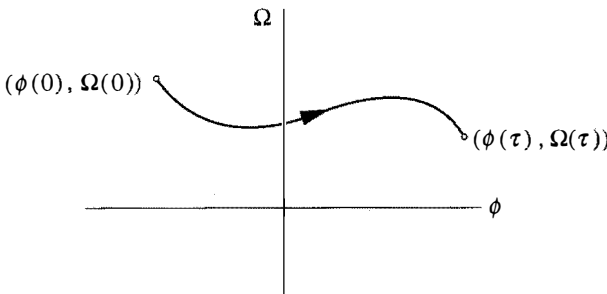


Figure 3.5.7

Our goal now is to see what those trajectories actually look like. As before, the key idea is that *the differential equation can be interpreted as a vector field on the phase space*. To convert (6) into a vector field, we first rewrite it as

$$\varepsilon\Omega' = f(\phi) - \Omega.$$

Along with the definition $\phi' = \Omega$, this yields the **vector field**

$$\phi' = \Omega \tag{8a}$$

$$\Omega' = \frac{1}{\varepsilon}(f(\phi) - \Omega). \tag{8b}$$

We interpret the vector (ϕ', Ω') at the point (ϕ, Ω) as the local velocity of a phase fluid flowing steadily on the plane. Note that the velocity vector now has two components, one in the ϕ -direction and one in the Ω -direction. To visualize the trajectories, we just imagine how the phase point would move as it is carried along by the phase fluid.

In general, the pattern of trajectories would be difficult to picture, but the pre-

sent case is simple because we are only interested in the limit $\varepsilon \rightarrow 0$. In this limit, *all trajectories slam straight up or down onto the curve C defined by $f(\phi) = \Omega$, and then slowly ooze along this curve until they reach a fixed point* (Figure 3.5.8).

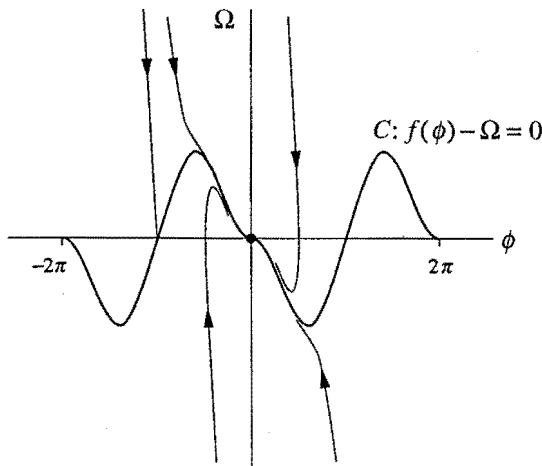


Figure 3.5.8

To arrive at this striking conclusion, let's do an order-of-magnitude calculation. Suppose that the phase point lies off the curve C . For instance, suppose (ϕ, Ω) lies an $O(1)$ distance below the curve C , i.e., $\Omega < f(\phi)$ and $f(\phi) - \Omega \approx O(1)$. Then (8b) shows that Ω' is enormously positive: $\Omega' \approx O(1/\varepsilon) \gg 1$. Thus the phase point zaps like lightning up to the region where $f(\phi) - \Omega \approx O(\varepsilon)$. In the limit $\varepsilon \rightarrow 0$, this region is indistinguishable from C . Once the phase point is on C , it evolves according to $\Omega \approx f(\phi)$; that is, it approximately satisfies the first-order equation $\dot{\phi} = f(\phi)$.

Our conclusion is that a typical trajectory is made of two parts: a rapid initial *transient*, during which the phase point zaps onto the curve where $\dot{\phi} = f(\phi)$, followed by a much slower drift along this curve.

Now we see how the paradox is resolved: The second-order system (6) *does* behave like the first-order system (7), but only after a rapid initial transient. During this transient, it is *not* correct to neglect the term $\varepsilon d^2\phi/dt^2$. The problem with our earlier approach is that we used only a single time scale $T = b/mg$; this time scale is characteristic of the slow drift process, but not of the rapid transient (Exercise 3.5.5).

A Singular Limit

The difficulty we have encountered here occurs throughout science and engineering. In some limit of interest (here, the limit of strong damping), the term con-

taining the highest order derivative drops out of the governing equation. Then the initial conditions or boundary conditions can't be satisfied. Such a limit is often called *singular*. For example, in fluid mechanics, the limit of high Reynolds number is a singular limit; it accounts for the presence of extremely thin "boundary layers" in the flow over airplane wings. In our problem, the rapid transient played the role of a boundary layer—it is a thin layer of *time* that occurs near the boundary $t = 0$.

The branch of mathematics that deals with singular limits is called *singular perturbation theory*. See Jordan and Smith (1987) or Lin and Segel (1988) for an introduction. Another problem with a singular limit will be discussed briefly in Section 7.5.

3.6 Imperfect Bifurcations and Catastrophes

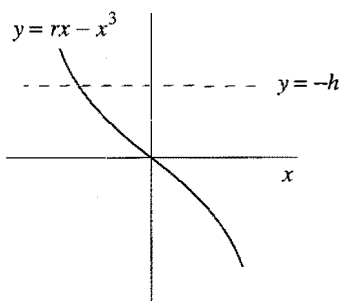
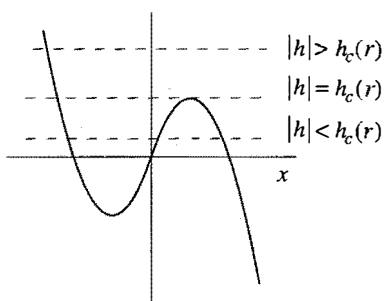
As we mentioned earlier, pitchfork bifurcations are common in problems that have a symmetry. For example, in the problem of the bead on a rotating hoop (Section 3.5), there was a perfect symmetry between the left and right sides of the hoop. But in many real-world circumstances, the symmetry is only approximate—an imperfection leads to a slight difference between left and right. We now want to see what happens when such imperfections are present.

For example, consider the system

$$\dot{x} = h + rx - x^3. \quad (1)$$

If $h = 0$, we have the normal form for a supercritical pitchfork bifurcation, and there's a perfect symmetry between x and $-x$. But this symmetry is broken when $h \neq 0$; for this reason we refer to h as an *imperfection parameter*.

Equation (1) is a bit harder to analyze than other bifurcation problems we've considered previously, because we have *two* independent parameters to worry about (h and r). To keep things straight, we'll think of r as fixed, and then examine the effects of varying h . The first step is to analyze the fixed points of (1). These can be found explicitly, but we'd have to invoke the messy formula for the roots of a cubic equation. It's clearer to use a graphical approach, as in Example 3.1.2. We plot the graphs of $y = rx - x^3$ and $y = -h$ on the same axes, and look for intersections (Figure 3.6.1). These intersections occur at the fixed points of (1). When $r \leq 0$, the cubic is monotonically decreasing, and so it intersects the horizontal line $y = -h$ in exactly one point (Figure 3.6.1a). The more interesting case is $r > 0$; then one, two, or three intersections are possible, depending on the value of h (Figure 3.6.1b).

(a) $r \leq 0$ (b) $r > 0$ **Figure 3.6.1**

The critical case occurs when the horizontal line is just *tangent* to either the local minimum or maximum of the cubic; then we have a *saddle-node bifurcation*. To find the values of h at which this bifurcation occurs, note that the cubic has a local maximum when $\frac{dx}{dr}(rx - x^3) = r - 3x^2 = 0$. Hence

$$x_{\max} = \sqrt{\frac{r}{3}},$$

and the value of the cubic at the local maximum is

$$rx_{\max} - (x_{\max})^3 = \frac{2r}{3} \sqrt{\frac{r}{3}}.$$

Similarly, the value at the minimum is the negative of this quantity. Hence saddle-node bifurcations occur when $h = \pm h_c(r)$, where

$$h_c(r) = \frac{2r}{3} \sqrt{\frac{r}{3}}.$$

Equation (1) has three fixed points for $|h| < h_c(r)$ and one fixed point for $|h| > h_c(r)$.

To summarize the results so far, we plot the **bifurcation curves** $h = \pm h_c(r)$ in the (r, h) plane (Figure 3.6.2). Note that the two bifurcation curves meet tangentially at $(r, h) = (0, 0)$; such a point is called a **cusp point**. We also label the regions that correspond to different numbers of fixed points. Saddle-node bifurcations occur all along the boundary of the regions, except at the cusp point, where we have a *codimension-2 bifurcation*. (This fancy terminology essentially means that we have had to tune *two* parameters, h and r , to achieve this type of bifurcation. Until now, all our bifurcations could be achieved by tuning a single parameter, and were therefore *codimension-1* bifurcations.)

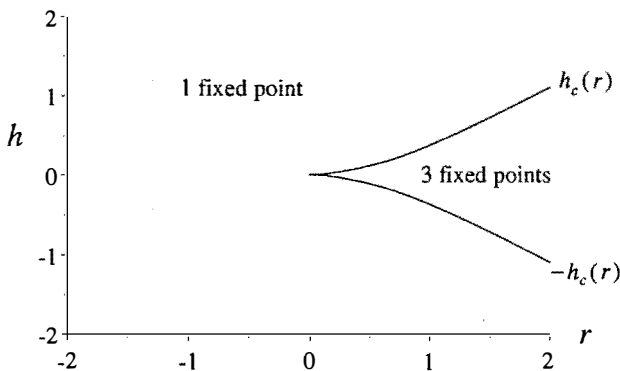


Figure 3.6.2

Pictures like Figure 3.6.2 will prove very useful in our future work. We will refer to such pictures as **stability diagrams**. They show the different types of behavior that occur as we move around in **parameter space** (here, the (r, h) plane).

Now let's present our results in a more familiar way by showing the bifurcation diagram of x^* vs. r , for fixed h (Figure 3.6.3).

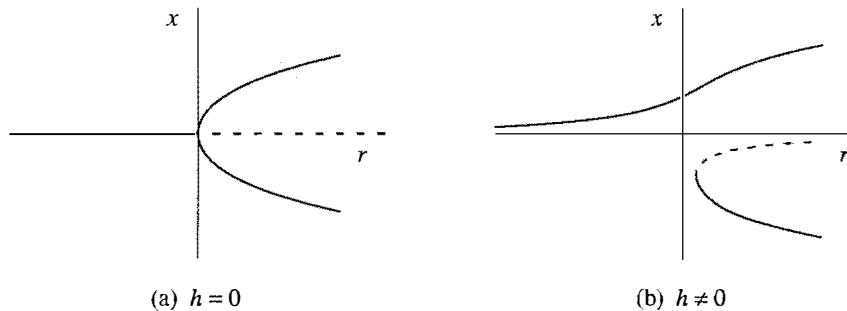


Figure 3.6.3

When $h = 0$ we have the usual pitchfork diagram (Figure 3.6.3a) but when $h \neq 0$, the pitchfork disconnects into two pieces (Figure 3.6.3b). The upper piece consists entirely of stable fixed points, whereas the lower piece has both stable and unstable branches. As we increase r from negative values, there's no longer a sharp transition at $r = 0$; the fixed point simply glides smoothly along the upper branch. Furthermore, the lower branch of stable points is not accessible unless we make a fairly large disturbance.

Alternatively, we could plot x^* vs. h , for fixed r (Figure 3.6.4).

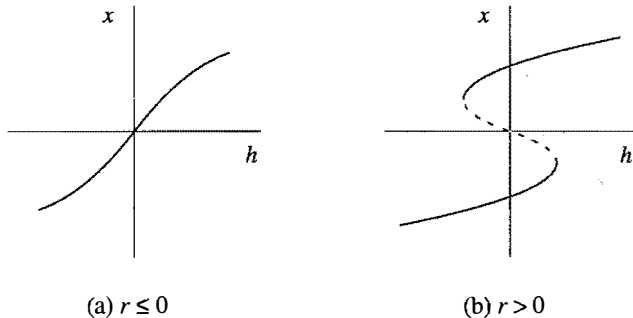


Figure 3.6.4

When $r \leq 0$ there's one stable fixed point for each h (Figure 3.6.4a). However, when $r > 0$ there are three fixed points when $|h| < h_c(r)$, and one otherwise (Figure 3.6.4b). In the triple-valued region, the middle branch is unstable and the upper and lower branches are stable. Note that these graphs look like Figure 3.6.1 rotated by 90°.

There is one last way to plot the results, which may appeal to you if you like to picture things in three dimensions. This method of presentation contains all of the others as cross sections or projections.

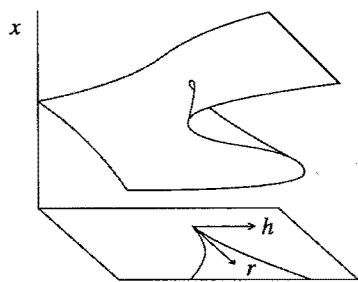


Figure 3.6.5

If we plot the fixed points x^* above the (r, h) plane, we get the **cusp catastrophe** surface shown in Figure 3.6.5. The surface folds over on itself in certain places. The projection of these folds onto the (r, h) plane yields the bifurcation curves shown in Figure 3.6.2. A cross section at fixed h yields Figure 3.6.3, and a cross section at fixed r yields Figure 3.6.4.

The term *catastrophe* is motivated by the fact that as parameters change, the state of the system can be carried over the edge of the upper surface, after which it drops discontinuously to the lower surface (Figure 3.6.6). This jump could be truly catastrophic for the equilibrium of a bridge or a building. We will see scientific examples of catastrophes in the context of insect outbreaks (Section 3.7) and in the following example from mechanics.

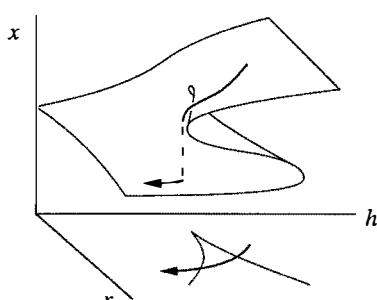


Figure 3.6.6

For more about catastrophe theory, see Zeeman (1977) or Poston and Stewart (1978). Incidentally, there was a violent controversy about this subject in the late

1970s. If you like watching fights, have a look at Zahler and Sussman (1977) and Kolata (1977).

Bead on a Tilted Wire

As a simple example of imperfect bifurcation and catastrophe, consider the following mechanical system (Figure 3.6.7).

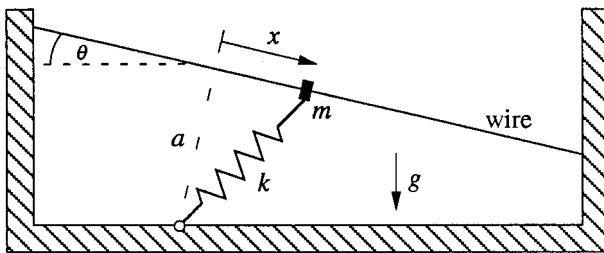


Figure 3.6.7

A bead of mass m is constrained to slide along a straight wire inclined at an angle θ with respect to the horizontal. The mass is attached to a spring of stiffness k and relaxed length L_0 , and is also acted on by gravity. We choose coordinates along the wire so that $x = 0$ occurs at the point closest to the support point of the spring; let a be the distance between this support point and the wire.

In Exercises 3.5.4 and 3.6.5, you are asked to analyze the equilibrium positions of the bead. But first let's get some physical intuition. When the wire is horizontal ($\theta = 0$), there is perfect symmetry between the left and right sides of the wire, and $x = 0$ is always an equilibrium position. The stability of this equilibrium depends on the relative sizes of L_0 and a : if $L_0 < a$, the spring is in tension and so the equilibrium should be stable. But if $L_0 > a$, the spring is compressed and so we expect an *unstable* equilibrium at $x = 0$ and a pair of stable equilibria to either side of it. Exercise 3.5.4 deals with this simple case.

The problem becomes more interesting when we tilt the wire ($\theta \neq 0$). For small tilting, we expect that there are still three equilibria if $L_0 > a$. However if the tilt becomes too steep, perhaps you can see intuitively that the uphill equilibrium might suddenly disappear, causing the bead to jump catastrophically to the downhill equilibrium. You might even want to build this mechanical system and try it. Exercise 3.6.5 asks you to work through the mathematical details.

3.7 Insect Outbreak

For a biological example of bifurcation and catastrophe, we turn now to a model for the sudden outbreak of an insect called the spruce budworm. This insect is a se-

rious pest in eastern Canada, where it attacks the leaves of the balsam fir tree. When an outbreak occurs, the budworms can defoliate and kill most of the fir trees in the forest in about four years.

Ludwig et al. (1978) proposed and analyzed an elegant model of the interaction between budworms and the forest. They simplified the problem by exploiting a separation of time scales: the budworm population evolves on a *fast* time scale (they can increase their density fivefold in a year, so they have a characteristic time scale of months), whereas the trees grow and die on a *slow* time scale (they can completely replace their foliage in about 7–10 years, and their life span in the absence of budworms is 100–150 years.) Thus, as far as the budworm dynamics are concerned, the forest variables may be treated as constants. At the end of the analysis, we will allow the forest variables to drift very slowly—this drift ultimately triggers an outbreak.

Model

The proposed model for the budworm population dynamics is

$$\dot{N} = RN \left(1 - \frac{N}{K}\right) - p(N).$$

In the absence of predators, the budworm population $N(t)$ is assumed to grow logistically with growth rate R and carrying capacity K . The carrying capacity depends

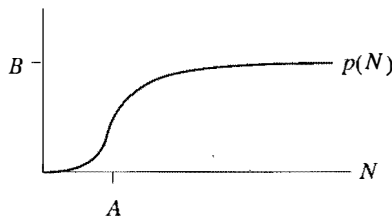


Figure 3.7.1

on the amount of foliage left on the trees, and so it is a slowly drifting parameter; at this stage we treat it as fixed. The term $p(N)$ represents the death rate due to *predation*, chiefly by birds, and is assumed to have the shape shown in Figure 3.7.1. There is almost no predation when budworms are scarce; the birds seek food elsewhere. However, once the population exceeds a certain

critical level $N = A$, the predation turns on sharply and then saturates (the birds are eating as fast as they can). Ludwig et al. (1978) assumed the specific form

$$p(N) = \frac{BN^2}{A^2 + N^2}$$

where $A, B > 0$. Thus the full model is

$$\dot{N} = RN \left(1 - \frac{N}{K}\right) - \frac{BN^2}{A^2 + N^2}. \quad (1)$$

We now have several questions to answer. What do we mean by an “outbreak” in the context of this model? The idea must be that, as parameters drift, the bud-

worm population suddenly jumps from a low to a high level. But what do we mean by “low” and “high,” and are there solutions with this character? To answer these questions, it is convenient to recast the model into a dimensionless form, as in Section 3.5.

Dimensionless Formulation

The model (1) has four parameters: R , K , A , and B . As usual, there are various ways to nondimensionalize the system. For example, both A and K have the same dimension as N , and so either N/A or N/K could serve as a dimensionless population level. It often takes some trial and error to find the best choice. In this case, our heuristic will be to scale the equation so that all the dimensionless groups are pushed into the *logistic* part of the dynamics, with none in the *predation* part. This turns out to ease the graphical analysis of the fixed points.

To get rid of the parameters in the predation term, we divide (1) by B and then let

$$x = N/A,$$

which yields

$$\frac{A}{B} \frac{dx}{dt} = \frac{R}{B} Ax \left(1 - \frac{Ax}{K}\right) - \frac{x^2}{1+x^2}. \quad (2)$$

Equation (2) suggests that we should introduce a dimensionless time τ and dimensionless groups r and k , as follows:

$$\tau = \frac{Bt}{A}, \quad r = \frac{RA}{B}, \quad k = \frac{K}{A}.$$

Then (2) becomes .

$$\frac{dx}{d\tau} = rx \left(1 - \frac{x}{k}\right) - \frac{x^2}{1+x^2}, \quad (3)$$

which is our final dimensionless form. Here r and k are the dimensionless growth rate and carrying capacity, respectively.

Analysis of Fixed Points

Equation (3) has a fixed point at $x^* = 0$; it is *always unstable* (Exercise 3.7.1). The intuitive explanation is that the predation is extremely weak for small x , and so the budworm population grows exponentially for x near zero.

The other fixed points of (3) are given by the solutions of

$$r \left(1 - \frac{x}{k}\right) = \frac{x}{1+x^2}. \quad (4)$$

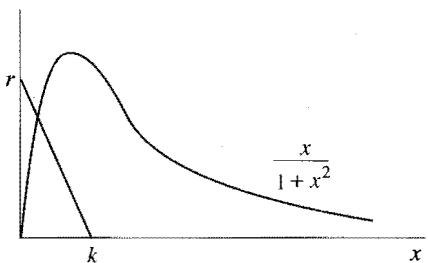


Figure 3.7.2

the curve doesn't—this convenient property is what motivated our choice of nondimensionalization.

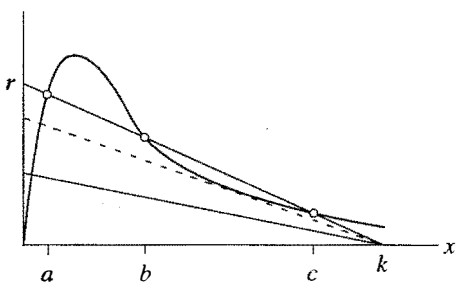


Figure 3.7.3

and eventually coalesce in a *saddle-node bifurcation* when the line intersects the curve *tangentially* (dashed line in Figure 3.7.3). After the bifurcation, the only remaining fixed point is a (in addition to $x^*=0$, of course). Similarly, a and b can collide and annihilate as r is increased.

To determine the stability of the fixed points, we recall that $x^*=0$ is unstable, and also observe that the stability type must alternate as we move along the x -axis.

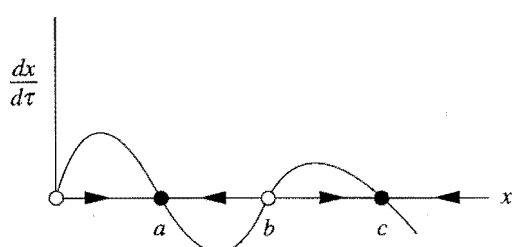


Figure 3.7.4

view of pest control, one would like to keep the population at a and away from c . The fate of the system is determined by the initial condition x_0 ; an outbreak occurs

This equation is easy to analyze graphically—we simply graph the right- and left-hand sides of (4), and look for intersections (Figure 3.7.2). The left-hand side of (4) represents a straight line with x -intercept equal to k and a y -intercept equal to r , and the right-hand side represents a curve that is *independent of the parameters!* Hence, as we vary the parameters r and k , the line moves but

Figure 3.7.2 shows that if k is sufficiently small, there is exactly one intersection for any $r > 0$. However, for large k , we can have one, two, or three intersections, depending on the value of r (Figure 3.7.3). Let's suppose that there are three intersections a , b , and c . As we decrease r with k fixed, the line rotates counter-clockwise about k . Then the fixed points b and c approach each other

Hence a is stable, b is unstable, and c is stable. Thus, for r and k in the range corresponding to three positive fixed points, the vector field is qualitatively like that shown in Figure 3.7.4. The smaller stable fixed point a is called the *refuge* level of the budworm population, while the larger stable point c is the *outbreak* level. From the point of

if and only if $x_0 > b$. In this sense the unstable equilibrium b plays the role of a **threshold**.

An outbreak can also be triggered by a saddle-node bifurcation. If the parameters r and k drift in such a way that the fixed point a disappears, then the population will jump suddenly to the outbreak level c . The situation is made worse by the hysteresis effect—even if the parameters are restored to their values before the outbreak, the population will not drop back to the refuge level.

Calculating the Bifurcation Curves

Now we compute the curves in (k, r) space where the system undergoes saddle-node bifurcations. The calculation is somewhat harder than that in Section 3.6: we will not be able to write r explicitly as a function of k , for example. Instead, the bifurcation curves will be written in the **parametric form** $(k(x), r(x))$, where x runs through all positive values. (Please don't be confused by this traditional terminology—one would call x the “parameter” in these parametric equations, even though r and k are themselves parameters in a different sense.)

As discussed earlier, the condition for a saddle-node bifurcation is that the line $r(1 - x/k)$ intersects the curve $x/(1 + x^2)$ tangentially. Thus we require *both*

$$r\left(1 - \frac{x}{k}\right) = \frac{x}{1 + x^2} \quad (5)$$

and

$$\frac{d}{dx} \left[r\left(1 - \frac{x}{k}\right) \right] = \frac{d}{dx} \left[\frac{x}{1 + x^2} \right]. \quad (6)$$

After differentiation, (6) reduces to

$$-\frac{r}{k} = \frac{1 - x^2}{(1 + x^2)^2}. \quad (7)$$

We substitute this expression for r/k into (5), which allows us to express r solely in terms of x . The result is

$$r = \frac{2x^3}{(1 + x^2)^2}. \quad (8)$$

Then inserting (8) into (7) yields

$$k = \frac{2x^3}{x^2 - 1}. \quad (9)$$

The condition $k > 0$ implies that x must be restricted to the range $x > 1$.

Together (8) and (9) define the bifurcation curves. For each $x > 1$, we plot the

corresponding point $(k(x), r(x))$ in the (k, r) plane. The resulting curves are shown in Figure 3.7.5. (Exercise 3.7.2 deals with some of the analytical properties of these curves.)

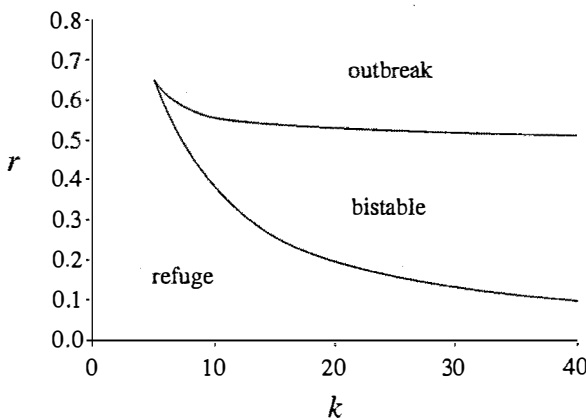


Figure 3.7.5

The different regions in Figure 3.7.5 are labeled according to the stable fixed points that exist. The refuge level a is the only stable state for low r , and the outbreak level c is the only stable state for large r . In the **bistable** region, both stable states exist.

The stability diagram is very similar to Figure 3.6.2. It too can be regarded as the projection of a cusp catastrophe surface, as schematically illustrated in Figure 3.7.6. You are hereby challenged to graph the surface accurately!

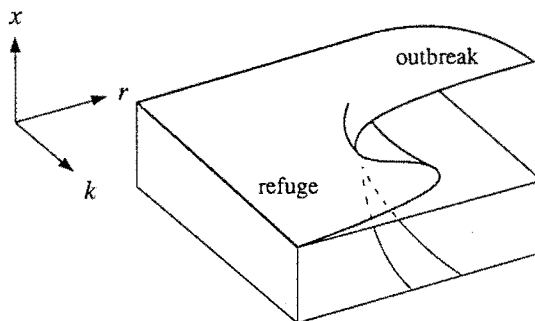


Figure 3.7.6

Comparison with Observations

Now we need to decide on biologically plausible values of the dimensionless groups $r = RA/B$ and $k = K/A$. A complication is that these parameters may drift

slowly as the condition of the forest changes. According to Ludwig et al. (1978), r increases as the forest grows, while k remains fixed.

They reason as follows: let S denote the average size of the trees, interpreted as the total surface area of the branches in a stand. Then the carrying capacity K should be proportional to the available foliage, so $K = K'S$. Similarly, the half-saturation parameter A in the predation term should be proportional to S ; predators such as birds search *units of foliage*, not acres of forest, and so the relevant quantity A' must have the dimensions of budworms per unit of branch area. Hence $A = A'S$ and therefore

$$r = \frac{RA'}{B}S, \quad k = \frac{K'}{A'}. \quad (10)$$

The experimental observations suggest that for a young forest, typically $k \approx 300$ and $r < 1/2$ so the parameters lie in the bistable region. The budworm population is kept down by the birds, which find it easy to search the small number of branches per acre. However, as the forest grows, S increases and therefore the point (k, r) drifts upward in parameter space toward the outbreak region of Figure 3.7.5. Ludwig et al. (1978) estimate that $r \approx 1$ for a fully mature forest, which lies dangerously in the outbreak region. After an outbreak occurs, the fir trees die and the forest is taken over by birch trees. But they are less efficient at using nutrients and eventually the fir trees come back—this recovery takes about 50–100 years (Murray 1989).

We conclude by mentioning some of the approximations in the model presented here. The tree dynamics have been neglected; see Ludwig et al. (1978) for a discussion of this longer time-scale behavior. We've also neglected the *spatial distribution* of budworms and their possible dispersal—see Ludwig et al. (1979) and Murray (1989) for treatments of this aspect of the problem.

EXERCISES FOR CHAPTER 3

3.1 Saddle-Node Bifurcation

For each of the following exercises, sketch all the qualitatively different vector fields that occur as r is varied. Show that a saddle-node bifurcation occurs at a critical value of r , to be determined. Finally, sketch the bifurcation diagram of fixed points x^* versus r .

3.1.1 $\dot{x} = 1 + rx + x^2$

3.1.2 $\dot{x} = r - \cosh x$

3.1.3 $\dot{x} = r + x - \ln(1+x)$

3.1.4 $\dot{x} = r + \frac{1}{2}x - x/(1+x)$

3.1.5 (Unusual bifurcations) In discussing the normal form of the saddle-node bi-

furcation, we mentioned the assumption that $a = \partial f / \partial r|_{(x^*, r_c)} \neq 0$. To see what can happen if $\partial f / \partial r|_{(x^*, r_c)} = 0$, sketch the vector fields for the following examples, and then plot the fixed points as a function of r .

- $\dot{x} = r^2 - x^2$
- $\dot{x} = r^2 + x^2$

3.2 Transcritical Bifurcation

For each of the following exercises, sketch all the qualitatively different vector fields that occur as r is varied. Show that a transcritical bifurcation occurs at a critical value of r , to be determined. Finally, sketch the bifurcation diagram of fixed points x^* vs. r .

3.2.1 $\dot{x} = rx + x^2$

3.2.2 $\dot{x} = rx - \ln(1+x)$

3.2.3 $\dot{x} = x - rx(1-x)$

3.2.4 $\dot{x} = x(r - e^x)$

3.2.5 (Chemical kinetics) Consider the chemical reaction system



This is a generalization of Exercise 2.3.2; the new feature is that X is used up in the production of C .

- Assuming that both A and B are kept at constant concentrations a and b , show that the law of mass action leads to an equation of the form $\dot{x} = c_1x - c_2x^2$, where x is the concentration of X , and c_1 and c_2 are constants to be determined.
- Show that $x^* = 0$ is stable when $k_2b > k_1a$, and explain why this makes sense chemically.

The next two exercises concern the normal form for the transcritical bifurcation. In Example 3.2.2, we showed how to reduce the dynamics near a transcritical bifurcation to the approximate form $\dot{X} = RX - X^2 + O(X^3)$. Our goal now is to show that the $O(X^3)$ terms can always be eliminated by a suitable nonlinear change of variables; in other words, the reduction to normal form can be made *exact*, not just approximate.

3.2.6 (Eliminating the cubic term) Consider the system $\dot{X} = RX - X^2 + O(X^4)$, where $R \neq 0$. We want to find a new variable x such that the system transforms into $\dot{x} = Rx - x^2 + O(x^4)$. This would be a big improvement, since the cubic term has been eliminated and the error term has been bumped up to fourth order.

Let $x = X + bX^3 + O(X^4)$, where b will be chosen later to eliminate the cubic term in the differential equation for x . This is called a *near-identity transformation*, since x and X are practically equal; they differ by a tiny cubic term. (We

have skipped the quadratic term X^2 , because it is not needed—you should check this later.) Now we need to rewrite the system in terms of x ; this calculation requires a few steps.

- Show that the near-identity transformation can be inverted to yield $X = x + cx^3 + O(x^4)$, and solve for c .
- Write $\dot{x} = \dot{X} + 3bX^2\dot{X} + O(X^4)$, and substitute for X and \dot{X} on the right-hand side, so that everything depends only on x . Multiply the resulting series expansions and collect terms, to obtain $\dot{x} = Rx - x^2 + kx^3 + O(x^4)$, where k depends on a , b , and R .
- Now the moment of triumph: Choose b so that $k = 0$.
- Is it really necessary to make the assumption that $R \neq 0$? Explain.

3.2.7 (Eliminating any higher-order term) Now we generalize the method of the last exercise. Suppose we have managed to eliminate a number of higher-order terms, so that the system has been transformed into $\dot{X} = RX - X^2 + a_nX^n + O(X^{n+1})$, where $n \geq 3$. Use the near-identity transformation $x = X + b_nX^n + O(X^{n+1})$ and the previous strategy to show that the system can be rewritten as $\dot{x} = Rx - x^2 + O(x^{n+1})$ for an appropriate choice of b_n . Thus we can eliminate as many higher-order terms as we like.

3.3 Laser Threshold

3.3.1 (An improved model of a laser) In the simple laser model considered in Section 3.3, we wrote an *algebraic* equation relating N , the number of excited atoms, to n , the number of laser photons. In more realistic models, this would be replaced by a *differential* equation. For instance, Milonni and Eberly (1988) show that after certain reasonable approximations, quantum mechanics leads to the system

$$\begin{aligned}\dot{n} &= GnN - kn \\ \dot{N} &= -GnN - fN + p.\end{aligned}$$

Here G is the gain coefficient for stimulated emission, k is the decay rate due to loss of photons by mirror transmission, scattering, etc., f is the decay rate for spontaneous emission, and p is the pump strength. All parameters are positive, except p , which can have either sign.

This two-dimensional system will be analyzed in Exercise 8.1.13. For now, let's convert it to a one-dimensional system, as follows.

- Suppose that N relaxes much more rapidly than n . Then we may make the quasi-static approximation $\dot{N} \approx 0$. Given this approximation, express $N(t)$ in terms of $n(t)$ and derive a first-order system for n . (This procedure is often called **adiabatic elimination**, and one says that the evolution of $N(t)$ is *slaved* to that of $n(t)$. See Haken (1983).)
- Show that $n^* = 0$ becomes unstable for $p > p_c$, where p_c is to be determined.

- c) What type of bifurcation occurs at the laser threshold p_c ?
d) (Hard question) For what range of parameters is it valid to make the approximation used in (a)?

3.3.2 (Maxwell–Bloch equations) The Maxwell–Bloch equations provide an even more sophisticated model for a laser. These equations describe the dynamics of the electric field E , the mean polarization P of the atoms, and the population inversion D :

$$\begin{aligned}\dot{E} &= \kappa(P - E) \\ \dot{P} &= \gamma_1(ED - P) \\ \dot{D} &= \gamma_2(\lambda + 1 - D - \lambda EP)\end{aligned}$$

where κ is the decay rate in the laser cavity due to beam transmission, γ_1 and γ_2 are decay rates of the atomic polarization and population inversion, respectively, and λ is a pumping energy parameter. The parameter λ may be positive, negative, or zero; all the other parameters are positive.

These equations are similar to the Lorenz equations and can exhibit chaotic behavior (Haken 1983, Weiss and Vilaseca 1991). However, many practical lasers do not operate in the chaotic regime. In the simplest case $\gamma_1, \gamma_2 \gg \kappa$; then P and D relax rapidly to steady values, and hence may be adiabatically eliminated, as follows.

- a) Assuming $\dot{P} \approx 0$, $\dot{D} \approx 0$, express P and D in terms of E , and thereby derive a first-order equation for the evolution of E .
b) Find all the fixed points of the equation for E .
c) Draw the bifurcation diagram of E^* vs. λ . (Be sure to distinguish between stable and unstable branches.)

3.4 Pitchfork Bifurcation

In the following exercises, sketch all the qualitatively different vector fields that occur as r is varied. Show that a pitchfork bifurcation occurs at a critical value of r (to be determined) and classify the bifurcation as supercritical or subcritical. Finally, sketch the bifurcation diagram of x^* vs. r .

3.4.1 $\dot{x} = rx + 4x^3$

3.4.2 $\dot{x} = rx - \sinh x$

3.4.3 $\dot{x} = rx - 4x^3$

3.4.4 $\dot{x} = x + \frac{rx}{1+x^2}$

The next exercises are designed to test your ability to distinguish among the various types of bifurcations—it's easy to confuse them! In each case, find the values of r at which bifurcations occur, and classify those as saddle-node, transcritical, supercritical pitchfork, or subcritical pitchfork. Finally, sketch the bifurcation diagram of fixed points x^* vs. r .

3.4.5 $\dot{x} = r - 3x^2$

3.4.6 $\dot{x} = rx - \frac{x}{1+x}$

3.4.7 $\dot{x} = 5 - re^{-x^2}$

3.4.8 $\dot{x} = rx - \frac{x}{1+x^2}$

3.4.9 $\dot{x} = x + \tanh(rx)$ **3.4.10** $\dot{x} = rx + \frac{x^3}{1+x^2}$

3.4.11 (An interesting bifurcation diagram) Consider the system $\dot{x} = rx - \sin x$.

- For the case $r = 0$, find and classify all the fixed points, and sketch the vector field.
- Show that when $r > 1$, there is only one fixed point. What kind of fixed point is it?
- As r decreases from ∞ to 0, classify *all* the bifurcations that occur.
- For $0 < r \ll 1$, find an approximate formula for values of r at which bifurcations occur.
- Now classify all the bifurcations that occur as r decreases 0 to $-\infty$.
- Plot the bifurcation diagram for $-\infty < r < \infty$, and indicate the stability of the various branches of fixed points.

3.4.12 (“Quadfurcation”) With tongue in cheek, we pointed out that the pitchfork bifurcation could be called a “trifurcation,” since three branches of fixed points appear for $r > 0$. Can you construct an example of a “quadfurcation,” in which $\dot{x} = f(x, r)$ has no fixed points for $r < 0$ and four branches of fixed points for $r > 0$? Extend your results to the case of an arbitrary number of branches, if possible.

3.4.13 (Computer work on bifurcation diagrams) For the vector fields below, use a computer to obtain a quantitatively accurate plot of the values of x^* vs. r , where $0 \leq r \leq 3$. In each case, there’s an easy way to do this, and a harder way using the Newton-Raphson method.

a) $\dot{x} = r - x - e^{-x}$

b) $\dot{x} = 1 - x - e^{-rx}$

3.4.14 (Subcritical pitchfork) Consider the system $\dot{x} = rx + x^3 - x^5$, which exhibits a subcritical pitchfork bifurcation.

- Find algebraic expressions for all the fixed points as r varies.
- Sketch the vector fields as r varies. Be sure to indicate all the fixed points and their stability.
- Calculate r_s , the parameter value at which the nonzero fixed points are born in a saddle-node bifurcation.

3.4.15 (First-order phase transition) Consider the potential $V(x)$ for the system $\dot{x} = rx + x^3 - x^5$. Calculate r_c , where r_c is defined by the condition that V has three equally deep wells, i.e., the values of V at the three local minima are equal.

(Note: In equilibrium statistical mechanics, one says that a *first-order phase transition* occurs at $r = r_c$. For this value of r , there is equal probability of finding the system in the state corresponding to any of the three minima. The freezing of water into ice is the most familiar example of a first-order phase transition.)

3.4.16 (Potentials) In parts (a)–(c), let $V(x)$ be the potential, in the sense that $\dot{x} = -dV/dx$. Sketch the potential as a function of r . Be sure to show all the qualitatively different cases, including bifurcation values of r .

- (Saddle-node) $\dot{x} = r - x^2$
- (Transcritical) $\dot{x} = rx - x^2$
- (Subcritical pitchfork) $\dot{x} = rx + x^3 - x^5$

3.5 Overdamped Bead on a Rotating Hoop

3.5.1 Consider the bead on the rotating hoop discussed in Section 3.5. Explain in physical terms why the bead cannot have an equilibrium position with $\phi > \pi/2$.

3.5.2 Do the linear stability analysis for all the fixed points for Equation (3.5.7), and confirm that Figure 3.5.6 is correct.

3.5.3 Show that Equation (3.5.7) reduces to $\frac{d\phi}{d\tau} = A\phi - B\phi^3 + O(\phi^5)$ near $\phi = 0$. Find A and B .

3.5.4 (Bead on a horizontal wire) A bead of mass m is constrained to slide along a straight horizontal wire. A spring of relaxed length L_0 and spring constant k is attached to the mass and to a support point a distance h from the wire (Figure 1).

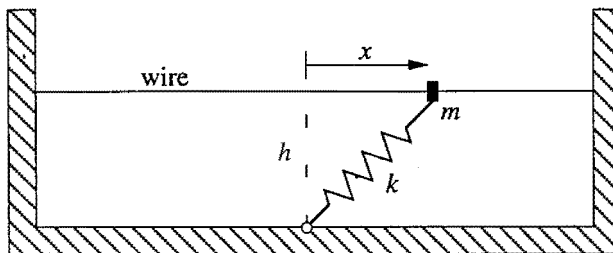


Figure 1

Finally, suppose that the motion of the bead is opposed by a viscous damping force $b\dot{x}$.

- Write Newton's law for the motion of the bead.
- Find all possible equilibria, i.e., fixed points, as functions of k , h , m , b , and L_0 .
- Suppose $m = 0$. Classify the stability of all the fixed points, and draw a bifurcation diagram.
- If $m \neq 0$, how small does m have to be to be considered negligible? In what sense is it negligible?

3.5.5 (Time scale for the rapid transient) While considering the bead on the rotating hoop, we used phase plane analysis to show that the equation

$$\varepsilon \frac{d^2\phi}{d\tau^2} + \frac{d\phi}{d\tau} = f(\phi)$$

has solutions that rapidly relax to the curve where $\frac{d\phi}{d\tau} = f(\phi)$.

- a) Estimate the time scale T_{fast} for this rapid transient in terms of ε , and then express T_{fast} in terms of the original dimensional quantities m , g , r , ω , and b .
- b) Rescale the original differential equation, using T_{fast} as the characteristic time scale, instead of $T_{slow} = b/mg$. Which terms in the equation are negligible on this time scale?
- c) Show that $T_{fast} \ll T_{slow}$ if $\varepsilon \ll 1$. (In this sense, the time scales T_{fast} and T_{slow} are *widely separated*.)

3.5.6 (A model problem about singular limits) Consider the *linear* differential equation

$$\varepsilon \ddot{x} + \dot{x} + x = 0,$$

subject to the initial conditions $x(0) = 1$, $\dot{x}(0) = 0$.

- a) Solve the problem analytically for all $\varepsilon > 0$.
- b) Now suppose $\varepsilon \ll 1$. Show that there are two widely separated time scales in the problem, and estimate them in terms of ε .
- c) Graph the solution $x(t)$ for $\varepsilon \ll 1$, and indicate the two time scales on the graph.
- d) What do you conclude about the validity of replacing $\varepsilon \ddot{x} + \dot{x} + x = 0$ with its singular limit $\dot{x} + x = 0$?
- e) Give two physical analogs of this problem, one involving a mechanical system, and another involving an electrical circuit. In each case, find the dimensionless combination of parameters corresponding to ε , and state the physical meaning of the limit $\varepsilon \ll 1$.

3.5.7 (Nondimensionalizing the logistic equation) Consider the logistic equation $\dot{N} = rN(1 - N/K)$, with initial condition $N(0) = N_0$.

- a) This system has three dimensional parameters r , K , and N_0 . Find the dimensions of each of these parameters.
- b) Show that the system can be rewritten in the dimensionless form

$$\frac{dx}{d\tau} = x(1 - x), \quad x(0) = x_0$$

for appropriate choices of the dimensionless variables x , x_0 , and τ .

- c) Find a different nondimensionalization in terms of variables u and τ , where u is chosen such that the initial condition is always $u_0 = 1$.
- d) Can you think of any advantage of one nondimensionalization over the other?

3.5.8 (Nondimensionalizing the subcritical pitchfork) The first-order system $\dot{u} = au + bu^3 - cu^5$, where $b, c > 0$, has a subcritical pitchfork bifurcation at $a = 0$. Show that this equation can be rewritten as

$$\frac{dx}{d\tau} = rx + x^3 - x^5$$

where $x = u/U$, $\tau = t/T$, and U , T , and r are to be determined in terms of a , b , and c .

3.6 Imperfect Bifurcations and Catastrophes

3.6.1 (Warm-up question about imperfect bifurcation) Does Figure 3.6.3b correspond to $h > 0$ or to $h < 0$?

3.6.2 (Imperfect transcritical bifurcation) Consider the system $\dot{x} = h + rx - x^2$. When $h = 0$, this system undergoes a transcritical bifurcation at $r = 0$. Our goal is to see how the bifurcation diagram of x^* vs. r is affected by the imperfection parameter h .

- a) Plot the bifurcation diagram for $\dot{x} = h + rx - x^2$, for $h < 0$, $h = 0$, and $h > 0$.
- b) Sketch the regions in the (r, h) plane that correspond to qualitatively different vector fields, and identify the bifurcations that occur on the boundaries of those regions.
- c) Plot the potential $V(x)$ corresponding to all the different regions in the (r, h) plane.

3.6.3 (A perturbation to the supercritical pitchfork) Consider the system $\dot{x} = rx + ax^2 - x^3$, where $-\infty < a < \infty$. When $a = 0$, we have the normal form for the supercritical pitchfork. The goal of this exercise is to study the effects of the new parameter a .

- a) For each a , there is a bifurcation diagram of x^* vs. r . As a varies, these bifurcation diagrams can undergo qualitative changes. Sketch all the qualitatively different bifurcation diagrams that can be obtained by varying a .
- b) Summarize your results by plotting the regions in the (r, a) plane that correspond to qualitatively different classes of vector fields. Bifurcations occur on the boundaries of these regions; identify the types of bifurcations that occur.

3.6.4 (Imperfect saddle-node) What happens if you add a small imperfection to a system that has a saddle-node bifurcation?

3.6.5 (Mechanical example of imperfect bifurcation and catastrophe) Consider the bead on a tilted wire discussed at the end of Section 3.6.

- a) Show that the equilibrium positions of the bead satisfy

$$mg \sin \theta = kx \left(1 - \frac{L_0}{\sqrt{x^2 + a^2}} \right).$$

- b) Show that this equilibrium equation can be written in dimensionless form as

$$1 - \frac{h}{u} = \frac{R}{\sqrt{1+u^2}}$$

for appropriate choices of R , h , and u .

- c) Give a graphical analysis of the dimensionless equation for the cases $R < 1$ and $R > 1$. How many equilibria can exist in each case?
- d) Let $r = R - 1$. Show that the equilibrium equation reduces to $h + ru - \frac{1}{2}u^3 \approx 0$ for small r , h , and u .
- e) Find an approximate formula for the saddle-node bifurcation curves in the limit of small r , h , and u .
- f) Show that the *exact* equations for the bifurcation curves can be written in parametric form as

$$h(u) = -u^3, \quad R(u) = (1+u^2)^{3/2},$$

where $-\infty < u < \infty$. (Hint: You may want to look at Section 3.7.) Check that this result reduces to the approximate result in part (d).

- g) Give a numerically accurate plot of the bifurcation curves in the (r,h) plane.
h) Interpret your results physically, in terms of the original dimensional variables.

3.6.6 (Patterns in fluids) Ahlers (1989) gives a fascinating review of experiments on one-dimensional patterns in fluid systems. In many cases, the patterns first emerge via supercritical or subcritical pitchfork bifurcations from a spatially uniform state. Near the bifurcation, the dynamics of the amplitude of the patterns are given approximately by $\tau \dot{A} = \varepsilon A - gA^3$ in the supercritical case, or $\tau \dot{A} = \varepsilon A - gA^3 - kA^5$ in the subcritical case. Here $A(t)$ is the amplitude, τ is a typical time scale, and ε is a small dimensionless parameter that measures the distance from the bifurcation. The parameter $g > 0$ in the supercritical case, whereas $g < 0$ and $k > 0$ in the subcritical case. (In this context, the equation $\tau \dot{A} = \varepsilon A - gA^3$ is often called the *Landau equation*.)

- a) Dubois and Bergé (1978) studied the supercritical bifurcation that arises in Rayleigh–Bénard convection, and showed experimentally that the steady-state amplitude depended on ε according to the power law $A^* \propto \varepsilon^\beta$, where $\beta = 0.50 \pm 0.01$. What does the Landau equation predict?
- b) The equation $\tau \dot{A} = \varepsilon A - gA^3 - kA^5$ is said to undergo a *tricritical bifurcation*

when $g = 0$; this case is the borderline between supercritical and subcritical bifurcations. Find the relation between A^* and ε when $g = 0$.

- c) In experiments on Taylor–Couette vortex flow, Aitta et al. (1985) were able to change the parameter g continuously from positive to negative by varying the aspect ratio of their experimental set-up. Assuming that the equation is modified to $\tau \dot{A} = h + \varepsilon A - gA^3 - kA^5$, where $h > 0$ is a slight imperfection, sketch the bifurcation diagram of A^* vs. ε in the three cases $g > 0$, $g = 0$, and $g < 0$. Then look up the actual data in Aitta et al. (1985, Figure 2) or see Ahlers (1989, Figure 15).
- d) In the experiments of part (c), the amplitude $A(t)$ was found to evolve toward a steady state in the manner shown in Figure 2 (redrawn from Ahlers (1989), Figure 18). The results are for the imperfect subcritical case $g < 0$, $h \neq 0$. In the experiments, the parameter ε was switched at $t = 0$ from a negative value to a positive value ε_f . In Figure 2, ε_f increases from the bottom to the top.

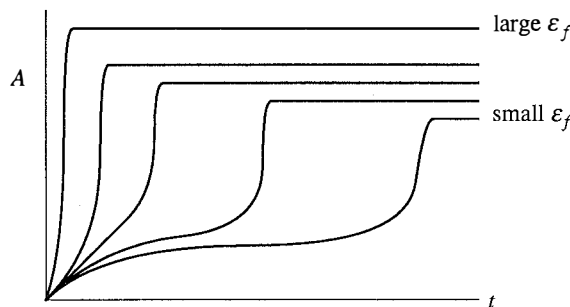


Figure 2

Explain intuitively why the curves have this strange shape. Why do the curves for large ε_f go almost straight up to their steady state, whereas the curves for small ε_f rise to a plateau before increasing sharply to their final level? (Hint: Graph \dot{A} vs. A for different ε_f .)

3.6.7 (Simple model of a magnet) A magnet can be modeled as an enormous collection of electronic spins. In the simplest model, known as the **Ising model**, the spins can point only up or down, and are assigned the values $S_i = \pm 1$, for $i = 1, \dots, N \gg 1$. For quantum mechanical reasons, the spins like to point in the same direction as their neighbors; on the other hand, the randomizing effects of temperature tend to disrupt any such alignment.

An important macroscopic property of the magnet is its average spin or *magnetization*

$$m = \left| \frac{1}{N} \sum_{i=1}^N S_i \right|.$$

At high temperature the spins point in random directions and so $m \approx 0$; the material is in the *paramagnetic* state. As the temperature is lowered, m remains near zero until a critical temperature T_c is reached. Then a ***phase transition*** occurs and the material spontaneously magnetizes. Now $m > 0$; we have a *ferromagnet*.

But the symmetry between up and down spins means that there are *two* possible ferromagnetic states. This symmetry can be broken by applying an external magnetic field h , which favors either the up or down direction. Then, in an approximation called *mean-field theory*, the equation governing the equilibrium value of m is

$$h = T \tanh^{-1} m - J n m$$

where J and n are constants; $J > 0$ is the ferromagnetic coupling strength and n is the number of neighbors of each spin (Ma 1985, p. 459).

- Analyze the solutions m^* of $h = T \tanh^{-1} m - J n m$, using a graphical approach.
- For the special case $h = 0$, find the critical temperature T_c at which a phase transition occurs.

3.7 Insect Outbreak

3.7.1 (Warm-up question about insect outbreak model) Show that the fixed point $x^* = 0$ is *always unstable* for Equation (3.7.3).

3.7.2 (Bifurcation curves for insect outbreak model)

- Using Equations (3.7.8) and (3.7.9), sketch $r(x)$ and $k(x)$ vs. x . Determine the limiting behavior of $r(x)$ and $k(x)$ as $x \rightarrow 1$ and $x \rightarrow \infty$.
- Find the exact values of r , k , and x at the cusp point shown in Figure 3.7.5.

3.7.3 (A model of a fishery) The equation $\dot{N} = rN(1 - \frac{N}{K}) - H$ provides an extremely simple model of a fishery. In the absence of fishing, the population is assumed to grow logistically. The effects of fishing are modeled by the term $-H$, which says that fish are caught or “harvested” at a constant rate $H > 0$, independent of their population N . (This assumes that the fishermen aren’t worried about fishing the population dry—they simply catch the same number of fish every day.)

- Show that the system can be rewritten in dimensionless form as

$$\frac{dx}{d\tau} = x(1 - x) - h,$$

for suitably defined dimensionless quantities x , τ , and h .

- Plot the vector field for different values of h .
- Show that a bifurcation occurs at a certain value h_c , and classify this bifurcation.
- Discuss the long-term behavior of the fish population for $h < h_c$ and $h > h_c$, and give the biological interpretation in each case.

There’s something silly about this model—the population can become nega-

tive! A better model would have a fixed point at zero population for all values of H . See the next exercise for such an improvement.

3.7.4 (Improved model of a fishery) A refinement of the model in the last exercise is

$$\dot{N} = rN\left(1 - \frac{N}{K}\right) - H \frac{N}{A + N}$$

where $H > 0$ and $A > 0$. This model is more realistic in two respects: it has a fixed point at $N = 0$ for all values of the parameters, and the rate at which fish are caught decreases with N . This is plausible—when fewer fish are available, it is harder to find them and so the daily catch drops.

- a) Give a biological interpretation of the parameter A ; what does it measure?
- b) Show that the system can be rewritten in dimensionless form as

$$\frac{dx}{d\tau} = x(1-x) - h \frac{x}{a+x},$$

for suitably defined dimensionless quantities x , τ , a , and h .

- c) Show that the system can have one, two, or three fixed points, depending on the values of a and h . Classify the stability of the fixed points in each case.
- d) Analyze the dynamics near $x = 0$ and show that a bifurcation occurs when $h = a$. What type of bifurcation is it?
- e) Show that another bifurcation occurs when $h = \frac{1}{4}(a+1)^2$, for $a < a_c$, where a_c is to be determined. Classify this bifurcation.
- f) Plot the stability diagram of the system in (a, h) parameter space. Can hysteresis occur in any of the stability regions?

3.7.5 (A biochemical switch) Zebra stripes and butterfly wing patterns are two of the most spectacular examples of biological pattern formation. Explaining the development of these patterns is one of the outstanding problems of biology; see Murray (1989) for an excellent review of our current knowledge.

As one ingredient in a model of pattern formation, Lewis et al. (1977) considered a simple example of a biochemical switch, in which a gene G is activated by a biochemical signal substance S . For example, the gene may normally be inactive but can be “switched on” to produce a pigment or other gene product when the concentration of S exceeds a certain threshold. Let $g(t)$ denote the concentration of the gene product, and assume that the concentration s_0 of S is fixed. The model is

$$\dot{g} = k_1 s_0 - k_2 g + \frac{k_3 g^2}{k_4^2 + g^2}$$

where the k 's are positive constants. The production of g is stimulated by s_0 at a

rate k_1 , and by an *autocatalytic* or positive feedback process (the nonlinear term). There is also a linear degradation of g at a rate k_2 .

- a) Show that the system can be put in the dimensionless form

$$\frac{dx}{d\tau} = s - rx + \frac{x^2}{1+x^2}$$

where $r > 0$ and $s \geq 0$ are dimensionless groups.

- b) Show that if $s = 0$, there are two positive fixed points x^* if $r < r_c$, where r_c is to be determined.
- c) Assume that initially there is no gene product, i.e., $g(0) = 0$, and suppose s is slowly increased from zero (the activating signal is turned on); what happens to $g(t)$? What happens if s then goes back to zero? Does the gene turn off again?
- d) Find parametric equations for the bifurcation curves in (r, s) space, and classify the bifurcations that occur.
- e) Use the computer to give a quantitatively accurate plot of the stability diagram in (r, s) space.

For further discussion of this model, see Lewis et al. (1977); Edelstein-Keshet (1988), Section 7.5; or Murray (1989), Chapter 15.

3.7.6 (Model of an epidemic) In pioneering work in epidemiology, Kermack and McKendrick (1927) proposed the following simple model for the evolution of an epidemic. Suppose that the population can be divided into three classes: $x(t)$ = number of healthy people; $y(t)$ = number of sick people; $z(t)$ = number of dead people. Assume that the total population remains constant in size, except for deaths due to the epidemic. (That is, the epidemic evolves so rapidly that we can ignore the slower changes in the populations due to births, emigration, or deaths by other causes.)

Then the model is

$$\begin{aligned}\dot{x} &= -kxy \\ \dot{y} &= kxy - \ell y \\ \dot{z} &= \ell y\end{aligned}$$

where k and ℓ are positive constants. The equations are based on two assumptions:

- (i) Healthy people get sick at a rate proportional to the product of x and y . This would be true if healthy and sick people encounter each other at a rate proportional to their numbers, and if there were a constant probability that each such encounter would lead to transmission of the disease.
- (ii) Sick people die at a constant rate ℓ .

The goal of this exercise is to reduce the model, which is a *third-order system*, to a first-order system that can be analyzed by our methods. (In Chapter 6 we will see

a simpler analysis.)

- a) Show that $x + y + z = N$, where N is constant.
- b) Use the \dot{x} and \dot{z} equation to show that $x(t) = x_0 \exp(-kz(t)/\ell)$, where $x_0 = x(0)$.
- c) Show that z satisfies the first-order equation $\dot{z} = \ell[N - z - x_0 \exp(-kz/\ell)]$.
- d) Show that this equation can be nondimensionalized to

$$\frac{du}{d\tau} = a - bu - e^{-u}$$

by an appropriate rescaling.

- e) Show that $a \geq 1$ and $b > 0$.
- f) Determine the number of fixed points u^* and classify their stability.
- g) Show that the maximum of $\dot{u}(t)$ occurs at the same time as the maximum of both $\dot{z}(t)$ and $y(t)$. (This time is called the *peak* of the epidemic, denoted t_{peak} . At this time, there are more sick people and a higher daily death rate than at any other time.)
- h) Show that if $b < 1$, then $\dot{u}(t)$ is increasing at $t = 0$ and reaches its maximum at some time $t_{\text{peak}} > 0$. Thus things get worse before they get better. (The term *epidemic* is reserved for this case.) Show that $\dot{u}(t)$ eventually decreases to 0.
- i) On the other hand, show that $t_{\text{peak}} = 0$ if $b > 1$. (Hence no epidemic occurs if $b > 1$.)
- j) The condition $b = 1$ is the *threshold* condition for an epidemic to occur. Can you give a biological interpretation of this condition?
- k) Kermack and McKendrick showed that their model gave a good fit to data from the Bombay plague of 1906. How would you improve the model to make it more appropriate for AIDS? Which assumptions need revising?

For an introduction to models of epidemics, see Murray (1989), Chapter 19, or Edelstein-Keshet (1988). Models of AIDS are discussed by Murray (1989) and May and Anderson (1987). An excellent review and commentary on the Kermack–McKendrick papers is given by Anderson (1991).

4

FLOWS ON THE CIRCLE

4.0 Introduction

So far we've concentrated on the equation $\dot{x} = f(x)$, which we visualized as a vector field on the line. Now it's time to consider a new kind of differential equation and its corresponding phase space. This equation,

$$\dot{\theta} = f(\theta),$$

corresponds to a *vector field on the circle*. Here θ is a point on the circle and $\dot{\theta}$ is the velocity vector at that point, determined by the rule $\dot{\theta} = f(\theta)$. Like the line, the circle is one-dimensional, but it has an important new property: by flowing in one direction, a particle can eventually return to its starting place (Figure 4.0.1). Thus periodic solutions become possible for the first time in this book! To put it another way, *vector fields on the circle provide the most basic model of systems that can oscillate*.

However, in all other respects, flows on the circle are similar to flows on the line, so this will be a short chapter. We will discuss the dynamics of some simple oscillators, and then show that these equations arise in a wide variety of applications. For example, the flashing of fireflies and the voltage oscillations of superconducting Josephson junctions have been modeled by the same equation, even though their oscillation frequencies differ by about ten orders of magnitude!

4.1 Examples and Definitions

Let's begin with some examples, and then give a more careful definition of vector fields on the circle.

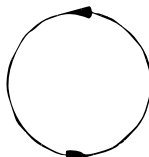


Figure 4.0.1

EXAMPLE 4.1.1:

Sketch the vector field on the circle corresponding to $\dot{\theta} = \sin \theta$.

Solution: We assign coordinates to the circle in the usual way, with $\theta = 0$ in the direction of “east,” and with θ increasing counterclockwise.

To sketch the vector field, we first find the fixed points, defined by $\dot{\theta} = 0$. These occur at $\theta^* = 0$ and $\theta^* = \pi$. To determine their stability, note that $\sin \theta > 0$ on the upper semicircle. Hence $\dot{\theta} > 0$, so the flow is counterclockwise. Similarly,

the flow is clockwise on the lower semicircle, where $\dot{\theta} < 0$. Hence $\theta^* = \pi$ is stable and $\theta^* = 0$ is unstable, as shown in Figure 4.1.1.

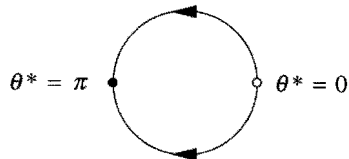


Figure 4.1.1

Actually, we've seen this example before—it's given in Section 2.1. There we regarded $\dot{x} = \sin x$ as a vector field on the *line*. Compare Figure 2.1.1 with Figure 4.1.1 and notice how much clearer it is to think of this system as a vector field on the circle. ■

EXAMPLE 4.1.2:

Explain why $\dot{\theta} = \theta$ cannot be regarded as a vector field on the circle, for θ in the range $-\infty < \theta < \infty$.

Solution: The velocity is not uniquely defined. For example, $\theta = 0$ and $\theta = 2\pi$ are two labels for the same point on the circle, but the first label implies a velocity of 0 at that point, while the second implies a velocity of 2π . ■

If we try to avoid this non-uniqueness by restricting θ to the range $-\pi < \theta \leq \pi$, then the velocity vector jumps discontinuously at the point corresponding to $\theta = \pi$. Try as we might, there's no way to consider $\dot{\theta} = \theta$ as a smooth vector field on the entire circle.

Of course, there's no problem regarding $\dot{\theta} = \theta$ as a vector field on the *line*, because then $\theta = 0$ and $\theta = 2\pi$ are different points, and so there's no conflict about how to define the velocity at each of them.

Example 4.1.2 suggests how to define vector fields on the circle. Here's a geometric definition: A **vector field on the circle** is a rule that assigns a unique velocity vector to each point on the circle.

In practice, such vector fields arise when we have a first-order system $\dot{\theta} = f(\theta)$, where $f(\theta)$ is a real-valued, 2π -periodic function. That is, $f(\theta + 2\pi) = f(\theta)$ for all real θ . Moreover, we assume (as usual) that $f(\theta)$ is smooth enough to guarantee existence and uniqueness of solutions. Although this system could be regarded as a special case of a vector field on the line, it is usually clearer to think of it as a vector field on the circle (as in Example 4.1.1). This means that we don't distin-

guish between θ 's that differ by an integer multiple of 2π . Here's where the periodicity of $f(\theta)$ becomes important—it ensures that the velocity $\dot{\theta}$ is uniquely defined at each point θ on the circle, in the sense that $\dot{\theta}$ is the same, whether we call that point θ or $\theta + 2\pi$, or $\theta + 2\pi k$ for any integer k .

4.2 Uniform Oscillator

A point on a circle is often called an *angle* or a *phase*. Then the simplest oscillator of all is one in which the phase θ changes uniformly:

$$\dot{\theta} = \omega$$

where ω is a constant. The solution is

$$\theta(t) = \omega t + \theta_0,$$

which corresponds to uniform motion around the circle at an angular frequency ω . This solution is *periodic*, in the sense that $\theta(t)$ changes by 2π , and therefore returns to the same point on the circle, after a time $T = 2\pi/\omega$. We call T the *period* of the oscillation.

Notice that we have said nothing about the *amplitude* of the oscillation. There really is no amplitude variable in our system. If we had an amplitude as well as a phase variable, we'd be in a *two-dimensional* phase space; this situation is more complicated and will be discussed later in the book. (Or if you prefer, you can imagine that the oscillation occurs at some *fixed* amplitude, corresponding to the radius of our circular phase space. In any case, amplitude plays no role in the dynamics.)

EXAMPLE 4.2.1:

Two joggers, Speedy and Pokey, are running at a steady pace around a circular track. It takes Speedy T_1 seconds to run once around the track, whereas it takes Pokey $T_2 > T_1$ seconds. Of course, Speedy will periodically overtake Pokey; how long does it take for Speedy to lap Pokey once, assuming that they start together?

Solution: Let $\theta_i(t)$ be Speedy's position on the track. Then $\dot{\theta}_i = \omega_i$ where $\omega_i = 2\pi/T_i$. This equation says that Speedy runs at a steady pace and completes

a circuit every T_i seconds. Similarly, suppose that $\dot{\theta}_2 = \omega_2 = 2\pi/T_2$ for Pokey.

The condition for Speedy to lap Pokey is that the angle between them has increased by 2π . Thus if we define the *phase difference* $\phi = \theta_1 - \theta_2$, we want to find how long it takes for ϕ to increase by 2π (Figure 4.2.1). By subtraction we find $\dot{\phi} = \dot{\theta}_1 - \dot{\theta}_2 = \omega_1 - \omega_2$. Thus ϕ increases by 2π after a time

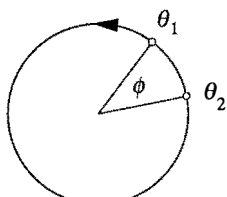


Figure 4.2.1

$$T_{\text{lap}} = \frac{2\pi}{\omega_1 - \omega_2} = \left(\frac{1}{T_1} - \frac{1}{T_2} \right)^{-1}.$$

Example 4.2.1 illustrates an effect called the ***beat phenomenon***. Two noninteracting oscillators with different frequencies will periodically go in and out of phase with each other. You may have heard this effect on a Sunday morning: sometimes the bells of two different churches will ring simultaneously, then slowly drift apart, and then eventually ring together again. If the oscillators *interact* (for example, if the two joggers try to stay together or the bell ringers can hear each other), then we can get more interesting effects, as we will see in Section 4.5 on the flashing rhythm of fireflies.

4.3 Nonuniform Oscillator

The equation

$$\dot{\theta} = \omega - a \sin \theta \quad (1)$$

arises in many different branches of science and engineering. Here is a partial list:

Electronics (phase-locked loops)

Biology (oscillating neurons, firefly flashing rhythm, human sleep-wake cycle)

Condensed-matter physics (Josephson junction, charge-density waves)

Mechanics (Overdamped pendulum driven by a constant torque)

Some of these applications will be discussed later in this chapter and in the exercises.

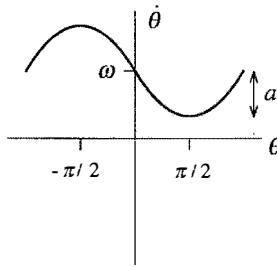


Figure 4.3.1

To analyze (1), we assume that $\omega > 0$ and $a \geq 0$ for convenience; the results for negative ω and a are similar. A typical graph of $f(\theta) = \omega - a \sin \theta$ is shown in Figure 4.3.1. Note that ω is the mean and a is the amplitude.

Vector Fields

If $a = 0$, (1) reduces to the uniform oscillator. The parameter a introduces a

nonuniformity in the flow around the circle: the flow is fastest at $\theta = -\pi/2$ and slowest at $\theta = \pi/2$ (Figure 4.3.2a). This nonuniformity becomes more pronounced as a increases. When a is slightly less than ω , the oscillation is very jerky: the phase point $\theta(t)$ takes a long time to pass through a *bottleneck* near $\theta = \pi/2$, after which it zips around the rest of the circle on a much faster time scale. When $a = \omega$, the system stops oscillating altogether: a half-stable fixed point has been born in a *saddle-node bifurcation* at $\theta = \pi/2$ (Figure 4.3.2b). Finally, when $a > \omega$, the half-stable fixed point splits into a stable and unstable fixed point (Figure 4.3.2c). All trajectories are attracted to the stable fixed point as $t \rightarrow \infty$.

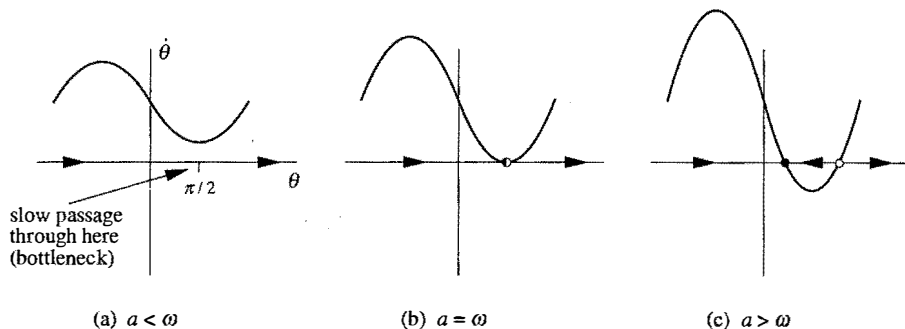


Figure 4.3.2

The same information can be shown by plotting the vector fields on the circle (Figure 4.3.3).

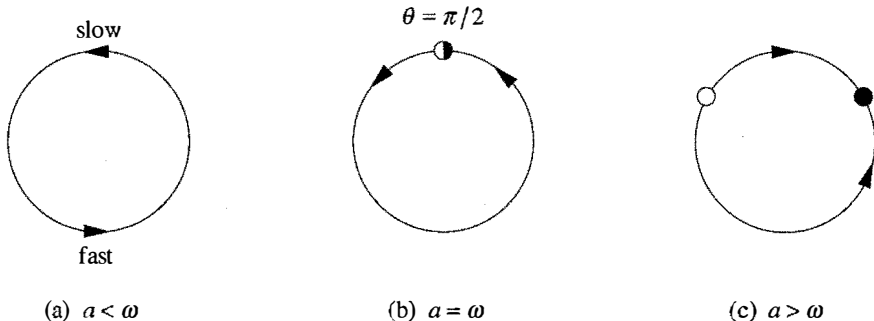


Figure 4.3.3

EXAMPLE 4.3.1:

Use linear stability analysis to classify the fixed points of (1) for $a > \omega$.

Solution: The fixed points θ^* satisfy

$$\sin \theta^* = \omega/a, \quad \cos \theta^* = \pm \sqrt{1 - (\omega/a)^2}.$$

Their linear stability is determined by

$$f'(\theta^*) = -a \cos \theta^* = \mp a \sqrt{1 - (\omega/a)^2}.$$

Thus the fixed point with $\cos \theta^* > 0$ is the stable one, since $f'(\theta^*) < 0$. This agrees with Figure 4.3.2c. ■

Oscillation Period

For $a < \omega$, the period of the oscillation can be found analytically, as follows: the time required for θ to change by 2π is given by

$$T = \int dt = \int_0^{2\pi} \frac{dt}{d\theta} d\theta$$

$$= \int_0^{2\pi} \frac{d\theta}{\omega - a \sin \theta}$$

where we have used (1) to replace $dt/d\theta$. This integral can be evaluated by complex variable methods, or by the substitution $u = \tan \frac{\theta}{2}$. (See Exercise 4.3.2 for details.) The result is

$$T = \frac{2\pi}{\sqrt{\omega^2 - a^2}}. \quad (2)$$

Figure 4.3.4 shows the graph of T as a function of a .

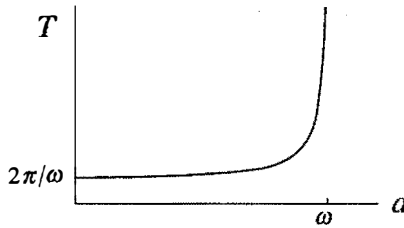


Figure 4.3.4

When $a = 0$, Equation (2) reduces to $T = 2\pi/\omega$, the familiar result for a uniform oscillator. The period increases with a and diverges as a approaches ω from below (we denote this limit by $a \rightarrow \omega^-$).

We can estimate the order of the divergence by noting that

$$\begin{aligned} \sqrt{\omega^2 - a^2} &= \sqrt{\omega + a} \sqrt{\omega - a} \\ &\approx \sqrt{2\omega} \sqrt{\omega - a} \end{aligned}$$

as $a \rightarrow \omega^-$. Hence

$$T = \left(\frac{\pi\sqrt{2}}{\sqrt{\omega}} \right) \frac{1}{\sqrt{\omega - a}}, \quad (3)$$

which shows that T blows up like $(a_c - a)^{-1/2}$, where $a_c = \omega$. Now let's explain the origin of this **square-root scaling law**.

Ghosts and Bottlenecks

The square-root scaling law found above is a *very general feature of systems that are close to a saddle-node bifurcation*. Just after the fixed points collide, there is a saddle-node remnant or **ghost** that leads to slow passage through a bottleneck.

For example, consider $\dot{\theta} = \omega - a \sin \theta$ for decreasing values of a , starting with $a > \omega$. As a decreases, the two fixed points approach each other, collide, and disappear (this sequence was shown earlier in Figure 4.3.3, except now you have to read from right to left.) For a slightly less than ω , the fixed points near $\pi/2$ no longer exist, but they still make themselves felt through a saddle-node ghost (Figure 4.3.5).

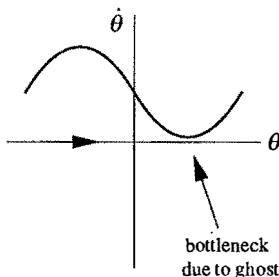


Figure 4.3.5

A graph of $\theta(t)$ would have the shape shown in Figure 4.3.6. Notice how the trajectory spends practically all its time getting through the bottleneck.

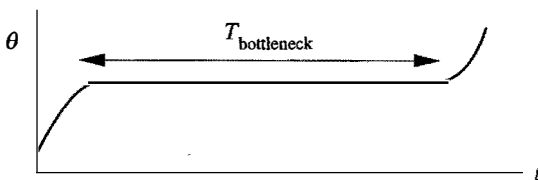


Figure 4.3.6

Now we want to derive a general scaling law for the time required to pass through a bottleneck. The only thing that matters is the behavior of θ in the immediate vicinity of the minimum, since the time spent there dominates all other time

scales in the problem. Generically, $\dot{\theta}$ looks *parabolic* near its minimum. Then the problem simplifies tremendously: the dynamics can be reduced to the normal form for a saddle-node bifurcation! By a local rescaling of space, we can rewrite the vector field as

$$\dot{x} = r + x^2$$

where r is proportional to the distance from the bifurcation, and $0 < r \ll 1$. The graph of \dot{x} is shown in Figure 4.3.7.

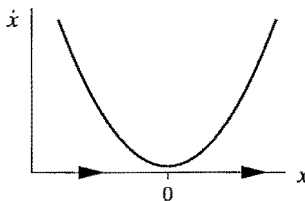


Figure 4.3.7

To estimate the time spent in the bottleneck, we calculate the time taken for x to go from $-\infty$ (all the way on one side of the bottleneck) to $+\infty$ (all the way on the other side). The result is

$$T_{\text{bottleneck}} \approx \int_{-\infty}^{\infty} \frac{dx}{r + x^2} = \frac{\pi}{\sqrt{r}}, \quad (4)$$

which shows the generality of the square-root scaling law. (Exercise 4.3.1 reminds you how to evaluate the integral in (4).)

EXAMPLE 4.3.2:

Estimate the period of $\dot{\theta} = \omega - a \sin \theta$ in the limit $a \rightarrow \omega^-$, using the normal form method instead of the exact result.

Solution: The period will be essentially the time required to get through the bottleneck. To estimate this time, we use a Taylor expansion about $\theta = \pi/2$, where the bottleneck occurs. Let $\phi = \theta - \pi/2$, where ϕ is small. Then

$$\begin{aligned}\dot{\phi} &= \omega - a \sin(\phi + \frac{\pi}{2}) \\ &= \omega - a \cos \phi \\ &= \omega - a + \frac{1}{2} a \phi^2 + \dots\end{aligned}$$

which is close to the desired normal form. If we let

$$x = (a/2)^{1/2} \phi, \quad r = \omega - a$$

then $(2/a)^{1/2} \dot{x} \approx r + x^2$, to leading order in x . Separating variables yields

$$T \approx (2/a)^{1/2} \int_{-\infty}^{\infty} \frac{dx}{r+x^2} = (2/a)^{1/2} \frac{\pi}{\sqrt{r}}.$$

Now we substitute $r = \omega - a$. Furthermore, since $a \rightarrow \omega^-$, we may replace $2/a$ by $2/\omega$. Hence

$$T \approx \left(\frac{\pi \sqrt{2}}{\sqrt{\omega}} \right) \frac{1}{\sqrt{\omega - a}},$$

which agrees with (3). ■

4.4 Overdamped Pendulum

We now consider a simple mechanical example of a nonuniform oscillator: an overdamped pendulum driven by a constant torque. Let θ denote the angle between the pendulum and the downward vertical, and suppose that θ increases counterclockwise (Figure 4.4.1).

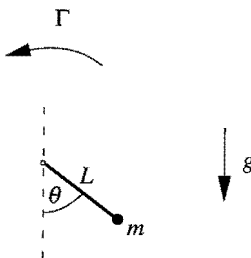


Figure 4.4.1

Then Newton's law yields

$$mL^2\ddot{\theta} + b\dot{\theta} + mgL\sin\theta = \Gamma \quad (1)$$

where m is the mass and L is the length of the pendulum, b is a viscous damping constant, g is the acceleration due to gravity, and Γ is a constant applied torque. All of these parameters are positive. In particular, $\Gamma > 0$ implies that the applied torque drives the pendulum counterclockwise, as shown in Figure 4.4.1.

Equation (1) is a second-order system, but in the *overdamped limit* of extremely large b , it may be approximated by a first-order system (see Section 3.5 and Exercise 4.4.1). In this limit the inertia term $mL^2\ddot{\theta}$ is negligible and so (1) becomes

$$b\dot{\theta} + mgL\sin\theta = \Gamma. \quad (2)$$

To think about this problem physically, you should imagine that the pendulum is immersed in molasses. The torque Γ enables the pendulum to plow through its vis-

cous surroundings. Please realize that this is the *opposite* limit from the familiar frictionless case in which energy is conserved, and the pendulum swings back and forth forever. In the present case, energy is lost to damping and pumped in by the applied torque.

To analyze (2), we first nondimensionalize it. Dividing by mgL yields

$$\frac{b}{mgL}\dot{\theta} = \frac{\Gamma}{mgL} - \sin \theta.$$

Hence, if we let

$$\tau = \frac{mgL}{b}t, \quad \gamma = \frac{\Gamma}{mgL} \quad (3)$$

then

$$\theta' = \gamma - \sin \theta \quad (4)$$

where $\theta' = d\theta/d\tau$.

The dimensionless group γ is the ratio of the applied torque to the maximum gravitational torque. If $\gamma > 1$ then the applied torque can never be balanced by the gravitational torque and *the pendulum will overturn continually*. The rotation rate is nonuniform, since gravity helps the applied torque on one side and opposes it on the other (Figure 4.4.2).

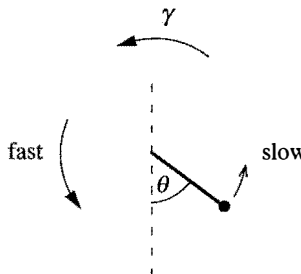


Figure 4.4.2

As $\gamma \rightarrow 1^+$, the pendulum takes longer and longer to climb past $\theta = \pi/2$ on the slow side. When $\gamma = 1$ a fixed point appears at $\theta^* = \pi/2$, and then splits into two when $\gamma < 1$ (Figure 4.4.3). On physical grounds, it's clear that the lower of the two equilibrium positions is the stable one.

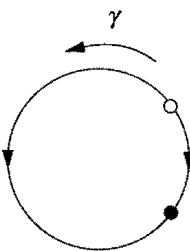


Figure 4.4.3

As γ decreases, the two fixed points move farther apart. Finally, when $\gamma = 0$, the applied torque vanishes and there is an unstable equilibrium at the top (inverted pendulum) and a stable equilibrium at the bottom.

4.5 Fireflies

Fireflies provide one of the most spectacular examples of synchronization in nature. In some parts of southeast Asia, thousands of male fireflies gather in trees at night and flash on and off in unison. Meanwhile the female fireflies cruise overhead, looking for males with a handsome light.

To really appreciate this amazing display, you have to see a movie or videotape of it. A good example is shown in David Attenborough's (1992) television series *The Trials of Life*, in the episode called "Talking to Strangers." See Buck and Buck (1976) for a beautifully written introduction to synchronous fireflies, and Buck (1988) for a more recent review. For mathematical models of synchronous fireflies, see Mirollo and Strogatz (1990) and Ermentrout (1991).

How does the synchrony occur? Certainly the fireflies don't start out synchronized; they arrive in the trees at dusk, and the synchrony builds up gradually as the night goes on. The key is that *the fireflies influence each other*: When one firefly sees the flash of another, it slows down or speeds up so as to flash more nearly in phase on the next cycle.

Hanson (1978) studied this effect experimentally, by periodically flashing a light at a firefly and watching it try to synchronize. For a range of periods close to the firefly's natural period (about 0.9 sec), the firefly was able to match its frequency to the periodic stimulus. In this case, one says that the firefly had been *entrained* by the stimulus. However, if the stimulus was too fast or too slow, the firefly could not keep up and entrainment was lost—then a kind of beat phenomenon occurred. But in contrast to the simple beat phenomenon of Section 4.2, the phase difference between stimulus and firefly did not increase uniformly. The phase difference increased slowly during part of the beat cycle, as the firefly struggled in vain to synchronize, and then it increased rapidly through 2π , after which

the firefly tried again on the next beat cycle. This process is called *phase walk-through* or *phase drift*.

Model

Ermentrout and Rinzel (1984) proposed a simple model of the firefly's flashing rhythm and its response to stimuli. Suppose that $\theta(t)$ is the phase of the firefly's flashing rhythm, where $\theta = 0$ corresponds to the instant when a flash is emitted. Assume that in the absence of stimuli, the firefly goes through its cycle at a frequency ω , according to $\dot{\theta} = \omega$.

Now suppose there's a periodic stimulus whose phase Θ satisfies

$$\dot{\Theta} = \Omega, \quad (1)$$

where $\Theta = 0$ corresponds to the flash of the stimulus. We model the firefly's response to this stimulus as follows: If the stimulus is ahead in the cycle, then we assume that the firefly speeds up in an attempt to synchronize. Conversely, the firefly slows down if it's flashing too early. A simple model that incorporates these assumptions is

$$\dot{\theta} = \omega + A \sin(\Theta - \theta) \quad (2)$$

where $A > 0$. For example, if Θ is ahead of θ (i.e., $0 < \Theta - \theta < \pi$) the firefly speeds up ($\dot{\theta} > \omega$). The *resetting strength* A measures the firefly's ability to modify its instantaneous frequency.

Analysis

To see whether entrainment can occur, we look at the dynamics of the phase difference $\phi = \Theta - \theta$. Subtracting (2) from (1) yields

$$\dot{\phi} = \dot{\Theta} - \dot{\theta} = \Omega - \omega - A \sin \phi, \quad (3)$$

which is a *nonuniform oscillator* equation for $\phi(t)$. Equation (3) can be nondimensionalized by introducing

$$\tau = At, \quad \mu = \frac{\Omega - \omega}{A}. \quad (4)$$

Then

$$\phi' = \mu - \sin \phi \quad (5)$$

where $\phi' = d\phi/d\tau$. The dimensionless group μ is a measure of the frequency difference, relative to the resetting strength. When μ is small, the frequencies are relatively close together and we expect that entrainment should be possible. This is

confirmed by Figure 4.5.1, where we plot the vector fields for (5), for different values of $\mu \geq 0$. (The case $\mu < 0$ is similar.)

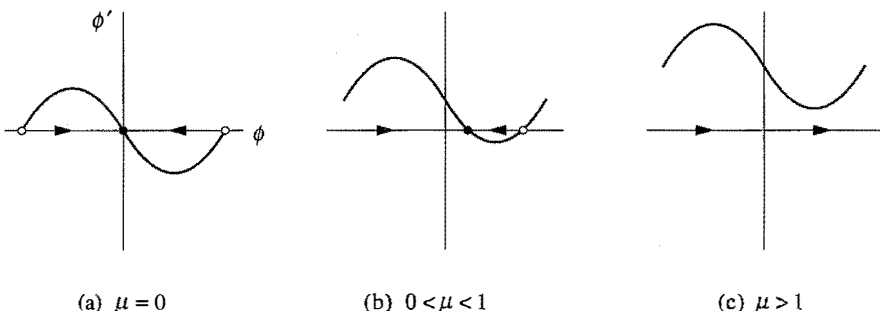


Figure 4.5.1

When $\mu = 0$, all trajectories flow toward a stable fixed point at $\phi^* = 0$ (Figure 4.5.1a). Thus the firefly eventually entrains with *zero phase difference* in the case $\Omega = \omega$. In other words, the firefly and the stimulus flash *simultaneously* if the firefly is driven at its natural frequency.

Figure 4.5.1b shows that for $0 < \mu < 1$, the curve in Figure 4.5.1a lifts up and the stable and unstable fixed points move closer together. All trajectories are still attracted to a stable fixed point, but now $\phi^* > 0$. Since the phase difference approaches a constant, one says that the firefly's rhythm is **phase-locked** to the stimulus.

Phase-locking means that the firefly and the stimulus run with the same instantaneous frequency, although they no longer flash in unison. The result $\phi^* > 0$ implies that the stimulus flashes *ahead* of the firefly in each cycle. This makes sense—we assumed $\mu > 0$, which means that $\Omega > \omega$; the stimulus is inherently faster than the firefly, and drives it faster than it wants to go. Thus the firefly falls behind. But it never gets lapped—it always lags in phase by a constant amount ϕ^* .

If we continue to increase μ , the stable and unstable fixed points eventually coalesce in a saddle-node bifurcation at $\mu = 1$. For $\mu > 1$ both fixed points have disappeared and now phase-locking is lost; the phase difference ϕ increases indefinitely, corresponding to *phase drift* (Figure 4.5.1c). (Of course, once ϕ reaches 2π the oscillators are in phase again.) Notice that the phases don't separate at a uniform rate, in qualitative agreement with the experiments of Hanson (1978): ϕ increases most slowly when it passes under the minimum of the sine wave in Figure 4.5.1c, at $\phi = \pi/2$, and most rapidly when it passes under the maximum at $\phi = -\pi/2$.

The model makes a number of specific and testable predictions. Entrainment is predicted to be possible only within a symmetric interval of driving frequencies, specifically $\omega - A \leq \Omega \leq \omega + A$. This interval is called the **range of entrainment** (Figure 4.5.2).

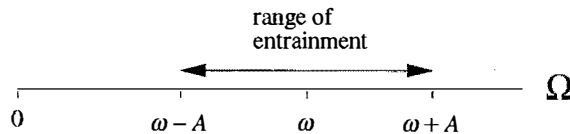


Figure 4.5.2

By measuring the range of entrainment experimentally, one can nail down the value of the parameter A . Then the model makes a rigid prediction for the phase difference during entrainment, namely

$$\sin \phi^* = \frac{\Omega - \omega}{A} \quad (6)$$

where $-\pi/2 \leq \phi^* \leq \pi/2$ corresponds to the *stable* fixed point of (3).

Moreover, for $\mu > 1$, the period of phase drift may be predicted as follows. The time required for ϕ to change by 2π is given by

$$T_{\text{drift}} = \int dt = \int_0^{2\pi} \frac{dt}{d\phi} d\phi \\ = \int_0^{2\pi} \frac{d\phi}{\Omega - \omega - A \sin \phi} .$$

To evaluate this integral, we invoke (2) of Section 4.3, which yields

$$T_{\text{drift}} = \frac{2\pi}{\sqrt{(\Omega - \omega)^2 - A^2}} . \quad (7)$$

Since A and ω are presumably fixed properties of the firefly, the predictions (6) and (7) could be tested simply by varying the drive frequency Ω . Such experiments have yet to be done.

Actually, the biological reality about synchronous fireflies is more complicated. The model presented here is reasonable for certain species, such as *Pteroptyx cribellata*, which behave as if A and ω were fixed. However, the species that is best at synchronizing, *Pteroptyx malaccae*, is actually able to shift its frequency ω toward the drive frequency Ω (Hanson 1978). In this way it is able to achieve nearly zero phase difference, even when driven at periods that differ from its natural period by ± 15 percent! A model of this remarkable effect has been presented by Ermentrout (1991).

4.6 Superconducting Josephson Junctions

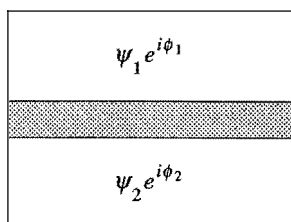
Josephson junctions are superconducting devices that are capable of generating voltage oscillations of extraordinarily high frequency, typically 10^{10} – 10^{11} cycles

per second. They have great technological promise as amplifiers, voltage standards, detectors, mixers, and fast switching devices for digital circuits. Josephson junctions can detect electric potentials as small as one quadrillionth of a volt, and they have been used to detect far-infrared radiation from distant galaxies. For an introduction to Josephson junctions, as well as superconductivity more generally, see Van Duzer and Turner (1981).

Although quantum mechanics is required to explain the *origin* of the Josephson effect, we can nevertheless describe the *dynamics* of Josephson junctions in classical terms. Josephson junctions have been particularly useful for experimental studies of nonlinear dynamics, because the equation governing a single junction is the same as that for a pendulum! In this section we will study the dynamics of a single junction in the overdamped limit. In later sections we will discuss underdamped junctions, as well as arrays of enormous numbers of junctions coupled together.

Physical Background

A Josephson junction consists of two closely spaced superconductors separated by a weak connection (Figure 4.6.1). This connection may be provided by an insulator, a normal metal, a semiconductor, a weakened superconductor, or some other



superconductor #1
weak coupling
superconductor #2

material that weakly couples the two superconductors. The two superconducting regions may be characterized by quantum mechanical wave functions $\psi_1 e^{i\phi_1}$ and $\psi_2 e^{i\phi_2}$ respectively. Normally a much more complicated description would be necessary because there are $\sim 10^{23}$ electrons to deal

Figure 4.6.1

with, but in the superconducting ground state, these electrons form “Cooper pairs” that can be described by a *single* macroscopic wave function. This implies an astonishing degree of coherence among the electrons. The Cooper pairs act like a miniature version of synchronous fireflies: they all adopt the same phase, because this turns out to minimize the energy of the superconductor.

As a 22-year-old graduate student, Brian Josephson (1962) suggested that it should be possible for a current to pass between the two superconductors, even if there were no voltage difference between them. Although this behavior would be impossible classically, it could occur because of quantum mechanical *tunneling* of Cooper pairs across the junction. An observation of this “Josephson effect” was made by Anderson and Rowell in 1963.

Incidentally, Josephson won the Nobel Prize in 1973, after which he lost interest in mainstream physics and was rarely heard from again. See Josephson (1982) for an interview in which he reminisces about his early work and discusses his

more recent interests in transcendental meditation, consciousness, language, and even psychic spoon-bending and paranormal phenomena.

The Josephson Relations

We now give a more quantitative discussion of the Josephson effect. Suppose that a Josephson junction is connected to a dc current source (Figure 4.6.2), so that

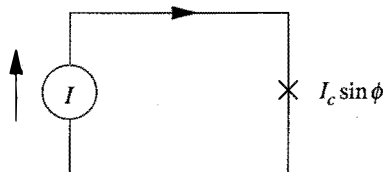


Figure 4.6.2

a constant current $I > 0$ is driven through the junction. Using quantum mechanics, one can show that if this current is less than a certain **critical current** I_c , no voltage will be developed across the junction; that is, the junction acts as if it had zero resistance! However, the phases of the two superconductors will be driven apart to a constant phase difference $\phi = \phi_2 - \phi_1$, where ϕ satisfies the *Josephson current-phase relation*

$$I = I_c \sin \phi. \quad (1)$$

Equation (1) implies that the phase difference increases as the **bias current** I increases.

When I exceeds I_c , a constant phase difference can no longer be maintained and a voltage develops across the junction. The phases on the two sides of the junction begin to slip with respect to each other, with the rate of slippage governed by the *Josephson voltage-phase relation*

$$V = \frac{\hbar}{2e} \dot{\phi}. \quad (2)$$

Here $V(t)$ is the instantaneous voltage across the junction, \hbar is Planck's constant divided by 2π , and e is the charge on the electron. For an elementary derivation of the Josephson relations (1) and (2), see Feynman's argument (Feynman et al. (1965), Vol. III), also reproduced in Van Duzer and Turner (1981).

Equivalent Circuit and Pendulum Analog

The relation (1) applies only to the *supercurrent* carried by the electron pairs. In general, the total current passing through the junction will also contain contributions from a *displacement current* and an *ordinary current*. Representing the displacement current by a capacitor, and the ordinary current by a resistor, we arrive at the equivalent circuit shown in Figure 4.6.3, first analyzed by Stewart (1968) and McCumber (1968).

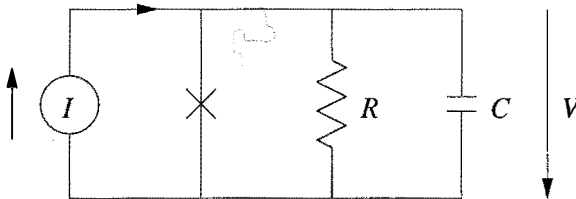


Figure 4.6.3

Now we apply Kirchhoff's voltage and current laws. For this parallel circuit, the voltage drop across each branch must be equal, and hence all the voltages are equal to V , the voltage across the junction. Hence the current through the capacitor equals CV and the current through the resistor equals V/R . The sum of these currents and the supercurrent $I_c \sin \phi$ must equal the bias current I ; hence

$$C\dot{V} + \frac{V}{R} + I_c \sin \phi = I. \quad (3)$$

Equation (3) may be rewritten solely in terms of the phase difference ϕ , thanks to (2). The result is

$$\frac{\hbar C}{2e} \ddot{\phi} + \frac{\hbar}{2eR} \dot{\phi} + I_c \sin \phi = I, \quad (4)$$

which is precisely analogous to the equation governing a damped pendulum driven by a constant torque! In the notation of Section 4.4, the pendulum equation is

$$mL^2 \ddot{\theta} + b\dot{\theta} + mgL \sin \theta = \Gamma.$$

Hence the analogies are as follows:

Pendulum	Josephson junction
Angle θ	Phase difference ϕ
Angular velocity $\dot{\theta}$	Voltage $\frac{\hbar}{2e} \dot{\phi}$
Mass m	Capacitance C
Applied torque Γ	Bias current I
Damping constant b	Conductance $1/R$
Maximum gravitational torque mgL	Critical current I_c

This mechanical analog has often proved useful in visualizing the dynamics of Josephson junctions. Sullivan and Zimmerman (1971) actually constructed such a mechanical analog, and measured the average rotation rate of the pendulum as a function of the applied torque; this is the analog of the physically important $I - V$ curve (current-voltage curve) for the Josephson junction.

Typical Parameter Values

Before analyzing (4), we mention some typical parameter values for Josephson junctions. The critical current is typically in the range $I_c \approx 1 \mu\text{A} - 1 \text{ mA}$, and a typical voltage is $I_c R \approx 1 \text{ mV}$. Since $2e/h \approx 4.83 \times 10^{14} \text{ Hz/V}$, a typical frequency is on the order of 10^{11} Hz . Finally, a typical length scale for Josephson junctions is around $1 \mu\text{m}$, but this depends on the geometry and the type of coupling used.

Dimensionless Formulation

If we divide (4) by I_c and define a dimensionless time

$$\tau = \frac{2eI_c R}{\hbar} t, \quad (5)$$

we obtain the dimensionless equation

$$\beta\phi'' + \phi' + \sin \phi = \frac{I}{I_c} \quad (6)$$

where $\phi' = d\phi/d\tau$. The dimensionless group β is defined by

$$\beta = \frac{2eI_c R^2 C}{\hbar}.$$

and is called the *McCumber parameter*. It may be thought of as a dimensionless capacitance. Depending on the size, the geometry, and the type of coupling used in the Josephson junction, the value of β can range from $\beta \approx 10^{-6}$ to much larger values ($\beta \approx 10^6$).

We are not yet prepared to analyze (6) in general. For now, let's restrict ourselves to the *overdamped limit* $\beta \ll 1$. Then the term $\beta\phi''$ may be neglected after a rapid initial transient, as discussed in Section 3.5, and so (6) reduces to a nonuniform oscillator:

$$\phi' = \frac{I}{I_c} - \sin \phi. \quad (7)$$

As we know from Section 4.3, the solutions of (7) tend to a stable fixed point when $I < I_c$, and vary periodically when $I > I_c$.

EXAMPLE 4.6.1:

Find the *current–voltage curve* analytically in the overdamped limit. In other words, find the average value of the voltage $\langle V \rangle$ as a function of the constant applied current I , assuming that all transients have decayed and the system has

reached steady-state operation. Then plot $\langle V \rangle$ vs. I .

Solution: It is sufficient to find $\langle \phi' \rangle$, since $\langle V \rangle = (\hbar/2e)\langle \dot{\phi} \rangle$ from the voltage-phase relation (2), and

$$\langle \dot{\phi} \rangle = \left\langle \frac{d\phi}{dt} \right\rangle = \left\langle \frac{d\tau}{dt} \frac{d\phi}{d\tau} \right\rangle = \frac{2eI_c R}{\hbar} \langle \phi' \rangle,$$

from the definition of τ in (5); hence

$$\langle V \rangle = I_c R \langle \phi' \rangle. \quad (8)$$

There are two cases to consider. When $I \leq I_c$, all solutions of (7) approach a fixed point $\phi^* = \sin^{-1}(I/I_c)$, where $-\pi/2 \leq \phi^* \leq \pi/2$. Thus $\phi' = 0$ in steady state, and so $\langle V \rangle = 0$ for $I \leq I_c$.

When $I > I_c$, all solutions of (7) are periodic with period

$$T = \frac{2\pi}{\sqrt{(I/I_c)^2 - 1}}, \quad (9)$$

where the period is obtained from (2) of Section 4.3, and time is measured in units of τ . We compute $\langle \phi' \rangle$ by taking the average over one cycle:

$$\langle \phi' \rangle = \frac{1}{T} \int_0^T \frac{d\phi}{d\tau} d\tau = \frac{1}{T} \int_0^{2\pi} d\phi = \frac{2\pi}{T}. \quad (10)$$

Combining (8)–(10) yields

$$\langle V \rangle = I_c R \sqrt{(I/I_c)^2 - 1} \quad \text{for } I > I_c.$$

In summary, we have found

$$\langle V \rangle = \begin{cases} 0 & \text{for } I \leq I_c \\ I_c R \sqrt{(I/I_c)^2 - 1} & \text{for } I > I_c. \end{cases} \quad (11)$$

The I - V curve (11) is shown in Figure 4.6.4.

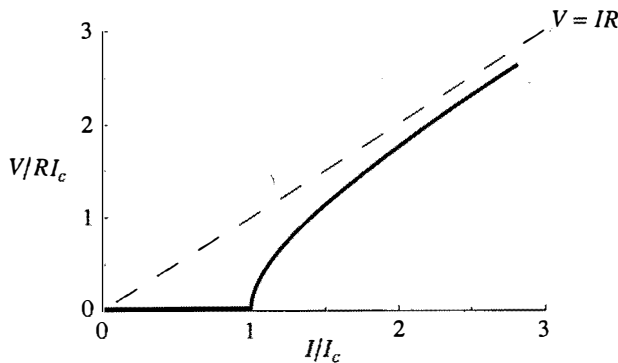


Figure 4.6.4

As I increases, the voltage remains zero until $I > I_c$; then $\langle V \rangle$ rises sharply and eventually asymptotes to the Ohmic behavior $\langle V \rangle \approx IR$ for $I \gg I_c$. ■

The analysis given in Example 4.6.1 applies only to the overdamped limit $\beta \ll 1$. The behavior of the system becomes much more interesting if β is not negligible. In particular, the I - V curve can be **hysteretic**, as shown in Figure 4.6.5. As the bias current is increased slowly from $I = 0$, the voltage remains at $V = 0$ until $I > I_c$. Then the voltage jumps up to a nonzero value, as shown by the upward arrow in Figure 4.6.5. The voltage increases with further increases of I . However, if we now slowly *decrease* I , the voltage doesn't drop back to zero at I_c —we have to go *below* I_c before the voltage returns to zero.

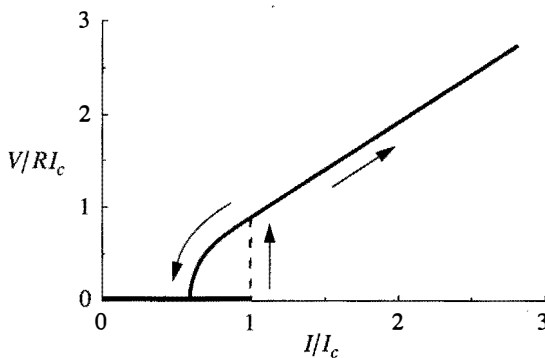


Figure 4.6.5

The hysteresis comes about because the system has **inertia** when $\beta \neq 0$. We can make sense of this by thinking in terms of the pendulum analog. The critical current I_c is analogous to the critical torque Γ_c needed to get the pendulum overturning. Once the pendulum has started whirling, its inertia keeps it going so that even if the torque is lowered *below* Γ_c , the rotation continues. The torque has to be low-

ered even further before the pendulum will fail to make it over the top.

In more mathematical terms, we'll show in Section 8.5 that this hysteresis occurs because a *stable fixed point coexists with a stable periodic solution*. We have never seen anything like *this* before! For vector fields on the line, only fixed points can exist; for vector fields on the circle, both fixed points and periodic solutions can exist, *but not simultaneously*. Here we see just one example of the new kinds of phenomena that can occur in two-dimensional systems. It's time to take the plunge.

EXERCISES FOR CHAPTER 4

4.1 Examples and Definitions

4.1.1 For which real values of a does the equation $\dot{\theta} = \sin(a\theta)$ give a well-defined vector field on the circle?

For each of the following vector fields, find and classify all the fixed points, and sketch the phase portrait on the circle.

4.1.2 $\dot{\theta} = 1 + 2 \cos \theta$

4.1.3 $\dot{\theta} = \sin 2\theta$

4.1.4 $\dot{\theta} = \sin^3 \theta$

4.1.5 $\dot{\theta} = \sin \theta + \cos \theta$

4.1.6 $\dot{\theta} = 3 + \cos 2\theta$

4.1.7 $\dot{\theta} = \sin k\theta$ where k is a positive integer.

4.1.8 (Potentials for vector fields on the circle)

- Consider the vector field on the circle given by $\dot{\theta} = \cos \theta$. Show that this system has a single-valued potential $V(\theta)$, i.e., for each point on the circle, there is a well-defined value of V such that $\dot{\theta} = -dV/d\theta$. (As usual, θ and $\theta + 2\pi k$ are to be regarded as the same point on the circle, for each integer k .)
- Now consider $\dot{\theta} = 1$. Show that there is no single-valued potential $V(\theta)$ for this vector field on the circle.
- What's the general rule? When does $\dot{\theta} = f(\theta)$ have a single-valued potential?

4.1.9 In Exercises 2.6.2 and 2.7.7, you were asked to give two analytical proofs that periodic solutions are impossible for vector fields on the line. Review these arguments and explain why they *don't* carry over to vector fields on the circle. Specifically, which parts of the argument fail?

4.2 Uniform Oscillator

4.2.1 (Church bells) The bells of two different churches are ringing. One bell rings every 3 seconds, and the other rings every 4 seconds. Assume that the bells have just rung at the same time. How long will it be until the next time they ring together? Answer the question in two ways: using common sense, and using the method of Example 4.2.1.

4.2.2 (Beats arising from linear superpositions) Graph $x(t) = \sin 8t + \sin 9t$ for $-20 < t < 20$. You should find that the amplitude of the oscillations is *modulated*—it grows and decays periodically.

- What is the period of the amplitude modulations?
- Solve this problem analytically, using a trigonometric identity that converts sums of sines and cosines to products of sines and cosines.

(In the old days, this beat phenomenon was used to tune musical instruments. You would strike a tuning fork at the same time as you played the desired note on the instrument. The combined sound $A_1 \sin \omega_1 t + A_2 \sin \omega_2 t$ would get louder and softer as the two vibrations went in and out of phase. Each maximum of total amplitude is called a beat. When the time between beats is long, the instrument is nearly in tune.)

4.2.3 (The clock problem) Here's an old chestnut from high school algebra: At 12:00, the hour hand and minute hand of a clock are perfectly aligned. When is the *next* time they will be aligned? (Solve the problem by the methods of this section, and also by some alternative approach of your choosing.)

4.3 Nonuniform Oscillator

4.3.1 As shown in the text, the time required to pass through a saddle-node bottleneck is approximately $T_{\text{bottleneck}} = \int_{-\infty}^{\infty} \frac{dx}{r+x^2}$. To evaluate this integral, let $x = \sqrt{r} \tan \theta$, use the identity $1 + \tan^2 \theta = \sec^2 \theta$, and change the limits of integration appropriately. Thereby show that $T_{\text{bottleneck}} = \pi / \sqrt{r}$.

4.3.2 The oscillation period for the nonuniform oscillator is given by the integral $T = \int_{-\pi}^{\pi} \frac{d\theta}{\omega - a \sin \theta}$, where $\omega > a > 0$. Evaluate this integral as follows.

- Let $u = \tan \frac{\theta}{2}$. Solve for θ and then express $d\theta$ in terms of u and du .
- Show that $\sin \theta = 2u/(1+u^2)$. (Hint: Draw a right triangle with base 1 and height u . Then $\frac{\theta}{2}$ is the angle opposite the side of length u , since $u = \tan \frac{\theta}{2}$ by definition. Finally, invoke the half-angle formula $\sin \theta = 2 \sin \frac{\theta}{2} \cos \frac{\theta}{2}$.)
- Show that $u \rightarrow \pm\infty$ as $\theta \rightarrow \pm\pi$, and use that fact to rewrite the limits of integration.
- Express T as an integral with respect to u .
- Finally, complete the square in the denominator of the integrand of (d), and reduce the integral to the one studied in Exercise 4.3.1, for a suitable choice of x and r .

For each of the following questions, draw the phase portrait as function of the control parameter μ . Classify the bifurcations that occur as μ varies, and find all the bifurcation values of μ .

$$4.3.3 \quad \dot{\theta} = \mu \sin \theta - \sin 2\theta$$

$$4.3.4 \quad \dot{\theta} = \frac{\sin \theta}{\mu + \cos \theta}$$

$$4.3.5 \quad \dot{\theta} = \mu + \cos \theta + \cos 2\theta$$

$$4.3.6 \quad \dot{\theta} = \mu + \sin \theta + \cos 2\theta$$

$$4.3.7 \quad \dot{\theta} = \frac{\sin \theta}{\mu + \sin \theta}$$

$$4.3.8 \quad \dot{\theta} = \frac{\sin 2\theta}{1 + \mu \sin \theta}$$

4.3.9 (Alternative derivation of scaling law) For systems close to a saddle-node bifurcation, the scaling law $T_{\text{bottleneck}} \sim O(r^{-1/2})$ can also be derived as follows.

a) Suppose that x has a characteristic scale $O(r^a)$, where a is unknown for now.

Then $x = r^a u$, where $u \sim O(1)$. Similarly, suppose $t = r^b \tau$, with $\tau \sim O(1)$. Show that $\dot{x} = r + x^2$ is thereby transformed to $r^{a-b} \frac{du}{d\tau} = r + r^{2a} u^2$.

b) Assume that all terms in the equation have the same order with respect to r , and thereby derive $a = \frac{1}{2}$, $b = -\frac{1}{2}$.

4.3.10 (Nongeneric scaling laws) In deriving the square-root scaling law for the time spent passing through a bottleneck, we assumed that \dot{x} had a quadratic minimum. This is the generic case, but what if the minimum were of higher order? Suppose that the bottleneck is governed by $\dot{x} = r + x^{2n}$, where $n > 1$ is an integer. Using the method of Exercise 4.3.9, show that $T_{\text{bottleneck}} \approx c r^b$, and determine b and c .

(It's acceptable to leave c in the form of a definite integral. If you know complex variables and residue theory, you should be able to evaluate c exactly by integrating around the boundary of the pie-slice $\{z = re^{i\theta} : 0 \leq \theta \leq \pi/n, 0 \leq r \leq R\}$ and letting $R \rightarrow \infty$.)

4.4 Overdamped Pendulum

4.4.1 (Validity of overdamped limit) Find the conditions under which it is valid to approximate the equation $mL^2\ddot{\theta} + b\dot{\theta} + mgL \sin \theta = \Gamma$ by its overdamped limit $b\dot{\theta} + mgL \sin \theta = \Gamma$.

4.4.2 (Understanding $\sin \theta(t)$) By imagining the rotational motion of an overdamped pendulum, sketch $\sin \theta(t)$ vs. t for a typical solution of $\theta' = \gamma - \sin \theta$. How does the shape of the waveform depend on γ ? Make a series of graphs for different γ , including the limiting cases $\gamma \approx 1$ and $\gamma \gg 1$. For the pendulum, what physical quantity is proportional to $\sin \theta(t)$?

4.4.3 (Understanding $\dot{\theta}(t)$) Redo Exercise 4.4.2, but now for $\dot{\theta}(t)$ instead of $\sin \theta(t)$.

4.4.4 (Torsional spring) Suppose that our overdamped pendulum is connected to a torsional spring. As the pendulum rotates, the spring winds up and generates

an opposing torque $-k\theta$. Then the equation of motion becomes $b\dot{\theta} + mgL \sin \theta = \Gamma - k\theta$.

- Does this equation give a well-defined vector field on the circle?
- Nondimensionalize the equation.
- What does the pendulum do in the long run?
- Show that many bifurcations occur as k is varied from 0 to ∞ . What kind of bifurcations are they?

4.5 Fireflies

4.5.1 (Triangle wave) In the firefly model, the sinusoidal form of the firefly's response function was chosen somewhat arbitrarily. Consider the alternative model $\dot{\Theta} = \Omega$, $\dot{\theta} = \omega + Af(\Theta - \theta)$, where f is given now by a triangle wave, not a sine wave. Specifically, let

$$f(\phi) = \begin{cases} \phi, & -\frac{\pi}{2} \leq \phi \leq \frac{\pi}{2} \\ \pi - \phi, & \frac{\pi}{2} \leq \phi \leq \frac{3\pi}{2} \end{cases}$$

on the interval $-\frac{\pi}{2} \leq \phi \leq \frac{3\pi}{2}$, and extend f periodically outside this interval.

- Graph $f(\phi)$.
- Find the range of entrainment.
- Assuming that the firefly is phase-locked to the stimulus, find a formula for the phase difference ϕ^* .
- Find a formula for T_{drift} .

4.5.2 (General response function) Redo as much of the previous exercise as possible, assuming only that $f(\phi)$ is a smooth, 2π -periodic function with a single maximum and minimum on the interval $-\pi \leq \phi \leq \pi$.

4.5.3 (Excitable systems) Suppose you stimulate a neuron by injecting it with a pulse of current. If the stimulus is small, nothing dramatic happens: the neuron increases its membrane potential slightly, and then relaxes back to its resting potential. However, if the stimulus exceeds a certain threshold, the neuron will "fire" and produce a large voltage spike before returning to rest. Surprisingly, the size of the spike doesn't depend much on the size of the stimulus—anything above threshold will elicit essentially the same response.

Similar phenomena are found in other types of cells and even in some chemical reactions (Winfree 1980, Rinzel and Ermentrout 1989, Murray 1989). These systems are called *excitable*. The term is hard to define precisely, but roughly speaking, an excitable system is characterized by two properties: (1) it has a unique, globally attracting rest state, and (2) a large enough stimulus can send the system on a long excursion through phase space before it returns to the resting state.

This exercise deals with the simplest caricature of an excitable system. Let $\dot{\theta} = \mu + \sin \theta$, where μ is slightly less than 1.

- Show that the system satisfies the two properties mentioned above. What object plays the role of the “rest state”? And the “threshold”?
- Let $V(t) = \cos \theta(t)$. Sketch $V(t)$ for various initial conditions. (Here V is analogous to the neuron’s membrane potential, and the initial conditions correspond to different perturbations from the rest state.)

4.6 Superconducting Josephson Junctions

4.6.1 (Current and voltage oscillations) Consider a Josephson junction in the overdamped limit $\beta = 0$.

- Sketch the supercurrent $I_c \sin \phi(t)$ as a function of t , assuming first that I/I_c is slightly greater than 1, and then assuming that $I/I_c \gg 1$. (Hint: In each case, visualize the flow on the circle, as given by Equation (4.6.7).)
- Sketch the instantaneous voltage $V(t)$ for the two cases considered in (a).

4.6.2 (Computer work) Check your qualitative solution to Exercise 4.6.1 by integrating Equation (4.6.7) numerically, and plotting the graphs of $I_c \sin \phi(t)$ and $V(t)$.

4.6.3 (Washboard potential) Here’s another way to visualize the dynamics of an overdamped Josephson junction. As in Section 2.7, imagine a particle sliding down a suitable potential.

- Find the potential function corresponding to Equation (4.6.7). Show that it is *not* a single-valued function on the circle.
- Graph the potential as a function of ϕ , for various values of I/I_c . Here ϕ is to be regarded as a real number, not an angle.
- What is the effect of increasing I ?

The potential in (b) is often called the “washboard potential” (Van Duzer and Turner 1981, p. 179) because its shape is reminiscent of a tilted, corrugated washboard.

4.6.4 (Resistively loaded array) *Arrays* of coupled Josephson junctions raise many fascinating questions. Their dynamics are not yet understood in detail. The questions are technologically important because arrays can produce much greater power output than a single junction, and also because arrays provide a reasonable model of the (still mysterious) high-temperature superconductors. For an introduction to some of the dynamical questions of current interest, see Tsang et al. (1991) and Strogatz and Mirolo (1993).

Figure 1 shows an array of two identical overdamped Josephson junctions. The junctions are in series with each other, and in parallel with a resistive “load” R .

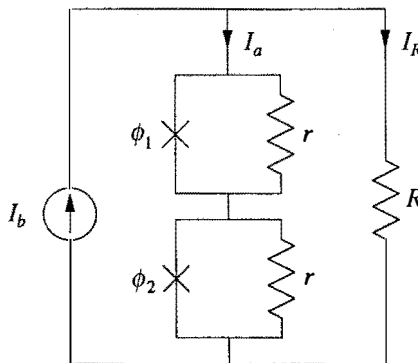


Figure 1

The goal of this exercise is to derive the governing equations for this circuit. In particular, we want to find differential equations for ϕ_1 and ϕ_2 .

- Write an equation relating the dc bias current I_b to the current I_a flowing through the array and the current I_R flowing through the load resistor.
- Let V_1 and V_2 denote the voltages across the first and second Josephson junctions. Show that $I_a = I_c \sin \phi_1 + V_1/r$ and $I_a = I_c \sin \phi_2 + V_2/r$.
- Let $k = 1, 2$. Express V_k in terms of $\dot{\phi}_k$.
- Using the results above, along with Kirchhoff's voltage law, show that

$$I_b = I_c \sin \phi_k + \frac{\hbar}{2er} \dot{\phi}_k + \frac{\hbar}{2eR} (\dot{\phi}_1 + \dot{\phi}_2) \text{ for } k = 1, 2.$$

- The equations in part (d) can be written in more standard form as equations for $\dot{\phi}_k$, as follows. Add the equations for $k = 1, 2$, and use the result to eliminate the term $(\dot{\phi}_1 + \dot{\phi}_2)$. Show that the resulting equations take the form

$$\dot{\phi}_k = \Omega + a \sin \phi_k + K \sum_{j=1}^2 \sin \phi_j,$$

and write down explicit expressions for the parameters Ω, a, K .

4.6.5 (N junctions, resistive load) Generalize Exercise 4.6.4 as follows. Instead of the two Josephson junctions in Figure 1, consider an array of N junctions in series. As before, assume the array is in parallel with a resistive load R , and that the junctions are identical, overdamped, and driven by a constant bias current I_b . Show that the governing equations can be written in dimensionless form as

$$\frac{d\phi_k}{d\tau} = \Omega + a \sin \phi_k + \frac{1}{N} \sum_{j=1}^N \sin \phi_j, \text{ for } k = 1, \dots, N,$$

and write down explicit expressions for the dimensionless groups Ω and a and the dimensionless time τ . (See Example 8.7.4 and Tsang et al. (1991) for further discussion.)

4.6.6 (N junctions, RLC load) Generalize Exercise 4.6.4 to the case where there are N junctions in series, and where the load is a resistor R in series with a capacitor C and an inductor L . Write differential equations for ϕ_k and for Q , where Q is the charge on the load capacitor. (See Strogatz and Miroollo 1993.)